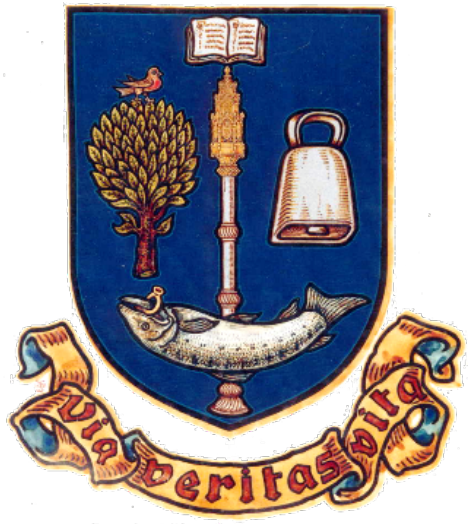

Essays on Natural Resource Evaluation and Management

by

Ruolan Ouyang

Submitted in Fulfilment of the Requirements for
the Degree of Doctor of Philosophy

Adam Smith Business School
College of Social Science
University of Glasgow

January 2017

Abstract

Derivatives markets, in particular futures markets, play an important role in the organization of production in commodity markets. While commodity markets for agricultural and natural resources like live cattle, soybean, oil, gas and minerals are well established, commodity markets for marine resources are very new. Located in Bergen (Norway), Fish Pool is a new derivatives market, where futures contracts written on fresh farmed salmon are traded in large quantities since 2006, continuing a strong upwards trend. Markets for forwards and futures on fresh salmon help companies which use fresh salmon in their production, for example, food processing companies, to hedge their price risk and plan ahead, by fixing the price in advance. In the same way, they help producers, i.e. salmon farmers, to reduce their selling price risk. In fact, according to Fish Pool News Archive released on 20/03/2012, not only consumers, processors and producers, but also speculative investors at Fish Pool play a more and more important role, which in consequence urges the issue of finding appropriate, theoretical well-founded and sound pricing formulas for the futures contracts traded there, as well as examining its effects on participants.

In this PhD thesis, we first discuss the valuation of futures on fresh farmed salmon as traded on the Fish Pool exchange and then explore how information reflected in the prices of futures contracts can be used to compute fair prices, i.e., arbitrage free prices, for lease and ownership of fish farms. Specifically, in the first chapter, we give a general background of the study and introduce the estimation methods adopted in the thesis, i.e., Kalman filter combined with the maximum likelihood estimation. In Chapter 2, we connect the popular Schwartz (1997) multi-factor approach, which features a stochastic convenience yield for the salmon spot price, with the classical literature

on fish-farming and aquaculture. We follow first principles, starting by modeling the aggregate salmon farming production process and modeling the demand using a Cobb-Douglas utility function for a representative consumer. In Chapter 3, we extend the Schwartz (1997) two-factor model by adding a seasonality feature to the mean-level of convenience yield. All models are estimated by means of Kalman filter, using a rich data set of contracts with different maturities traded at Fish Pool. The estimates are also discussed in the context of other commodity markets, specifically live cattle which acts as a substitute. Our results show that the framework presented is able to produce an excellent fit to the actual term structure of salmon futures. A comparison with live cattle futures traded within the same period reveals subtle difference, for example within the level of the convenience yield, the speed of mean reversion of the convenience yield and the convenience yield risk premium. In Chapter 4, we consider the optimal harvesting problem for a fish farmer. We take account of the existence of Fish Pool, which determines risk premia and other relevant variables, that influence the fish farmer in his decision. We assess the optimal strategy, harvesting time and value against two alternative setups. The first alternative involves simple strategies which lack managerial flexibility, the second alternative allows for managerial flexibility and risk aversion as modeled by a constant relative risk aversion utility function, but without access to the salmon futures market. In both cases, the loss in project value can be very significant, and in the second case is only negligible for extremely low levels of risk aversion. In consequence, for a risk-averse fish farmer, the presence of a salmon futures market as well as managerial flexibility are highly important.

Contents

List of Tables

List of Figures

Acknowledgement

First and foremost, I would like to express my deepest gratitude to my principal supervisor Prof. Christian Ewald, for his tremendous academic support. He has been my mentor since I was a postgraduate student, and I would not dream of starting a PhD without his encouragement. My PhD has been an amazing experience, and I am really grateful for all valuable opportunities he offered.

My sincere gratitude also goes to my second supervisor Dr Konstantinos Angelopoulos, for his patient guidance and continuous support. I benefited a lot from the stimulating discussions with him.

Besides my supervisors, special thanks must go to Prof. Sjur Westgaard and Prof. Bart Taub. It is my great honour to have them as my examiners. I am truly grateful for their time and efforts put into my work. Moreover, I would like to thank Prof. Stein-Erik Fleten, Prof. Mario Cerrato and Dr Michael Coulon, for their insightful comments and encouragements provided on workshops and conferences. Likewise, I would like to thank editors and anonymous referees of *Quantitative Finance* and *American Journal of Agricultural Economics* for their remarks and suggestions which greatly helped to improve the research.

Additionally, I acknowledge the financial support from the Adam Smith Business School. I also wish to thank all faculty members and administrative staffs who make efforts to create such a pleasant research environment.

Moreover, I am deeply indebted to all my friends. In particular, I am grateful to Jia Xie, Miao Huang, Yuanyuan Qu, Chaona Chen, Ying Zheng and Yun Yu, for all the good times and hard times we have been through in the last three years.

Last but not the least, I would like to thank my beloved parents wholeheartedly. Without the inspiration, love and support that they have given me, I cannot be the person I am today. My every success belongs to them as well.

Dedication

To my family

Declaration

I declare that, except where explicit reference is made to the contribution of others, that this dissertation is the result of my own work and has not been submitted for any other degree at he University of Glasgow or any other institution.

Signature: _____

Printed Name: Ruolan Ouyang

Chapter 1

Introduction

Derivatives markets, in particular futures markets, play an important role in the organization of production in commodity markets. This is well known, at least since the fundamental work of Hirshleifer (1988). Futures contracts on commodities help producers and processors to hedge against a significant part of the price risk they are exposed to. Although some recent claims link the activity of speculators on commodity futures markets to high world food prices, most farmers and food processing companies would not be able to survive without them. While commodity markets for agricultural and natural resources like live cattle, soybean, oil, gas and minerals are well established, commodity markets for marine resources are very new. So called seafood futures on frozen shrimp have been traded on the Minneapolis Grain Exchange for some time in the 1990s, but trading has ceased since. Reasons for this have been discussed in Sanders and Manfredo (2002). These include market specific inefficiencies as well as a general lack of knowledge regarding futures markets among the shrimp industry. In this chapter, we first give a general background and a broad outline of this study. After that, preliminaries of estimation techniques adopted in the thesis, i.e, Kalman filter combined with the maximum likelihood estimation, are presented.

1.1 General Background

Fish Pool is a new derivatives market, where futures and options on fresh farmed salmon are traded in large quantities since 2006. Located in Bergen (Norway), contract volumes traded at this market have reached 97,000 tons, equivalent to 4.3 billion *NOK* (457 million Euro), during 2014, continuing a strong upwards trend. Following its great success in the start-up phase, the Oslo Stock Exchange acquired 71% of Fish Pool in December 2012 and currently owns 94.3%, and Nasdaq offers clearing of salmon derivatives traded on it. Bergfjord (2007), Dalton (2005) and Bulte and Pennings (1997) provide possible explanations for this trend. Bergfjord (2007) in particular highlights the aspect of non-storability of the fresh salmon at Fish Pool, as compared to the frozen and storable shrimp products traded previously at the Minneapolis Grain Exchange, a fact which clearly distinguishes the new salmon futures market from the old shrimps futures market.

Markets for forwards and futures on fresh salmon help companies which use fresh salmon in their production, for example, food processing companies, to hedge their price risk and plan ahead, by fixing the price in advance. In the same way, they help producers, i.e. salmon farmers, to reduce their selling price risk. An analysis of the welfare effects of futures markets in a rather general context is presented in Hirshleifer (1988). He discusses a two-period model which includes consumers, processors, producers and speculators. In fact speculative investors at Fish Pool play a more and more important role, compare Fish Pool News Archive (2012), which in consequence urges the issue of finding appropriate, theoretical well-founded and sound pricing formulas for the futures and options traded there.

Markets like the Norwegian Fish Pool are also highly relevant for other countries. Minyanville, an Emmy award winning financial media company, reports in an article on 29/06/2010, that a US based futures market in fish is inevitable. The UK is the third largest producer of farmed salmon in the world with all production based in Scotland. In fact farmed salmon accounts for more than 50% of Scottish food exports.

It is further believed that the creation of futures and derivatives markets for ocean resources can contribute to the conservation of ocean species, see Dalton (2005) as well as Bulte and Pennings (1997). A consortium lead by George Sugihara from University of California San Diego supported by the National Marine Fisheries Service of USA has been campaigning for the creation of the Ocean Resource Exchange. Quoting Sugihara (see Dalton (2005)) "The first derivative is likely to be a futures contract for a certain percentage of a fisherman's catch at an agreed price at a specified time." The questions here are whether financial markets where appropriately designed financial contracts are traded can provide the incentives for fisheries to harvest marine resources in a way that is economically and environmentally sustainable, or if in fact there is evidence that a similar UK based market could improve the competitiveness of the UK's salmon industry.

Theoretical models of aquaculture and the fish farm production have been discussed since the mid 1980's. Early work includes important contributions by Karp, Sadeh, and Griffin (1986), Hannesson (1986) and Bjørndal (1988) who define the problem in its elementary form as a sequential optimal stopping problem. This is similar in nature to the typical problem encountered in forestry, when to cut a tree and plant a new one. Various aspects such as density dependent growth of the farmed fish population, optimal feeding schedules and weight dependent prices have since been discussed in Arnason (1992), Heaps (1993), Heaps (1995), Guttormsen (2008), Mistiaen and Strand (1998) and Yu and Leung (2006). The setup in the latter articles is fully deterministic and does not allow for any form of uncertainty. The methodology applied is deterministic optimal control in form of dynamic programming and the Pontryagin maximum principle. Stochastic models are far less common. Karp et al. (1986) includes a discrete time model which allows for uncertainty in the weight of the farmed shrimp and Rizzo and Spagnolo (1996) allow for stochastic effects in growth and mortality. To the best of our knowledge there do not yet exist any continuous time stochastic models which specifically address the fish farm production process. There are however continuous time real option models that have been applied to wild-catch fisheries by Li (1998) and Sarkar (2009). Other important literature in the continuous time stochastic context,

outwith the real options context, include Beddington and May (1977), May (1973), Lande, Engen, and Saether (1995), Alvarez (1998) and Alvarez and Shepp (1998) as well as Hanson and Ryan (1998). Finally, Ewald and Wang (2010) present a continuous time stochastic model which includes multiple species and ecological interactions, as well as different fishery regimes. None of the models above are addressing the aspect of financial markets where marine resources or certain derivative contracts on them are traded. Given the existence of the derivatives markets on salmon, i.e., Fish Pool, we can find a proper way to connect the classical literature on fish-farming and aquaculture to theoretically sound models in financial markets. Such framework will enable us to analyse the salmon prices and further explore its implications on salmon farming, for instance, how to make decisions regarding the price process which correctly accounts for risk premia. As mentioned earlier, for these derivative contracts to be meaningful, we require uncertainty in our model. In order to better blend in with the financial literature, we are mainly focusing on continuous time stochastic models. The models by Sarkar (2009), Li (1998), Hanson and Ryan (1998) and Alvarez and Shepp (1998) build an excellent foundation for such purpose.

1.2 Structures

To better organize the work in this study, we will structure it into three main chapters which all link into each other.[1] In Chapter 2, we study the futures contracts written on fresh farmed salmon, which have been actively traded at the Fish Pool Market in Norway since 2006, by the popular Schwartz (1997) multifactor approach. This approach features a stochastic convenience yield for the salmon spot price. We connect this approach with the classical literature on fish-farming and aquaculture using first principles, starting by modeling the aggregate salmon farming production process and modeling the demand using a Cobb-Douglas utility function for a representative consumer. The model is estimated by means of Kalman filter, using a rich data set of contracts with different maturities traded at Fish Pool. The results are also discussed in the context of other commodity markets, specifically live cattle which acts as a substitute. Our results show that the framework presented is able to produce an excellent fit to the actual term structure of salmon futures. A comparison with live cattle futures traded within the same period reveals subtle difference, for example within the level of the convenience yield, the speed of mean reversion of the convenience yield and the convenience yield risk premium.

The Chapter 2 is structured as follows. In section 2 we briefly review the Schwartz (1997) multifactor approach, while in section 3 we discuss farmed salmon supply and demand leading to an equilibrium price. Section 4 contains our empirical analysis, using Kalman filter to estimate the parameters within our model for different sub-samples of our data-set. In section 5 we draw comparisons with live cattle futures and identify subtle differences in the two markets. Our main conclusions are summarized in section 6. The appendices contain a number of figures which support the findings in the main text.

In Chapter 3, we develop a model based on the Schwartz (1997) two-factor model by adding a seasonality feature to the mean-level of convenience yield. To place our study

[1] These chapters are broadly based on three research papers co-authored with my supervisor Christian Ewald, as well as Roy Nawar and Tak-Kuen Siu.

into the context of other commodities, we have also included the live-cattle futures contracts traded on the Chicago Mercantile Exchange into our analysis as in Chapter 2. All models in Chapter 2 and Chapter 3 are estimated by the mean of Kalman filter. Chapter 3 is structured as follows. In section 2, we give a description of the models. In section 3, data and empirical study are discussed. Following that, in section 4, we draw comparison between the futures contracts written on live-cattle and salmon. Our conclusions are summarized in the final section. The appendices contain the derivation of joint distribution and additional figures.

In Chapter 4, we consider the optimal harvesting problem for a fish farmer in a model which accounts for stochastic prices featuring a Schwartz (1997) two-factor price dynamics. We presented a methodological approach, which can be used to determine the values of lease or ownership of a fish farm in a way which is consistent with market data obtained from the Fish Pool market, where futures on fresh farmed salmon are traded. Our approach correctly accounts for risk premia due to stochastically fluctuating prices. We assess the optimal strategy, harvesting time and value against two alternative setups. The first alternative involves simple strategies which lack managerial flexibility, the second alternative allows for managerial flexibility and risk aversion as modeled by a constant relative risk aversion utility function, but without access to the salmon futures market. In both cases, the loss in project value can be very significant, and in the second case is only negligible for extremely low levels of risk aversion. In consequence, for a risk averse fish farmer, the presence of a salmon futures market as well as managerial flexibility are highly important.

The Chapter 4 is structured as follows. In section 2, we briefly review the Schwartz (1997) two-factor approach, while in the following section we summarize the results of our empirical estimation of the model. The optimal harvesting and rotation problem of an individual fish farmer and in consequence the valuation for lease and ownership of a model fish farm are discussed in detail in the penultimate section. The final section contains our main conclusions.

1.3 Methods and Techniques: Preliminaries

In this section we introduce the methods and techniques involved in the estimation procedure in this study. Specifically, how the Kalman filter technique can be combined with the maximum likelihood method to estimate the unknown state variables and the parameters of model. We start from the formulation of the state space model, and then give a brief review of the Kalman filter as well as the maximum likelihood estimation. We refer to Harvey (1990) for details.

1.3.1 State Space Form

The state space form is a powerful way to deal with situations in which the state variables are not observable. In general, the state space form applies to an observable multivariate time series $\mathbf{y_t}$. These observable variables are related to the unobservable state variables $\mathbf{\Phi}_t$, which are known to be generated by a first-order Markov process. We can write the state space form into two sets of equations, the measurement equation (1.1) and the transition equation (1.2).

$$\mathbf{y}_t = \mathbf{d}_t + Z_t\mathbf{\Phi}_t + \boldsymbol{\epsilon}_t \tag{1.1}$$

$$\mathbf{\Phi}_t = \mathbf{c}_t + Q_t\mathbf{\Phi}_{t-1} + \boldsymbol{\eta}_t, \tag{1.2}$$

where

- $\mathbf{y}_t$ is an $(n \times 1)$ vector,
- $\mathbf{d}_t$ is an $(n \times 1)$ vector,
- Z_t is an $(n \times m)$ matrix,
- $\boldsymbol{\epsilon}_t$ is an $(n\times1)$ vector of serially uncorrelated and normally distributed disturbance with

$$\mathrm{E}(\boldsymbol{\epsilon}_t) = 0, \qquad \mathrm{Var}(\boldsymbol{\epsilon}_t) = H_t$$

H_t is an $(n \times n)$ matrix which is symmetric and positive semidefinite.

- $\mathbf{\Phi}_t$ is an $(m \times 1)$ vector,
- $\mathbf{c}_t$ is an $(m \times 1)$ vector,
- Q_t is an $(m \times m)$ matrix,
- $\boldsymbol{\eta}_t$ is an $(m \times 1)$ vector of serially uncorrelated and normally distributed disturbance with

$$\mathrm{E}(\boldsymbol{\eta}_t) = 0, \qquad \mathrm{Var}(\boldsymbol{\eta}_t) = R_t$$

  R_t is an $(m \times m)$ matrix which is symmetric and positive semidefinite.

The matrices $\mathbf{d}_t$, Z_t and H_t in the measurement equation (1.1) and the matrices $\mathbf{c}_t$, Q_t and R_t in the transition equation (1.2) are called the system matrices. These system matrices may be time-variant and depend on a set of unknown parameters $\boldsymbol{\psi}$, i.e., $\mathbf{d}_t(\boldsymbol{\psi})$, $Z_t(\boldsymbol{\psi})$, $H_t(\boldsymbol{\psi})$, $\mathbf{c}_t(\boldsymbol{\psi})$, $Q_t(\boldsymbol{\psi})$ and $R_t(\boldsymbol{\psi})$. Given such setup, a recursion algorithm such as Kalman filter can be applied to estimate both the unobservable state variables $\mathbf{\Phi}$ and the unknown parameter set $\boldsymbol{\psi}$ of the model. We will cover this important topic in the following sections. To complete the specification of the state space system, two further assumptions are made as follows.

i the initial state vector, $\mathbf{\Phi}_0$ is normally distributed with[2]

$$\mathrm{E}(\mathbf{\Phi}_0) = \mathbf{a}_0, \qquad \mathrm{Var}(\mathbf{\Phi}_0) = \mathbf{P}_0$$

ii the disturbances $\boldsymbol{\epsilon}_t$ and $\boldsymbol{\eta}_t$ are uncorrelated with each other in all time periods, and uncorrelated with the initial state $\mathbf{\Phi}_0$.

[2]This assumption may be relaxed and has been discussed in Harvey (1990).

1.3.2 Kalman Filter

Once a model has been put in a state space form, Kalman filter can be applied. The Kalman filter is an efficient data fusion algorithm, delivering the optimal estimator of the state vector $\mathbf{\Phi}_t$, based on all the information available at time t, through a recursive procedure. This recursive procedure can be divided into two steps in general:

i Prediction Step (Time Update): in this step, Kalman filter gives an optimal predictor of the unobservable state variable $\mathbf{\Phi}_t$ based on all information available up to time $t-1$. After that, a state vector called prior estimates at time t are calculated.

ii Correction Step (Measurement Update): once the new observation $\mathbf{y}_t$ becomes available, it is used to update the prior estimates. As a result, a posterior estimates can be produced.

To better illustrate this algorithm, we also provide equations involved in each step here. We denote the starting values for the Kalman filter as $\mathbf{a}_0$, a vector giving the initial value of the state variable, and $\mathbf{P}_0$, the corresponding covariance matrix of the estimation error.[3] Note, the system matrices as well as the $\mathbf{a}_0$ and $\mathbf{P}_0$ are assumed to be known in all time periods. Given these initial set up, the Kalman filter can run the following steps recursively from the starting point t_0 to the ending point T, and yield the optimal estimator based on the full information set.

i Calculate the prior estimates $\mathbf{a}_{t|t-1}$ and the corresponding covariance matrix $\mathbf{P}_{t|t-1}$ via the prediction equations

$$\mathbf{a}_{t|t-1} = \mathbf{c}_t + Q_t \mathbf{a}_{t-1}, \tag{1.3}$$

$$\mathbf{P}_{t|t-1} = Q_t \mathbf{P}_{t-1} Q_t' + R_t \tag{1.4}$$

ii Once the new observation $\mathbf{y}_t$ is available, we can get the prediction errors $\mathbf{v}_t$ and

[3] They may also be specified as $\mathbf{a}_{1|0}$ and $\mathbf{P}_{1|0}$.

the corresponding covariance matrix $\mathbf{F}_t$

$$\mathbf{v}_t = \mathbf{y}_t - Z_t\mathbf{a}_{t|t-1} - \mathbf{d}_t, \tag{1.5}$$

$$\mathbf{F}_t = Z_t\mathbf{P}_{t|t-1}Z_t' + H_t \tag{1.6}$$

iii Obtain the Kalman gain

$$\mathbf{K}_t = \mathbf{P}_{t|t-1}Z_t'\mathbf{F}_t^{-1} \tag{1.7}$$

iv Calculate the posteriori estimates $\mathbf{a}_t$ and the corresponding covariance matrix $\mathbf{P}_t$ via the updating equations

$$\mathbf{a}_t = \mathbf{a}_{t|t-1} + \mathbf{K}_t\mathbf{v}_t, \tag{1.8}$$

$$\mathbf{P}_t = (\mathbb{I} - \mathbf{K}_tZ_t)\mathbf{P}_{t|t-1} \tag{1.9}$$

Given the assumption that disturbances and initial state vector are normally distributed, the derivation of the Kalman filter shows that the recursion above can provide an optimal estimator of $\mathbf{\Phi}_t$, in the sense that the mean of the conditional distribution of $\mathbf{\Phi}_t$ is the estimator minimizing the mean square error (MSE). When the normality assumption is dropped, the conditional mean of the state vector is still an optimal estimator minimizing the mean square error within the class of all linear estimators. The derivation of Kalman filter, and the Kalman filter for non-normally distributed disturbances or nonlinear system are beyond the scope of this work, which are omitted here.

1.3.3 Maximum Likelihood Estimation

As indicated by Harvey (1990), one reason for the central role of the Kalman filter is that when the disturbances and the initial state vector are normally distributed, it enables the likelihood function to be calculated via the prediction error decomposition, which allows us to estimate the unknown parameters in the model. The likelihood function $\mathcal{L}$ of a linear state space model, in which the observations $\mathbf{Y}_T = (\mathbf{y}_1, \mathbf{y}_2, \cdots, \mathbf{y}_T)$ are independently and identically distributed, is given by

$$\mathcal{L}(\mathbf{Y}_T; \boldsymbol{\psi}) = \prod_{t=1}^{T} p(\mathbf{y}_t) \tag{1.10}$$

where $p(\mathbf{y}_t)$ is the probability density function of the $t-th$ set of observations. The maximum likelihood estimator is found by maximizing this function with respect to the parameter set $\boldsymbol{\psi}$. For most time series, the observations are not independent, which lead us to write the joint density function as

$$\mathcal{L}(\mathbf{Y}_T; \boldsymbol{\psi}) = \prod_{t=1}^{T} p(\mathbf{y}_t | \mathbf{Y}_{t-1}) \tag{1.11}$$

where $p(\mathbf{y}_t|\mathbf{Y}_{t-1})$ denotes the density of $\mathbf{y}_t$ conditional on the information set at time $t-1$ and $\mathbf{Y}_{t-1} = (\mathbf{y}_1, \mathbf{y}_2, \cdots, \mathbf{y}_{t-1})$. Due to the Markovian feature of the state space model, the future observation only depend on the value of current observation, which gives us the reduced form as

$$\mathcal{L}(\mathbf{Y}_T; \boldsymbol{\psi}) = \prod_{t=1}^{T} p(\mathbf{y}_t | \mathbf{y}_{t-1}) \tag{1.12}$$

As mentioned earlier, we use the algorithm, in which the Kalman filter is embedded in the maximum likelihood method, to achieve the goal of parameter estimation. The algorithm starts with an initial guess of the parameter set $\boldsymbol{\psi}_0$ and the state vector $\mathbf{a}_0$ as well as its covariance matrix $\mathbf{P}_0$. After that, the Kalman filter runs as introduced before. Once the last observation is reached, the log-likelihood will be calculated and a new parameter set can be selected to reach the maximum likelihood value. The recursive procedure will continue until the log-likelihood value cannot be improved with

regard to the predefined abortion criteria.

Based on all assumptions made in the Kalman filter, we can easily conclude that the conditional distribution of $\mathbf{y}_t$ or the density function $p(\mathbf{y}_t|\mathbf{y}_{t-1})$, is normal with conditional mean $\mathbf{y}_{t|t-1}$ and covariance matrix $\mathbf{F}_t$. For a Gaussian model, the likelihood function can then be written as

$$\mathcal{L}(\mathbf{Y}_T;\boldsymbol{\psi}) = \prod_{t=1}^{T}(2\pi)^{-\frac{n}{2}}|\mathbf{F}_t|^{-\frac{1}{2}}\exp(-\frac{1}{2}\mathbf{v}_t'\mathbf{F}_t^{-1}\mathbf{v}_t) \tag{1.13}$$

where n is the number of observations at each time point. Clearly, information needed to calculate the likelihood function can all be obtained when running the Kalman filter. Note, $\mathbf{v}_t$ and $\mathbf{F}_t$ have been defined in (1.5) and (1.6) respectively. The logarithm of the likelihood can be expressed immediately as

$$\ln\mathcal{L}(\mathbf{Y}_T;\boldsymbol{\psi}) \;=\; -\frac{nT}{2}\log 2\pi - \frac{1}{2}\sum_{t=1}^{T}\log|\mathbf{F}_t| - \frac{1}{2}\sum_{t=1}^{T}\mathbf{v}_t'\mathbf{F}_t^{-1}\mathbf{v}_t \tag{1.14}$$

and the maximum likelihood estimates $\hat{\boldsymbol{\psi}}_{ML}$ is obtained by

$$\hat{\boldsymbol{\psi}}_{ML} = \arg\max_{\boldsymbol{\psi}\in\boldsymbol{\Psi}} \ln\mathcal{L}(\mathbf{Y}_T;\boldsymbol{\psi}) \tag{1.15}$$

where $\boldsymbol{\Psi} \subset \mathbb{R}^n$ is the parameter space. Since the $\mathbf{v}_t$ can be interpreted as a vector of prediction errors, (1.14) is also known as the prediction error decomposition form of the likelihood.

Another important issue, namely how to get the standard error of each parameter, can be solved easily via three steps below.

i Calculate the information matrix ($\mathbf{I}$). The information matrix can be written as the negative expected value of the Hessian matrix. The Hessian matrix (Hess) is defined as the matrix of second-order partial derivatives of the log-likelihood

function with respect to each parameter.

$$\mathbf{I}(\hat{\boldsymbol{\psi}}_{ML}) = -\mathrm{E}(\mathrm{Hess}(\hat{\boldsymbol{\psi}}_{ML})) \tag{1.16}$$

$$\mathrm{Hess}(\hat{\boldsymbol{\psi}}_{ML}) = \frac{\partial^2 \ln \mathcal{L}(\hat{\boldsymbol{\psi}}_{ML})}{\partial \hat{\boldsymbol{\psi}}_{ML} \partial \hat{\boldsymbol{\psi}}'_{ML}} \tag{1.17}$$

ii Obtain the covariance matrix. In large samples, the inverse of the information matrix ($\mathbf{I}^{-1}$) is the covariance matrix of the maximum likelihood estimates.

iii Once the covariance matrix is got, the asymptotic standard errors of the estimates are the square roots of the diagonal elements of this matrix.

The Hessian matrix is generated automatically within the estimation procedure that combines the Kalman filter and the maximum likelihood method.

Bibliography

Alvarez, L. H. (1998). Optimal harvesting under stochastic fluctuations and critical depensation. *Mathematical Biosciences*, *152*(1), 63–85.

Alvarez, L. H., & Shepp, L. A. (1998). Optimal harvesting of stochastically fluctuating populations. *Journal of Mathematical Biology*, *37*(2), 155–177.

Arnason, R. (1992). Optimal feeding schedules and harvesting time in aquaculture. *Marine Resource Economics*, 15–35.

Beddington, J. R., & May, R. M. (1977). Harvesting natural populations in a randomly fluctuating environment. *Science*, *197*(4302), 463–465.

Bergfjord, O. J. (2007). Is there a future for salmon futures? an analysis of the prospects of a potential futures market for salmon. *Aquaculture Economics & Management*, *11*(2), 113–132.

Bjørndal, T. (1988). Optimal harvesting of farmed fish. *Marine Resource Economics*, 139–159.

Bulte, E., & Pennings, J. (1997). A note on overfishing, fishing rights and futures markets. *European journal of law and economics*, *4*(4), 327–335.

Dalton, R. (2005). Conservation policy: Fishy futures. *Nature*, *437*(7058), 473–474.

Ewald, C.-O., & Wang, W.-K. (2010). Sustainable yields in fisheries: Uncertainty, risk-aversion, and mean-variance analysis. *Natural Resource Modeling*, *23*(3), 303–323.

Fish Pool News Archive. (2012). *Fish pool news archive.* Retrieved 2012-09-30, from http://fishpool.eu/default.aspx?pageId=1&articleId=76&news=1

Guttormsen, A. G. (2008). Faustmann in the sea: optimal rotation in aquaculture. *Marine Resource Economics*, 401–410.

Hannesson, R. (1986). The effect of the discount rate on the optimal exploitation of

renewable resources. *Marine Resource Economics*, *3*(4), 319–329.

Hanson, F. B., & Ryan, D. (1998). Optimal harvesting with both population and price dynamics. *Mathematical Biosciences*, *148*(2), 129–146.

Harvey, A. C. (1990). *Forecasting, structural time series models and the kalman filter*. Cambridge university press.

Heaps, T. (1993). The optimal feeding of farmed fish. *Marine Resource Economics*, 89–99.

Heaps, T. (1995). Density dependent growth and the culling of farmed fish. *Marine Resource Economics*, 285–298.

Hirshleifer, D. (1988). Risk, futures pricing, and the organization of production in commodity markets. *The Journal of Political Economy*, 1206–1220.

Karp, L., Sadeh, A., & Griffin, W. L. (1986). Cycles in agricultural production: the case of aquaculture. *American Journal of Agricultural Economics*, *68*(3), 553–561.

Lande, R., Engen, S., & Saether, B.-E. (1995). Optimal harvesting of fluctuating populations with a risk of extinction. *American naturalist*, 728–745.

Li, E. (1998). Option value of harvesting: theory and evidence. *Marine Resource Economics*, 135–142.

May, R. M. (1973). Stability in randomly fluctuating versus deterministic environments. *American Naturalist*, 621–650.

Mistiaen, J. A., & Strand, I. (1998). Optimal feeding and harvest time for fish with weight-dependent prices. *Marine Resource Economics*, 231–246.

Rizzo, G., & Spagnolo, M. (1996). A model for the optimal management of sea bass dicentrarchus labrax aquaculture. *Marine resource economics*, 267–286.

Sanders, D. R., & Manfredo, M. R. (2002). The white shrimp futures market: lessons in contract design and marketing. *Agribusiness*, *18*(4), 505–522.

Sarkar, S. (2009). Optimal fishery harvesting rules under uncertainty. *Resource and Energy Economics*, *31*(4), 272–286.

Schwartz, E. S. (1997). The stochastic behavior of commodity prices: Implications for valuation and hedging. *The Journal of Finance*, *52*(3), 923–973.

Yu, R., & Leung, P. (2006). Optimal partial harvesting schedule for aquaculture operations. *Marine Resource Economics*, 301–315.

Chapter 2

The Market for Salmon Futures: An Empirical Analysis of Fish Pool Using the Schwartz Multifactor Model

Abstract

Using the popular Schwartz 97 two-factor approach, we study future contracts written on fresh farmed salmon, which have been actively traded at the Fish Pool Market in Norway since 2006. This approach features a stochastic convenience yield for the salmon spot price. We connect this approach with the classical literature on fish-farming and aquaculture using first principles, starting by modeling the aggregate salmon farming production process and modeling the demand using a Cobb-Douglas utility function for a representative consumer. The model is estimated by means of Kalman filter, using a rich data set of contracts with different maturities traded at Fish Pool between 12/06/2006 and 22/03/2012. The results are then discussed in the context of other commodity markets, specifically live cattle which acts as a substitute.

Keywords: Futures, Commodities, Aquaculture, Fisheries Economics

2.1 Introduction

In this chapter we discuss the valuation of futures on fresh farmed salmon as traded on the Fish Pool exchange. Our major concern is the accurate and market consistent pricing of the futures contracts, taking into account at least some of the key-elements describing the salmon farming process as well as the demand for farmed salmon and combining these coherently with the methodology of arbitrage free pricing developed in the derivatives pricing literature. More specifically we are connecting the Schwartz (1997) multifactor approach with stochastic convenience yield to the classical literature in fish farming and aquaculture. We estimate the parameters in our model on the basis of an extensive data set obtained from the Fish Pool market covering the period from 12/06/2006 until 22/03/2012. Solibakke (2012) presents an approach using stochastic volatility to model the Fish Pool market. However, only front months contracts are considered and the term structure, which can only be obtained from contracts with longer maturities, is not accounted for. In fact, it is well known that stochastic volatility alone cannot produce realistic term structures. While stochastic volatility is without doubt an important feature, modeling the term structure of the future contracts and identifying the stochastic convenience yield is generally considered to be more important.

The classical salmon farming literature, e.g. Bjørndal (1988), Arnason (1992), Heaps (1995), Cacho (1997), Yu and Leung (2006) as well as Guttormsen (2008) focuses on the harvesting behavior of one individual salmon farmer. In contrast to this, our focus is on the aggregate salmon production, as the aggregate production alone will affect the market price, which features prominently in our financial model. In order to get there, we assume that at any given time, a constant proportion of salmon farmers (or farming units) will harvest. This assumption accurately reflects how salmon farming companies operate world wide and salmon can be harvested at any time, reflecting consumer demand. The demand for farmed salmon is then modeled in a rather classical way by attaching a Cobb Douglas type utility function to a representative consumer, who chooses between farmed salmon and an alternative consumption good. The market

clearing price will then be used in the analysis of futures contracts within the Schwartz (1997) framework. To place our study into context and compare the estimated parameters of our model with those obtained for other commodities, we have also included a data set for live-cattle future contracts as traded on the Chicago Mercantile Exchange into our analysis.

A problem related to pricing farmed salmon futures and options has been discussed in Ewald (2013). The difference there, is that the population is assumed to be wild and not farmed, and managed as an open access fishery. Further the driving dynamics, e.g. the biomass of the wild population in the sea, is assumed to be of different type. Ewald (2013) uses stochastic logistic growth, which is mainly motivated by the classical fishery economics as well as population ecology literature such as Beddington and May (1977), May (1973), Lande, Engen, and Saether (1995), Alvarez (1998) as well as Alvarez and Shepp (1998). This specification however does only allow for approximate pricing formulas for futures and options, and hence causes problems in the calibration of the model. A mean variance approach in the context of optimizing sustainable yields under uncertainty in the same dynamic setup has been presented in Ewald and Wang (2010).

The rest of the paper is structured as follows. In section 2 we will briefly review the Schwartz (1997) multifactor approach, while in section 3 we discuss farmed salmon supply and demand leading to an equilibrium price. Section 4 contains our empirical analysis, using Kalman filter to estimate the parameters within our model for different sub-samples of our data-set. In section 5 we draw comparisons with live cattle futures and identify subtle differences in the two markets. Our main conclusions are summarized in section 6. The appendices contain a number of tables and figures which support our findings.

2.2 Schwartz (1997) Multifactor Framework

Let us denote with $P(t)$ the price of a commodity at time t. In the Schwartz (1997) framework the state variables $P(t)$, $\delta(t)$ and $r(t)$ are given by

$$dP(t) = (\mu - \delta(t))P(t)dt + \sigma_1 P(t)dZ_1(t) \tag{2.1}$$

$$d\delta(t) = \kappa(\alpha - \delta(t))dt + \sigma_2 dZ_2(t) \tag{2.2}$$

$$dr(t) = a(m - r(t))dt + \sigma_3 dZ_3(t) \tag{2.3}$$

with constants μ, κ, α, a, m, σ_1, σ_2 and σ_3 under the real world probability $\mathbb{P}$. The Brownian motions $Z_1(t)$, $Z_2(t)$ and $Z_3(t)$ are assumed to be correlated, according to

$$dZ_1(t)dZ_2(t) = \rho_1 dt, dZ_2(t)dZ_3(t) = \rho_2 dt, dZ_1(t)dZ_3(t) = \rho_3 dt. \tag{2.4}$$

We assume $\kappa, a \geq 0$. The process $r(t)$ denotes the stochastic interest rate. Under the assumption $\sigma_3 = 0$ and $a = 0$, the interest rate remains constant and the model in fact becomes a two-factor model, also known as Schwartz (1997) two-factor model. The process $\delta(t)$ represents the stochastic convenience yield and can be recognized as a mean reverting Ornstein-Uhlenbeck process. It reflects the utility that an agent receives when holding the commodity, or storage/maintenance costs that the agent needs to pay. The price dynamics (2.1) has an implicit mean reversion feature. If $\rho_1 > 0$, then the instantaneous correlation between $P(t)$ and $\delta(t)$ is positive. Hence $P(t)$ is likely to be large when $\delta(t)$ is large and in this case $\delta(t)$ is likely to be larger than μ. The drift term in (2.1) will then push $P(t)$ downwards. The opposite happens if $P(t)$ is small, pushing $P(t)$ upwards. If in fact one chooses $\delta(t) = \kappa \ln(P(t))$, one obtains the dynamics of a geometric Ornstein-Uhlenbeck process in (2.1), and $\delta(t)$ defined in this way satisfies (2.2) with $\rho = 1$. In this case we obtain the so called Schwartz (1997) one-factor model. In its full generality, i.e. without any coefficient restrictions other than $\kappa, a \geq 0$ the model is known as Schwartz (1997) three-factor model.

A forward contract in this context is an agreement established at a time $s < T$ to deliver or receive the renewable resource at time T for a price K, which is specified at

time s. In financial terms, the payoff at time of maturity T of such a forward contract is

$$H = P(T) - K. \tag{2.5}$$

The value K that lets this contract have a value zero under a no-arbitrage assumption is given by

$$F_P^{forw}(s,T) = \frac{1}{B(s,T)} \mathbb{E}_{\mathbb{Q}} \left(e^{-\int_s^T r(t)dt} \cdot P(T) | \mathcal{F}_s \right), \tag{2.6}$$

where $B(s,T) = \mathbb{E}_{\mathbb{Q}} \left(e^{-\int_s^T r(t)dt} \right)$ denotes the prize of a zero coupon bond maturing at time T at current time s. This is called the forward price at time s. The symbol $\mathcal{F}_s$ denotes the information available at time s and we denote in the following with $\mathbb{F} = (\mathcal{F}_s)$ the associated filtration which represents the information flow.[1]

The expectation in (2.6) is taken with respect to the pricing measure $\mathbb{Q}$, which takes into account a market price of convenience yield risk λ, i.e.

$$\begin{aligned} dP(t) &= (r - \delta(t))P(t)dt + \sigma_1 P(t) d\tilde{Z}_1(t) && (2.7) \\ d\delta(t) &= (\kappa(\alpha - \delta(t)) - \lambda)dt + \sigma_2 d\tilde{Z}_2(t) && (2.8) \\ dr(t) &= a(m^* - r(t))dt + \sigma_3 d\tilde{Z}_3(t) && (2.9) \end{aligned}$$

with

$$d\tilde{Z}_1(t)d\tilde{Z}_2(t) = \rho_1 dt, d\tilde{Z}_2(t)d\tilde{Z}_3(t) = \rho_2 dt, d\tilde{Z}_1(t)d\tilde{Z}_3(t) = \rho_3 dt. \tag{2.10}$$

Here m^* denotes the risk adjusted long-term mean interest rate.

A futures contract is basically a type of forward contract which is centrally cleared on a daily basis. The clearing exchange then usually requires the agent to set up a margin account, the amount held reflecting price movements in the market, protecting buyer and seller from possible default of the other party. The mechanism of the margin account affects the price as determined above and in fact the futures price is then

[1] More precisely, $\mathbb{F} = (\mathcal{F}_s)$ denotes the augmented and completed filtration generated by the Brownian motions $Z_1(s)$, $Z_2(s)$ and $Z_3(s)$.

provided via

$$F_P^{fut}(s,T) = \mathbb{E}_{\mathbb{Q}}\left(P(T)|\mathcal{F}_s\right). \tag{2.11}$$

It is a direct consequence from equations (2.6) and (2.11), that if the interest rate process $r(t)$ and the commodity price $P(t)$ are uncorrelated, the forward and futures prices coincide. This is in particular the case, if the interest rate is assumed to be deterministic, which is the case in the Schwartz (1997) two-factor model. While until 19/07/2007 contracts traded at Fish Pool had been exclusively bilateral and of forward type, the majority of contracts traded after that date had been cleared, and in fact close to 100% of contracts are nowadays cleared daily via Fish Pool's link with NASDAQ, hence are of futures type. This will be reflected in our empirical analysis. To simplify the notation, we write $F_P(s,T) = F_P^{fut}(s,T)$.

Let us assume initially that the interest rate is constant and equal to r, corresponding to the case $a = \sigma_3 = 0$. As indicated above, in this case, forward prices and futures prices coincide, and we do not need to distinguish these any further. In fact we use the notion forwards and futures as synonymous here. We can always assume that current time is normalized to 0 and that the time of maturity T is relative to this, hence the same as time-to-maturity. Since our model is Markovian, we can then denote the futures price in (2.11) as $F(P,\delta,T)$ depending on current spot price, level of convenience yield and time-to-maturity T. With this notation, Schwartz (1997) refers to Jamshidian and Fein (1990) and Bjerksund (1991) for an explicit expression for (2.11)

$$F(P,\delta,T) = P\cdot\exp\left(A(T)+\delta\cdot B(T)\right) \tag{2.12}$$

with

$$\begin{aligned} A(T) &= \left(r-\alpha+\frac{\lambda}{\kappa}+\frac{1}{2}\frac{\sigma_2^2}{\kappa^2}-\frac{\sigma_1\sigma_2\rho}{\kappa}\right)T+\frac{1}{4}\sigma_2^2\left(\frac{1-e^{-2\kappa T}}{\kappa^3}\right) \\ &\quad +\left(\alpha\kappa-\lambda+\sigma_1\sigma_2\rho-\frac{\sigma_2^2}{\kappa}\right)\left(\frac{1-e^{-\kappa T}}{\kappa^2}\right) \qquad (2.13) \\ B(T) &= -\frac{1-e^{-\kappa T}}{\kappa}. \qquad (2.14) \end{aligned}$$

Note, that the futures price (2.12) has a log-normal distribution, which makes the analytical pricing of options in this framework possible. On the other hand note that at least one of the state variables, the convenience yield $\delta(t)$ is unobservable. In fact Schwartz (1997) assumes that both the commodity price $P(t)$ and the convenience yield $\delta(t)$ are unobservable, and only the future prices (2.12) are observable. In order to estimate the model, Schwartz (1997) then applies Kalman filter techniques.

The case of stochastic interest rates is slightly more involved, but more of notational means rather than mathematical complexity, as the futures prices remain log-normal. The futures price in the Schwartz (1997) three-factor model is given as

$$F(P,\delta,r,T) = P \cdot \exp\left(-\delta \cdot \left(\frac{1-e^{-\kappa T}}{\kappa}\right) + r \cdot \left(\frac{1-e^{-aT}}{a}\right) + C(T)\right) \tag{2.15}$$

with

$$\begin{aligned} C(T) \quad = \quad & \frac{(\kappa(\alpha - \frac{\lambda}{\kappa}) + \sigma_1\sigma_2\rho_1)(1-e^{-\kappa T} - \kappa T)}{\kappa^2} \\ & - \frac{\sigma_2^2(4(1-e^{-\kappa T}) - (1-e^{-2\kappa T}) - 2\kappa T)}{4\kappa^3} \\ & - \frac{(am^* + \sigma_1\sigma_3\rho_3)(1-e^{-aT} - aT)}{a^2} \\ & - \frac{\sigma_3^2(4(1-e^{-aT}) - (1-e^{-2aT}) - 2aT)}{4a^3} \\ & + \sigma_2\sigma_3\rho_2\left(\frac{(1-e^{-\kappa T}) + (1-e^{-aT}) - (1-e^{-(\kappa+a)T})}{\kappa a(\kappa+a)}\right) \\ & + \left(\frac{\kappa^2(1-e^{-aT}) + a^2(1-e^{-\kappa T}) - \kappa a^2 T - a\kappa^2 T}{\kappa^2 a^2(\kappa+a)}\right). \end{aligned} \tag{2.16}$$

The empirical analysis in section 4 predominantly focuses on the application of the two factor model. The function of the three factor model in the context of this paper lies mainly in assessing how robust the results from the two factor model are in light of stochastically fluctuating interest rates, in particular when longer term contracts are used in the analysis.

2.3 Farmed Salmon Production

Aggregate salmon supply and demand in the context of market interactions on a global level has been discussed in Asche, Bremnes, and Wessells (1999) and Asche, Bjørndal, and Young (2001), but from a mostly exogenous and empirical point of view. We attempt to provide a micro founded model of aggregate salmon supply and demand.

Let us look at the farmed salmon production. We follow a more or less classical approach, which is outlined in Cacho (1997) for example, and presents a consensus of many models that are available in the literature. The total number of salmon in all pens contributing to the salmon production process is denoted with $n(t)$. We assume that mortality $m(t)$ follows an adapted stochastic process on $(\Omega, \mathbb{P}, \mathbb{F})$, and therefore at any time before harvesting

$$dn(t) = -m(t) \cdot n(t)dt. \tag{2.17}$$

Note that salmon does not reproduce in the pens, and therefore the number of salmon in each pen has to decrease over time. However, salmon gain in weight and it is assumed that the average weight of one fish is assumed to follow the dynamic

$$dw(t) = (\Theta - \beta(t))\, w(t)dt + \sigma_w w(t)dB(t), \tag{2.18}$$

where $B(t)$ represents a standard Brownian motion on $(\Omega, \mathbb{P}, \mathbb{F})$ and $\beta(t)$ an arbitrary adapted stochastic process, such that the dynamics (2.18) is well defined. In fact $\beta(t)$ represents the weight saturation, and should be positively correlated with $w(t)$, introducing a mean reversion feature in the weight dynamics towards the mean reversion level Θ, which is assumed to be constant. We denote with

$$X(t) = n(t)w(t) \tag{2.19}$$

the total biomass at time t. The dynamics of $X(t)$ in the absence of harvesting can be

easily derived and follows

$$dX(t) = (\Theta - m(t) - \beta(t))\, X(t)dt + \sigma_w X(t)dB(t). \tag{2.20}$$

An individual salmon farmer would now try to optimize the time of harvest, so as to achieve an optimal profit. The classical aquaculture literature around Bjørndal (1988), Cacho (1997), Yu and Leung (2006), Guttormsen (2008), Heaps (1995) and Arnason (1992) focuses on this and adopts the methodology of optimal stopping and control. In the present context however, it is the aggregate farmed salmon production that matters. Assuming that salmon farmers are heterogeneous and that because of limited market demand it cannot be optimal for all salmon farmers to harvest at the same time, no unique harvesting time can be identified.[2] We assume that at each instant of time t a proportion $\nu(t)$ of salmon farmers will harvest. Assuming that salmon farmers own equally sized portions of the total biomass, the biomass will then evolve according to the equation

$$dX(t) = (\Theta - (m(t) + \nu(t)) - \beta(t))\, X(t)dt + \sigma_w X(t)dB(t). \tag{2.21}$$

which is of the same type as (2.20).[3] The salmon supply in each infinitesimal time interval dt will then be $\nu(t)X(t)dt$.

Let us now look at the consumer side. We assume that a representative consumer chooses between farmed salmon and an alternative consumption good, and that the utility from consumption is of Cobb-Douglas type. The consumer's problem is at each time t to maximize utility

$$\max \quad \left(x(t)^{\alpha(t)} y(t)^{1-\alpha(t)}\right) \tag{2.22}$$

$$\text{subject to:} \quad P(t) \cdot x(t) + y(t) = c(t), \tag{2.23}$$

[2]The oligopolistic aquaculture harvesting problem does not seem to have been discussed in the literature.

[3]Note that while individual farmers still do complete harvests rather than continuously harvesting a proportion of the biomass, in aggregation the affect is like continuous harvesting. Even for a single salmon farming unit consisting of multiple pens, it would be unwise to harvest all pens at once.

where $x(t)$ denotes the amount of farmed salmon and $y(t)$ the amount of the alternative consumption good consumed. The total budget of the consumer is limited to $c(t)$ and can vary stochastically over time, while $P(t)$ denotes the price of farmed salmon and the price of the alternative consumption good is normalized to one. The preference parameter $\alpha(t)$ is also assumed to be stochastic at this point, taking into account changes in the consumer preferences, which are known to effect the price of salmon significantly.

The solution of the consumer problem is then given by

$$x(t) = \frac{\alpha(t)c(t)}{P(t)}. \tag{2.24}$$

In equilibrium we must have $x(t) = \nu(t)X(t)$ and hence we obtain the inverse demand function

$$P(t) = \frac{\epsilon(t)}{X(t)}, \tag{2.25}$$

where

$$\epsilon(t) = \frac{\alpha(t)c(t)}{\nu(t)}. \tag{2.26}$$

This price functional will be used in the following, and interpreted as the Fish Pool Index, which in turn corresponds to the salmon spot price.[4] Without further specifying the functional forms of $\alpha(t)$,$c(t)$ and $\nu(t)$ it is however impossible to obtain any explicit pricing formulas. However, rather than looking at each factor individually, we assume that the various effects of $\alpha(t)$,$c(t)$ and $\nu(t)$ aggregate to

$$d\epsilon(t) = \epsilon(t)\left(\gamma(t)dt + \eta dW(t)\right) \tag{2.27}$$

where $W(t)$ is a second Brownian motion, which is correlated with $B(t)$ according to the relationship

$$dB(t)dW(t) = \rho_D dt, \tag{2.28}$$

[4]The Fish Pool price index is based on a weighted weekly average of salmon categories 3-4 kg: 30 %, 4-5 kg: 40 %, 5-6 kg: 30 %, superior quality, head-on gutted. Further details are available on $http://fishpool.asp.manamind.com/?page\_id = 65$.

and $\gamma(t)$ is as yet unspecified.[5] A simple application of the Ito-formula yields

$$\begin{aligned} dP(t) &= P(t)\left(m(t)+\nu(t)+\sigma_w^2-\eta\sigma_w\rho_D+(\beta(t)+\gamma(t))-\Theta\right)dt \\ &\quad +P(t)\left(\eta dW(t)-\sigma_w dB(t)\right). \end{aligned} \tag{2.29}$$

Noticing that $var\left(\eta dW(t)-\sigma_w dB(t)\right)=\left(\eta^2+\sigma_w^2-2\eta\sigma_w\rho_D\right)dt$, this can be rewritten as

$$\begin{aligned} dP(t) &= P(t)\left(\sigma_w^2-\eta\sigma_w\rho_D-\Theta-\delta(t)\right)dt \\ &\quad +P(t)\sqrt{(\eta^2+\sigma_w^2-2\eta\sigma_w\rho_D)}dZ_1(t), \end{aligned} \tag{2.30}$$

where $Z_1(t)$ is a standard Brownian motion and

$$\delta(t)=-\left(m(t)+\nu(t)+\beta(t)+\gamma(t)\right). \tag{2.31}$$

Now, taking into account that $\delta(t)$ is an aggregation of four seemingly unrelated processes of which at least some feature mean-reversion, we are led to assume that $\delta(t)$, at least in approximation, follows an Ornstein-Uhlenbeck process, as described in (2.2). As for the dynamics of $P(t)$, we see that it exactly matches the dynamics (2.1), with the following choice of parameters

$$\mu = \sigma_w^2-\eta\sigma_w\rho_D-\Theta \tag{2.32}$$

$$\sigma_1 = \eta^2+\sigma_w^2-2\eta\sigma_w\rho_D. \tag{2.33}$$

With this parametrization it is worthwhile to keep in mind, what generates the uncertainty here: σ_W takes account of volatility generated by the fluctuations in weights of individual fish, due to sources such as nutrition, weather and disease, while η takes account of volatility generated by fluctuations in consumer income and preferences. At most times, it will be the case that $\sigma_W<\eta$.

[5] As $\gamma(t)$ at this point can be an arbitrary stochastic process, the only assumption made here is that the volatility of $\epsilon(t)$ is proportional to its level, which is a simplifying but intuitive assumption.

Table 2.1. Sub Data Sets

	Time Period	Interest Rate	Observations	Description
$Data_1$	12/06/2006-1/11/2006	2.88%	103	Medium interest regime
$Data_2$	2/11/2006-17/12/2008	4.00%	545	High interest regime
$Data_3$	18/12/2008-22/03/2012	1.93%	849	Low interest regime

Note: The whole sample period is divided into three different regimes according to the level of Norwegian interest rates.

2.4 Empirical Estimates

The data used to test the model developed so far consist of daily observations of futures prices in Fish Pool ASA from 12/06/2006 to 22/03/2012. For the whole sample period, complete data on the first 29 futures contracts sorted by different maturities are available. We use a similar notation as in Schwartz (1997) and denote with F1 the contract closest to maturity (with average maturity of 0.041 year) counting up to F29 which represents the contract farthest to maturity (with average maturity of 2.427 years). We further divide the whole sample period into three different regimes according to the level of Norwegian interest rates as shown in Table 2.1 leading to sub-samples $Data_1$, $Data_2$ and $Data_3$.[6] These have been chosen in order to take account of interest rate movements due to the financial crisis. Under each regime, contracts in Panel A, Panel B and Panel C are chosen as proxies for short-term, medium-term and long-term futures contracts respectively. In each test, five contracts (i.e., N=5) are used for the estimation. More precisely, Panel A contains F1, F3, F5, F7 and F9; Panel B contains F12, F14, F16, F18, F20 and Panel C contains F24, F25, F26, F28 and F29. A summary statistics on the contracts being used can be found in Tables A.1-A.3 in Appendix A. In this paper we use an approach based on Kalman filter in order to estimate the parameters in the model. To place our empirical results better into context we also include a comparison involving live-cattle data.

[6]Average interest rate r over the whole sample time period is 2.13%.

2.4.1 Empirical Models

In our model, both the commodity price (P) and the convenience yield (δ) are assumed to be unobservable, and only the futures price (F) can be observed.[7] Once the model has been cast in the state space form, model parameters can be estimated by the Kalman filter. Let $\mathbf{y}_t$ denote a $(n \times 1)$ vector of futures prices observed at time t and $\mathbf{\Phi}_t$ denote a (2×1) vector of state variables, i.e., the log spot price (X) and the convenience yield (δ). The state space representation can be written as

$$\mathbf{y}_t = \mathbf{d}_t + Z_t \mathbf{\Phi}_t + \boldsymbol{\epsilon}_t \tag{2.34}$$

$$\mathbf{\Phi}_{t+1} = \mathbf{c}_t + Q_t \mathbf{\Phi}_t + \boldsymbol{\eta}_t, \tag{2.35}$$

Unlike Schwartz (1997) uses linear approximations for estimation, we follow Erb, Lüthi, and Otziger (2014) here. For the two-factor model, (2.34) is the measurement equation with components

$$\mathbf{y}_t = \begin{pmatrix} \ln F(T_1) \\ \vdots \\ \ln F(T_n) \end{pmatrix}, \qquad \mathbf{d}_t = \begin{pmatrix} A(T_1) \\ \vdots \\ A(T_n) \end{pmatrix}, \qquad \mathbf{Z}_t = \begin{pmatrix} 1 & B(T_1) \\ \vdots & \vdots \\ 1 & B(T_n) \end{pmatrix} \tag{2.36}$$

and $\boldsymbol{\epsilon}_t$ is a $(n \times 1)$ vector of serially uncorrelated disturbance with

$$\mathrm{E}(\boldsymbol{\epsilon}_t) = 0, \qquad \mathrm{Var}(\boldsymbol{\epsilon}_t) = H \tag{2.37}$$

(2.35) is the transition equation with components

$$\mathbf{\Phi}_t = \begin{pmatrix} X(t) \\ \delta(t) \end{pmatrix} \tag{2.38}$$

$$\mathbf{c}_t = \begin{pmatrix} \left(\mu - \frac{1}{2}\sigma_1^2 - \alpha\right)\Delta t + \frac{\alpha}{\kappa}\left(1 - e^{-\kappa \Delta t}\right) \\ \alpha\left(1 - e^{-\kappa \Delta t}\right) \end{pmatrix} \tag{2.39}$$

$$\mathbf{Q}_t = \begin{pmatrix} 1 & \frac{1}{\kappa}\left(e^{-\kappa \Delta t} - 1\right) \\ 0 & e^{-\kappa \Delta t} \end{pmatrix} \tag{2.40}$$

[7] As indicated by Schwartz (1997), one major difficulty in the implementation of commodity price models arises from the indirectly observable state variables. In most cases, the spot price is quite uncertain and the instantaneous convenience yield is hardly estimated, but the futures contracts traded on exchanges are more attainable.

and $\boldsymbol{\eta}_t$ is serially uncorrelated disturbance with

$$\mathrm{E}(\boldsymbol{\eta}_t) = 0, \qquad \mathrm{Var}(\boldsymbol{\eta}_t) = \begin{pmatrix} \sigma_X^2(\Delta t) & \sigma_{X\delta}(\Delta t) \\ \sigma_{X\delta}(\Delta t) & \sigma_\delta^2(\Delta t) \end{pmatrix} \tag{2.41}$$

where

$$\sigma_X^2 = \frac{\sigma_2^2}{\kappa^2}\left\{\frac{1}{2\kappa}\left(1-e^{-2\kappa t}\right) - \frac{2}{\kappa}\left(1-e^{-\kappa t}\right) + t\right\} + 2\frac{\sigma_1\sigma_2\rho}{\kappa}\left(\frac{1-e^{-\kappa t}}{\kappa} - t\right) + \sigma_1^2 t \tag{2.42}$$

$$\sigma_\delta^2 = \frac{\sigma_2^2}{2\kappa}\left(1-e^{-2\kappa t}\right) \tag{2.43}$$

$$\sigma_{X\delta} = \frac{1}{\kappa}\left[\left(\sigma_1\sigma_2\rho - \frac{\sigma_2^2}{\kappa}\right)\left(1-e^{-\kappa t}\right) + \frac{\sigma_2^2}{2\kappa}\left(1-e^{-2\kappa t}\right)\right] \tag{2.44}$$

Note, $\Delta t = t_{k+1} - t_k$ represents the time interval and T_i denotes the given and fixed maturity of the i-th closest-to-maturity futures contract. The functions $F(\cdot)$, $A(\cdot)$ and $B(\cdot)$ are defined in (2.12), (2.13) and (2.14) respectively.

2.4.2 Data

As shown in Table 2.1, $Data_1$ ranges from 12/06/2006 to 1/11/2006 with average interest rate of 2.88%; $Data_2$ ranges from 2/11/2006 to 17/12/2008 with average interest rate of 4.00%; $Data_3$ ranges from 18/12/2008 to 22/03/2012 with average interest rate of 1.93%. Contracts used for tests in each data set are described in Tables A.1-A.3 respectively. Naturally, for each contract with a fixed maturity, the time-to-maturity changes as time progresses. Figure A.1 shows the time-to-maturity pattern for each contract used in Panel A of $Data_3$, which fluctuates but remains within a narrow range during the sample period. This pattern of time-to-maturity is representative of all the data used in this study.

2.4.3 Empirical Results for $Data_1$, 12/06/2006-1/11/2006

Table 2.2 shows the results for the estimation of the two-factor model based on $Data_1$. It can be observed that the correlation coefficient $\rho = \rho_1$ is large;[8] the speed of mean-reversion of the convenience yield κ, the expected return on the spot commodity μ,

[8]In the context of the two-factor model, where there is only one relevant correlation, we omit sub-indices and denote $\rho = \rho_1$.

Table 2.2. Estimation Results for $Data_1$, 12/06/2006-1/11/2006

Parameter	Panel A F1, F3, F5, F7, F9 (Short Term)	Panel B F12, F14, F16, F18, F20 (Medium Term)	Panel C F24, F25, F26, F28, F29 (Long Term)
μ	0.299 (0.446)	0.567 (0.567)	0.832 (0.345)**
κ	2.348 (0.203)***	1.009 (0.373)***	1.035 (0.277)***
α	0.084 (1.106)	1.311 (0.976)	1.484 (0.562)***
σ_1	0.236 (0.027)***	0.135 (0.031)***	0.128 (0.014)***
σ_2	1.444 (0.136)***	0.185 (0.095)**	0.162 (0.047)***
ρ	0.624 (0.103)***	0.866 (0.050)***	0.847 (0.030)***
λ	0.097 (2.615)	1.240 (1.364)	1.507 (0.809)*
Log-Likelihood	-1238	-1914.3	-2600.5

Note: Standard errors in parentheses. [***] Significant at 1% level; [**] Significant at 5% level; [*] Significant at 10% level. μ is the expected return on the spot commodity; κ is the speed of mean-reversion of the convenience yield; α is the mean level of the convenience yield; σ_1 is the volatility of the spot price; σ_2 is the volatility of the convenience yield; ρ is the correlation coefficient of spot price and convenience yield; λ is the market price of the convenience yield risk.

the mean-level of convenience yield α and the market price of convenience yield risk λ are all positive and reasonable. For Panel A and B however, the parameters μ, α and λ are not significant. This changes for panel C, where all coefficients are significant, most at the 1% level. Besides, it is also worth to note that the expected return on the spot commodity μ increases while the speed of mean-reversion κ decreases as the term of contracts increases. The Kalman filter based estimation is an iterative procedure. Figures A.2 in Appendix B shows the parameter evolution for $Data_1$ exemplary. The convergence is good in all cases.

Figure 2.1 shows the filtered state variables, i.e. the spot price and the instantaneous convenience yield along with a number of selected futures prices for Panel A.[9] Prices of futures contracts contained in Panel A are also included in the figure. The figure seems to indicate strong correlation between state variables as well as a strong relationship between futures prices and spot price. As one would expect the ability of futures contracts to proxy spot prices becomes weaker when maturity increases. The futures prices determined by the model are at most times within 2% of the market prices, which presents a good fit. Figures 2.2 represents the term structure, where the left part shows the actual term structures and the right part shows the model generated

[9]The figures for Panel B and C look similar, but are included in Appendix B.

term structures. To have a better view of curves in Figure 2.2, we further show the term structure on a randomly picked day as an example in Figure 2.3. In general, the model makes a good prediction for the short-term panel but finds it more difficult to capture the shapes of longer-term panels, where the actual term structure appears to be rather unconventional, see figures A.4 and A.6 in Appendix B.[10]

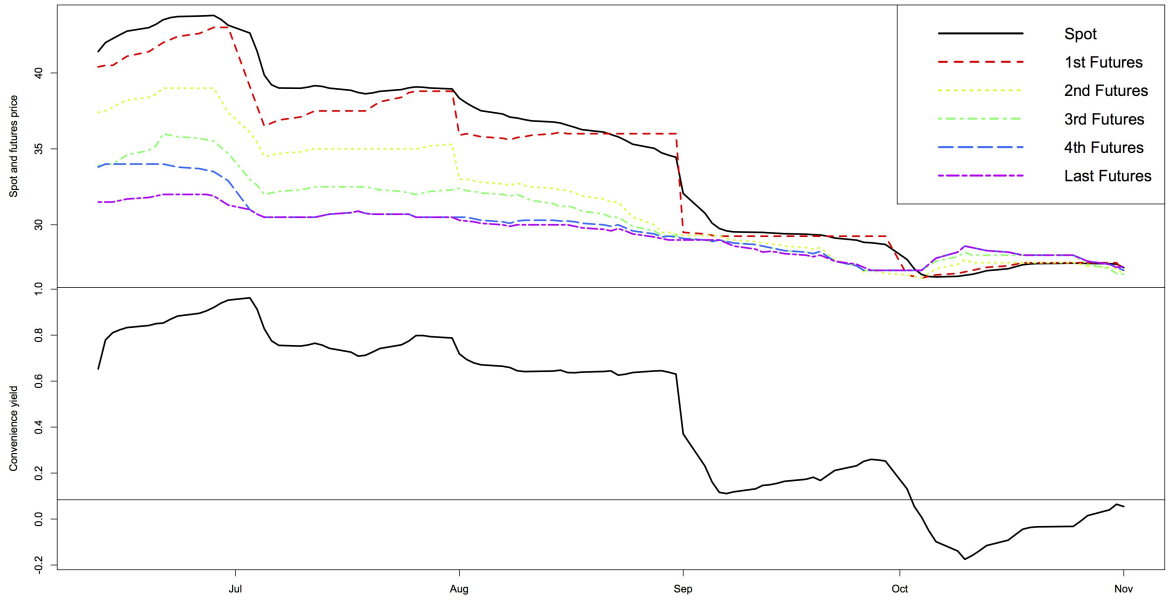

Figure 2.1. State variables for Panel A in $Data_1$, 12/06/2006-1/11/2006

Note: Spot and futures prices are on the top of convenience yield; F1, F3, F5, F7 and F9 correspond to the 1st Futures, 2nd Futures, 3rd Futures, 4th Futures and Last Futures in the figure.

2.4.4 Empirical Results for $Data_2$, 2/11/2006-17/12/2008

Table 2.3 shows the results for the two-factor model obtained from $Data_2$. Similar as before the correlation coefficient ρ is large; the expected return on the spot commodity μ, the mean-reversion level of the convenience yield α and the market price of convenience yield risk λ are all positive and reasonable. However, the speed of mean-reversion of the convenience yield κ for Panel A is significantly larger than before, and volatilities σ_1 and σ_2 are significantly lower. For Panel A, the parameters μ, α and λ are not significant. This changes for panel B and C though, where all coefficients are highly significant at the 1% level. Furthermore, it is worth mentioning that the expected return on the spot commodity μ increases while the speed of mean-reversion

[10]The slightly odd looking actual term structure for longer dated salmon future contracts is likely to be caused by the rather low trading volume of these contracts.

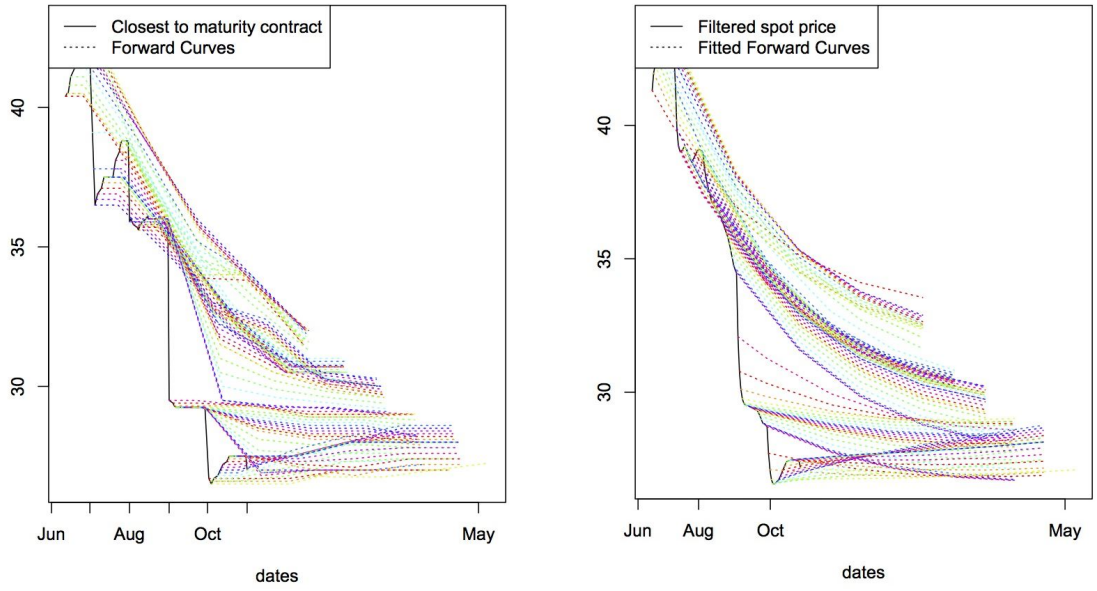

Figure 2.2. Term structures for Panel A in $Data_1$: actual forward curves on the left; model generated forward curves on the right

Note: Each colored curve is a static picture of futures prices (y-axis) against contract maturities (x-axis), which is analogous to a plot of the term structure of interest rates. On the left side of the figure, the solid line represents the price of the closest-to-maturity futures contract, i.e., $F1$ in this case; while the dashed line consists of the actual prices of other futures contracts with different maturities in this panel. On the right side of the figure, the solid line is the filtered spot price obtained through the estimation procedure; while the dashed line consists of the estimated futures prices given by the pricing formula.

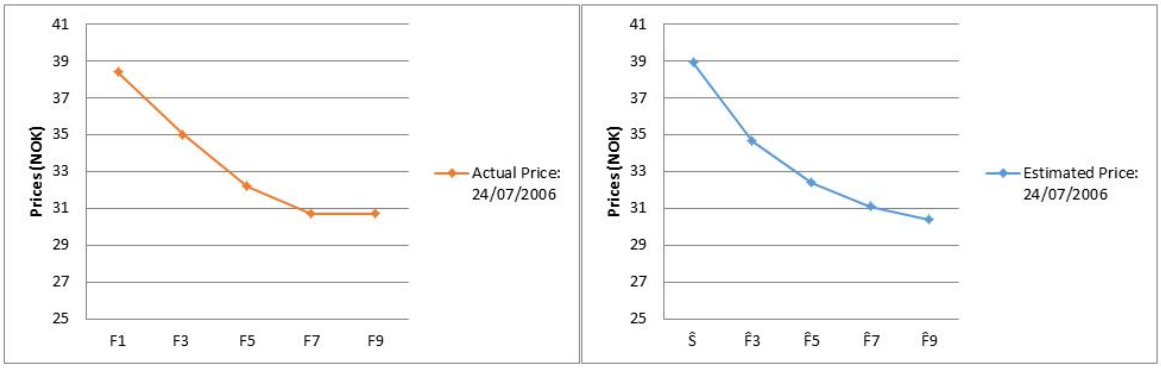

Figure 2.3. Term structure on 24/07/2006: actual forward curve on the left; model generated forward curve on the right

Note: This figure shows the term structure on a specific day. Each line corresponds to one colored line in Figure 2.2 on the same side. The observed term structure of salmon prices is on the left; while the estimated term structure is on the right. F1 - F9 denote the actual futures prices with different maturities on 24/07/2006. $\hat{S}$ is the filtered spot price on that day and $\hat{F}3$ - $\hat{F}9$ represent the estimated futures prices.

Table 2.3. Estimation Results for $Data_2$, 2/11/2006-17/12/2008

Parameter	Panel A F1, F3, F5, F7, F9 (Short Term)	Panel B F12, F14, F16, F18, F20 (Medium Term)	Panel C F24, F25, F26, F28, F29 (Long Term)
μ	0.214 (0.160)	0.747 (0.177)***	0.854 (0.122)***
κ	5.776 (0.616)***	1.387 (0.155)***	0.660 (0.018)***
α	0.216 (0.257)	0.951 (0.216)***	1.356 (0.069)***
σ_1	0.109 (0.006)***	0.141 (0.003)***	0.159 (0.023)***
σ_2	0.651 (0.059)***	0.223 (0.018)***	0.142 (0.022)***
ρ	0.580 (0.108)***	0.811 (0.021)***	0.895 (0.038)***
λ	0.818 (1.402)	1.290 (0.427)***	0.865 (0.098)***
Log-Likelihood	-8279.7	-9822.6	-12745

Note: Standard errors in parentheses. [***] Significant at 1% level; [**] Significant at 5% level; [*] Significant at 10% level. μ is the expected return on the spot commodity; κ is the speed of mean-reversion of the convenience yield; α is the mean level of the convenience yield; σ_1 is the volatility of the spot price; σ_2 is the volatility of the convenience yield; ρ is the correlation coefficient of spot price and convenience yield; λ is the market price of the convenience yield risk.

κ decreases as the terms of contracts increase. For all cases, the convergence of the Kalman filter is very good.

Figures 2.4 shows the filtered state variables for Panel A, i.e. the spot price and the instantaneous convenience yield, along with selected futures prices.[11] As before, we observe strong correlation between state variables as well as a close relationship between futures price and spot price. The ability of futures contracts to proxy spot prices becomes weaker when maturity extends. Again, the model presents a good fit, with model prices at most times being within 2% of market prices. Figure 2.5 presents the term structures for Panel A contracts, where once more the left part shows the real term structures while the right part shows the model generated term structures. Term structure on a randomly picked day is shown in Figure 2.6. In general, the model makes a good prediction for the short-term panel but again finds it difficult to capture the shapes of longer-term panels, which show the rather odd looking actual term structure already observed in the first case, compare figures A.8 and A.10 in Appendix B.

[11]The figures for Panel B and C look similar, but are included in Appendix B.

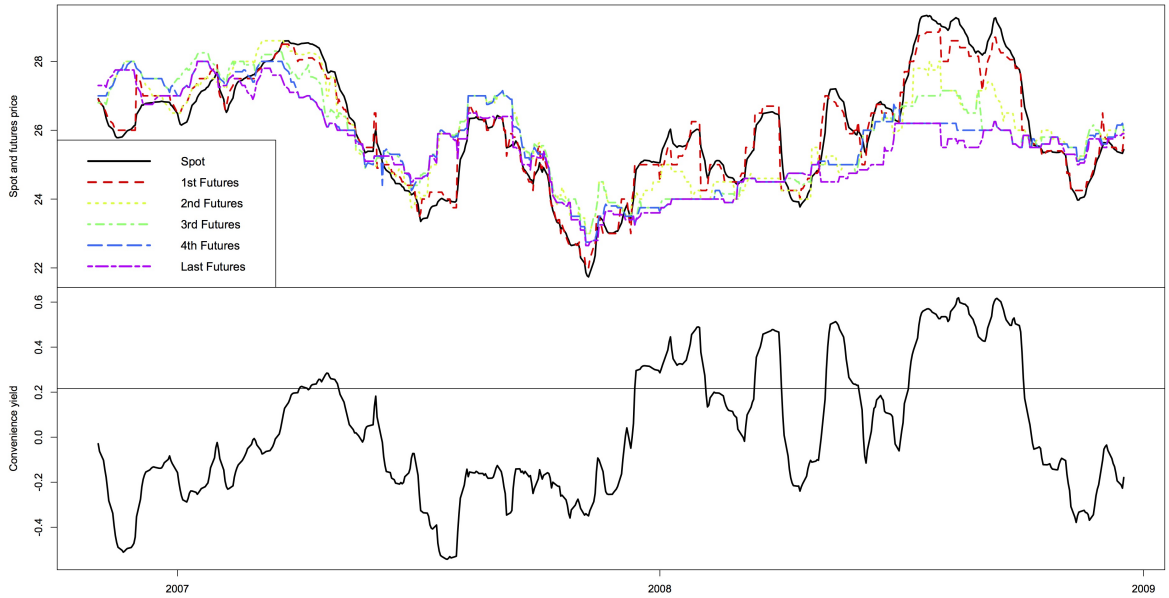

Figure 2.4. State variables for Panel A in $Data_2$, 2/11/2006-17/12/2008

Note: Spot and futures prices are on the top of convenience yield; F1, F3, F5, F7 and F9 correspond to the 1st Futures, 2nd Futures, 3rd Futures, 4th Futures and Last Futures in the figure.

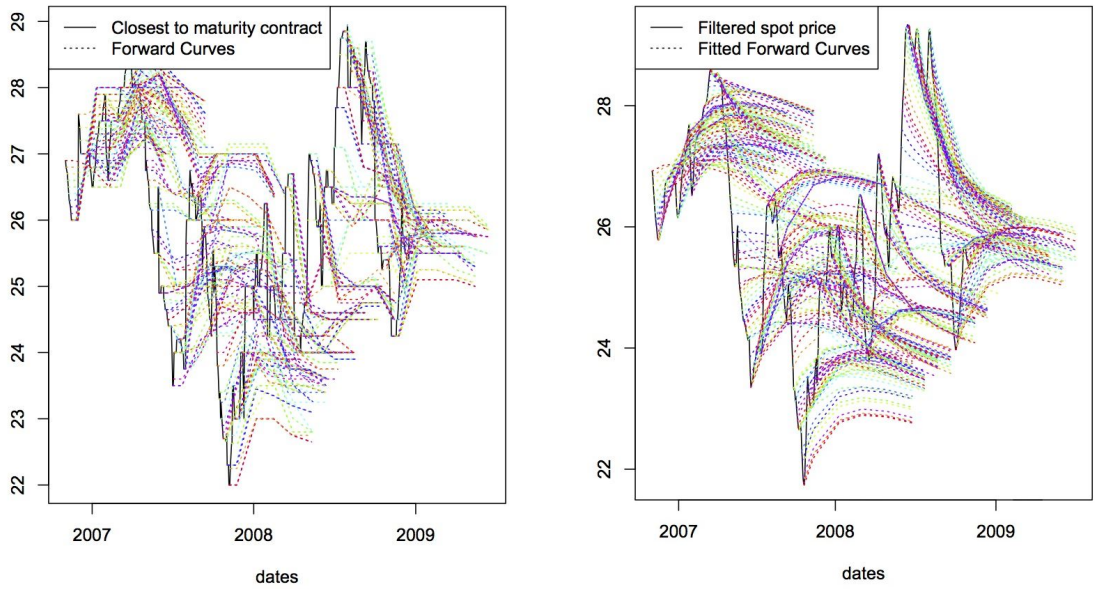

Figure 2.5. Term structures for Panel A in $Data_2$: actual forward curves on the left; model generated forward curves on the right

Note: Each colored curve is a static picture of futures prices (y-axis) against contract maturities (x-axis), which is analogous to a plot of the term structure of interest rates. On the left side of the figure, the solid line represents the price of the closest-to-maturity futures contract, i.e., $F1$ in this case; while the dashed line consists of the actual prices of other futures contracts with different maturities in this panel. On the right side of the figure, the solid line is the filtered spot price obtained through the estimation procedure; while the dashed line consists of the estimated futures prices given by the pricing formula.

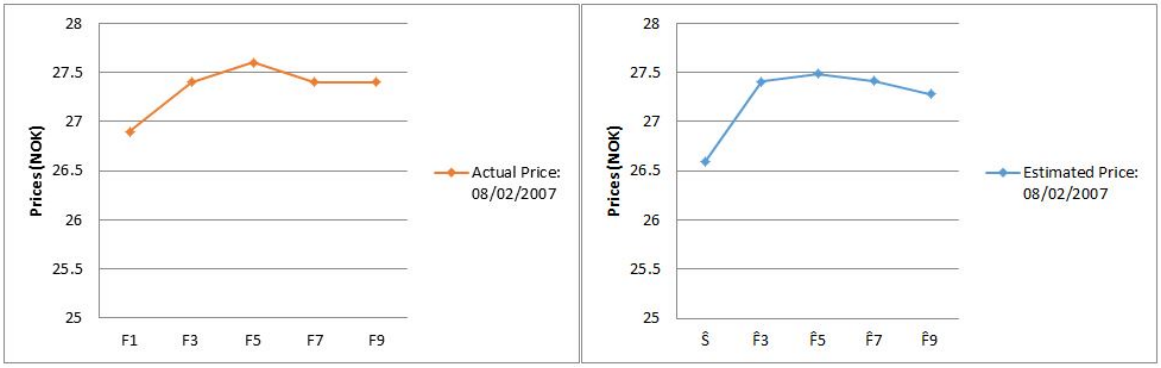

Figure 2.6. Term structure on 08/02/2007: actual forward curve on the left; model generated forward curve on the right

Note: This figure shows the term structure on a specific day. Each line corresponds to one colored line in Figure 2.5 on the same side. The observed term structure of salmon prices is on the left; while the estimated term structure is on the right. F1 - F9 denote the actual futures prices with different maturities on 08/02/2007. $\hat{S}$ is the filtered spot price on that day and $\hat{F}3$ - $\hat{F}9$ represent the estimated futures prices.

2.4.5 Empirical Results for $Data_3$, 18/12/2008-22/03/2012

Table 2.4 shows the results for the two-factor model obtained from $Data_3$. As in the other two cases, the correlation coefficient ρ is large; the expected return on the spot commodity μ, the mean-reversion level of convenience yield α and the market price of convenience yield risk λ are all positive and reasonable. The speed of mean-reversion of the convenience yield κ for Panel A is significantly larger than for the other two panels. However, α and λ are insignificant for Panel's A and B, and μ is insignificant for Panel B. As before, all parameters are significant at 1% level for Panel C. Further, it is worth to mention that the expected return on the spot commodity μ increases while the speed of mean-reversion κ decreases as the terms of the contracts increase. As in the previous cases, the convergence of the Kalman filter is very good.

Figure 2.7 shows the filtered state variables for Panel A, i.e. the spot price and the instantaneous convenience yield, along with selected futures prices.[12] As before, we observe strong correlation between the state variables as well as a close relationship between futures price and spot price, which however becomes weaker as maturities extends. Model prices are still within 2% of market prices at most times, however, in particular for panel A, fall out of the 2% range more frequently, than for $Data_1$ and

[12]The figures for Panel B and C look similar, but are included in Appendix B.

Table 2.4. Estimation Results of $Data_3$, 18/12/2008-22/03/2012

Parameter	Panel A F1, F3, F5, F7, F9 (Short Term)	Panel B F12, F14, F16, F18, F20 (Medium Term)	Panel C F24, F25, F26, F28, F29 (Long Term)
μ	0.255 (0.113)**	0.398 (0.323)	0.917 (0.167)***
κ	3.554 (0.191)***	0.347 (0.125)***	0.232 (0.032)***
α	0.181 (0.134)	1.000 (1.066)	1.821 (0.261)***
σ_1	0.182 (0.020)***	0.188 (0.040)***	0.189 (0.004)***
σ_2	0.698 (0.099)***	0.161 (0.020)***	0.104 (0.004)***
ρ	0.740 (0.156)***	0.905 (0.065)***	0.908 (0.007)***
λ	0.297 (0.476)	0.351 (0.251)	0.418 (0.101)***
Log-Likelihood	-9341.1	-11804	-12870

Note: Standard errors in parentheses. [***] Significant at 1% level; [**] Significant at 5% level; [*] Significant at 10% level. μ is the expected return on the spot commodity; κ is the speed of mean-reversion of the convenience yield; α is the mean level of the convenience yield; σ_1 is the volatility of the spot price; σ_2 is the volatility of the convenience yield; ρ is the correlation coefficient of spot price and convenience yield; λ is the market price of the convenience yield risk.

$Data_2$. Figure 2.8 and Figure 2.9 show the actual and model generated term structures as before. Similar as in the previous two cases the model makes a good prediction for the short-term panel but cannot capture the shapes of longer-term panels which as in the previous cases show odd looking actual term structures, most likely to be caused by the illiquidity of these contracts, compare Figure A.12 and Figure A.14 in Appendix B.

2.4.6 Three-Factor Model

Accounting for stochastic interest rates and their term structure is of particular importance for longer term contracts. The longest maturity contract included in our study has a 2 1/2 year time-to-maturity. Since we have formally linked the salmon production process to the Schwartz (1997) two-factor approach, it is also worth evaluating the performance of other models under this framework.[13] In both cases it makes sense to consider stochastic rates and to assess in how far this effects the results obtained in the previous sections. We therefore consider the full three factor model represented as in equations (2.1)-(2.3) under $\mathbb{P}$ and (2.7)-(2.9) under the pricing measure $\mathbb{Q}$. Once the three-factor model has been cast in state space form, the Kalman filter can be

[13]It is well known that the the two-factor and three-factor models clearly outperform the one-factor model. So we will not look into the one-factor model here.

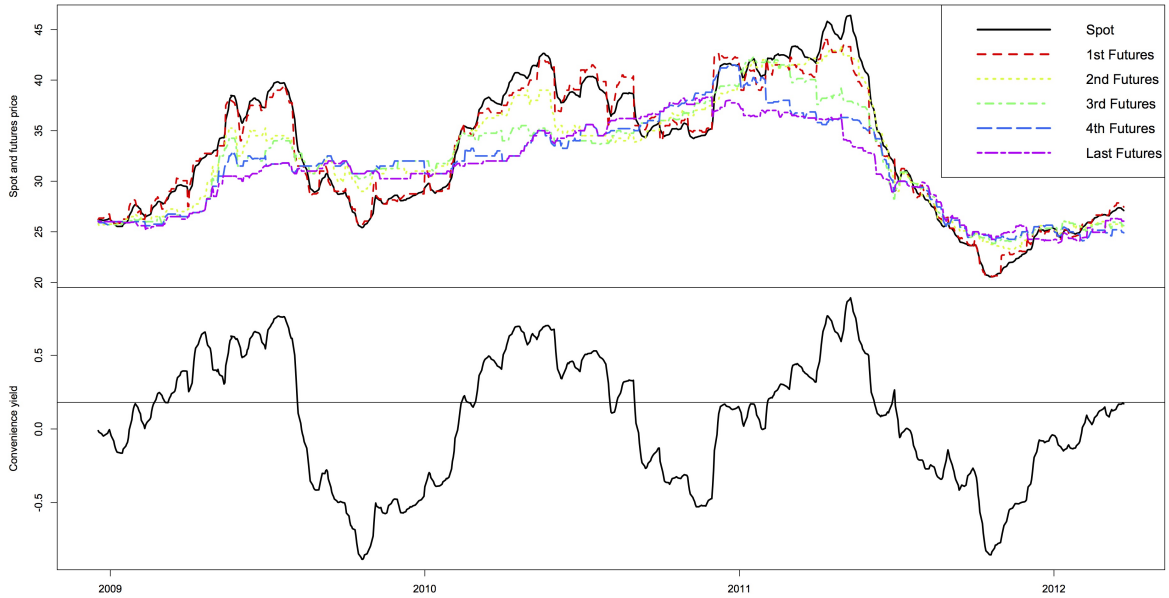

Figure 2.7. State variables for Panel A in $Data_3$, 18/12/2008-22/03/2012

Note: Spot and futures prices are on the top of convenience yield; F1, F3, F5, F7 and F9 correspond to the 1st Futures, 2nd Futures, 3rd Futures, 4th Futures and Last Futures in the figure.

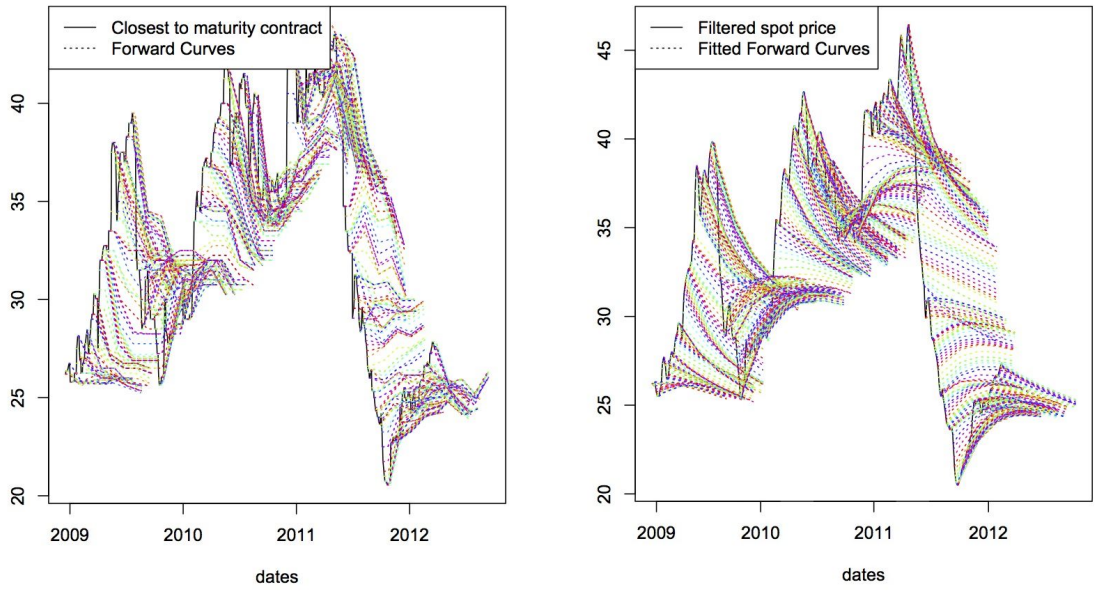

Figure 2.8. Term structures for Panel A in $Data_3$: actual forward curves on the left; model generated forward curves on the right

Note: Each colored curve is a static picture of futures prices (y-axis) against contract maturities (x-axis), which is analogous to a plot of the term structure of interest rates. On the left side of the figure, the solid line represents the price of the closest-to-maturity futures contract, i.e., $F1$ in this case; while the dashed line consists of the actual prices of other futures contracts with different maturities in this panel. On the right side of the figure, the solid line is the filtered spot price obtained through the estimation procedure; while the dashed line consists of the estimated futures prices given by the pricing formula.

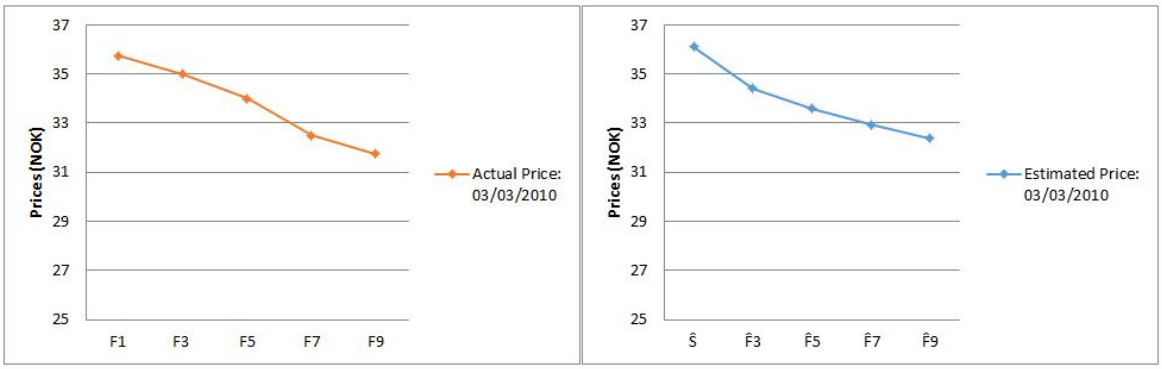

Figure 2.9. Term structure on 03/03/2010: actual forward curve on the left; model generated forward curve on the right

Note: This figure shows the term structure on a specific day. Each line corresponds to one colored line in Figure 2.8 on the same side. The observed term structure of salmon prices is on the left; while the estimated term structure is on the right. F1 - F9 denote the actual futures prices with different maturities on 03/03/2010. $\hat{S}$ is the filtered spot price on that day and $\hat{F}3$ - $\hat{F}9$ represent the estimated futures prices.

applied to estimate model parameters. Although ideally parameters in all three processes should be estimated simultaneously, here we will follow Schwartz (1997) by first estimating the interest rate process by fitting to the term structure of interests and then using the full three-factor model in order to determine the other two processes.

For the three-factor model, the transition equation is also (2.35) as in the two-factor model, since we estimate the same state variables. But the measurement equation is with components

$$\mathbf{y}_t = \begin{pmatrix} \ln F(T_1) \\ \vdots \\ \ln F(T_n) \end{pmatrix}, \qquad \mathbf{d}_t = \begin{pmatrix} \frac{r_t(1-e^{-aT_1})}{a} + C(T_1) \\ \vdots \\ \frac{r_t(1-e^{-aT_n})}{a} + C(T_n) \end{pmatrix}, \qquad \mathbf{Z}_t = \begin{pmatrix} 1 & B(T_1) \\ \vdots & \vdots \\ 1 & B(T_n) \end{pmatrix} \tag{2.45}$$

and $\boldsymbol{\epsilon}_t$ is a $(n \times 1)$ vector of serially uncorrelated disturbance with

$$\mathrm{E}(\boldsymbol{\epsilon}_t) = 0, \qquad \mathrm{Var}(\boldsymbol{\epsilon}_t) = H \tag{2.46}$$

Note, T_i denotes the given and fixed maturity of the i-th closest-to-maturity futures contract. The functions $F(\cdot)$, $B(\cdot)$ and $C(\cdot)$ are defined in (2.15), (2.14) and (2.16) respectively.

In this paper, Norwegian Treasury Bill yields are used to estimate the interest rate

process over the whole sample period. The Euler discretion of equation (2.9) can be expressed as

$$r(t_{n+1},\psi) \;=\; r(t_n,\psi) + a(m^* - r(t_n,\psi))\Delta t + \sigma_3 \Delta \tilde{Z}_3(t_n), \tag{2.47}$$

where ψ stands for Norwegian Treasury Bill with different maturities. We can estimate parameters by rewriting (2.47) and solving the equation below

$$(\hat{a},\hat{m}^*) = \arg\min_{a,m^*} \sum_{n=1}^{T-1} (r(t_{n+1},\psi) - r(t_n,\psi) - am^*\Delta t + ar(t_n,\psi)\Delta t)^2 \tag{2.48}$$

Once we have solved (2.48), $\hat{\sigma_3}$ can also be obtained by $\frac{\sigma_\epsilon}{\sqrt{\Delta t}}$, where σ_ϵ is the standard deviation of residuals. Since (2.9) is only capable of describing the short-term behavior, the 3-month, 6-month, 9-month and 12-month Norwegian Treasury Bills yields during the sample period are selected to estimate the interest rate process, accordingly only short-term futures contracts, i.e., Panel A consisting of F1, F3, F5, F7, and F9 in each data-set, are used to test the three-factor model. Moreover, ρ_2 and ρ_3 are approximated by the correlations between the 3-month Norwegian Treasury Bill yields and the filtered state variables, i.e. spot price and convenience yield, obtained from the corresponding two-factor model. The estimation results are displayed in Table 2.5.

As shown in Table 2.5, the estimated coefficients for the three-factor model are very close to those obtained from using the two-factor approach. However some of the estimates, which had been insignificant with the two-factor approach, now appear as significant. Specifically, the coefficients μ, α and λ for Panel A $Data_2$ now become highly significant at the 1% level, while being insignificant before, compare Table 2.3. Some problems however remain within the analysis of $Data_1$. Besides insignificant μ, α and λ, the absolute values of ρ_2 and ρ_3 in $Data1$ are close to 1, which suggests that the three factor model used might be inappropriate to deal with this particular data-set. Most likely, the fact that the data-set $Data_1$ contains much fewer data points than the other two is to blame for this. By and large, the three-factor approach confirms the results from the two-factor approach. In other words, the results obtained are rather robust under the two-factor and the three-factor models; the three-factor model

Table 2.5. Estimation Results of Three Factor Model: Panel A

Parameter	$Data_1$	$Data_2$	$Data_3$
μ	0.102 (0.466)	0.294 (0.109)***	0.647 (0.143)***
κ	2.520 (0.200)***	5.950 (0.209)***	3.429 (0.142)***
α	1.884 (1.181)	0.402 (0.121)***	0.681 (0.164)***
σ_1	0.280 (0.032)***	0.143 (0.008)***	0.228 (0.012)***
σ_2	1.792 (0.171)***	0.935 (0.069)***	0.878 (0.061)***
ρ	0.843 (0.038)***	0.857 (0.023)***	0.901 (0.016)***
λ	4.646 (2.95)	1.978 (0.748)***	2.046 (0.551)***
Log-Likelihood	-1241.7	-8357.7	-9381.7
a	0.543	0.543	0.543
m^*	0.027	0.027	0.027
ρ_2	-0.926	0.560	0.127
ρ_3	-0.961	0.031	0.277
σ_3	0.017	0.017	0.017

Note: Standard errors in parentheses. [***] Significant at 1% level; [**] Significant at 5% level; [*] Significant at 10% level. μ is the expected return on the spot commodity; κ is the speed of mean-reversion of the convenience yield; α is the mean level of the convenience yield; σ_1 is the volatility of the spot price; σ_2 is the volatility of the convenience yield; ρ is the correlation coefficient of spot price and convenience yield; λ is the market price of the convenience yield risk; a is the speed of mean-reversion of the interest rate; m^* is the mean level of the interest rate; ρ_2 is the correlation coefficient of convenience yield and interest rate; ρ_3 is the correlation coefficient of spot price and interest rate; σ_3 is the volatility of the interest rate.

only marginally outperforms the two-factor model, which is also confirmed by Schwartz (1997). Taking the complexity and the performance of models into consideration, it is sufficient to adopt the two-factor approach.

2.5 Comparison Between Cattle and Salmon

How do the salmon futures compare to futures traded on other related commodities? Live-cattle seems to reflect some of the properties of farmed salmon as a commodity and futures on live-cattle are traded in high volume on the Chicago Mercantile Exchange. Based on data availability for both the Fish Pool market and the live-cattle futures market, we have chosen 6 live-cattle contracts covering the period from 12/06/2006 to 07/09/2010. In analogy to our previous analysis, we divide the whole sample period into three different regimes as described in Table 2.1, but cut off at 07/09/2010. We continue to use Norwegian interest rates for the salmon contracts, but use the corresponding 3-month U.S treasury bill rates for each of the periods, i.e., 4.9%, 3.07% and 0.14%, for cattle contracts, which are traded in the US. Further, we select 6 salmon contracts F2, F5, F7, F10, F13 and F16 which have similar maturities as the live-cattle contracts. C1, C2, C3, C4, C5 and C6 are used to represent the live cattle contracts, whose statistic features are shown in Table A.4. The average maturity of these contracts is 0.126 years, 0.383 years, 0.554 years, 0.810 years, 1.065 years and 1.321 years respectively. The empirical results of our analysis are shown in Table 2.6. We observe that in general, there are no significant differences between the expected returns on the spot commodity μ of salmon and cattle contracts. More interesting perhaps is that salmon contracts show significantly higher mean-reversion speeds κ and mean-reversion level of the convenience yield α as compared to cattle contracts.[14] In addition, the market price of convenience yield risk in the case of salmon is notably higher, at least for the time periods corresponding to $Data_2$ and $Data_3$.

As before Convergence of the Kalman filter is very good in all cases. Figures 2.10 and 2.11 show the filtered state variables, i.e. the spot price and the instantaneous convenience yield, along with selected futures prices. The model fit is about the same, slightly better for salmon than for live-cattle where the relative error remains within 3% for most times. Figures 2.12 and 2.14 plot the term structures for both cattle and salmon.

[14]Note that for $Data_1$ the α's for both cattle and salmon are insignificant.

(a) $Data_1$

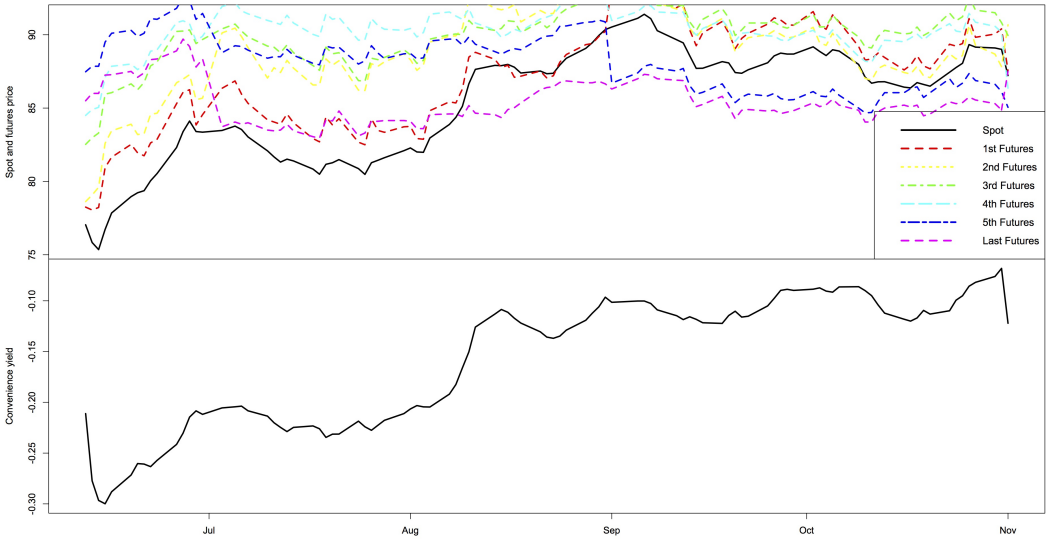

(b) $Data_2$

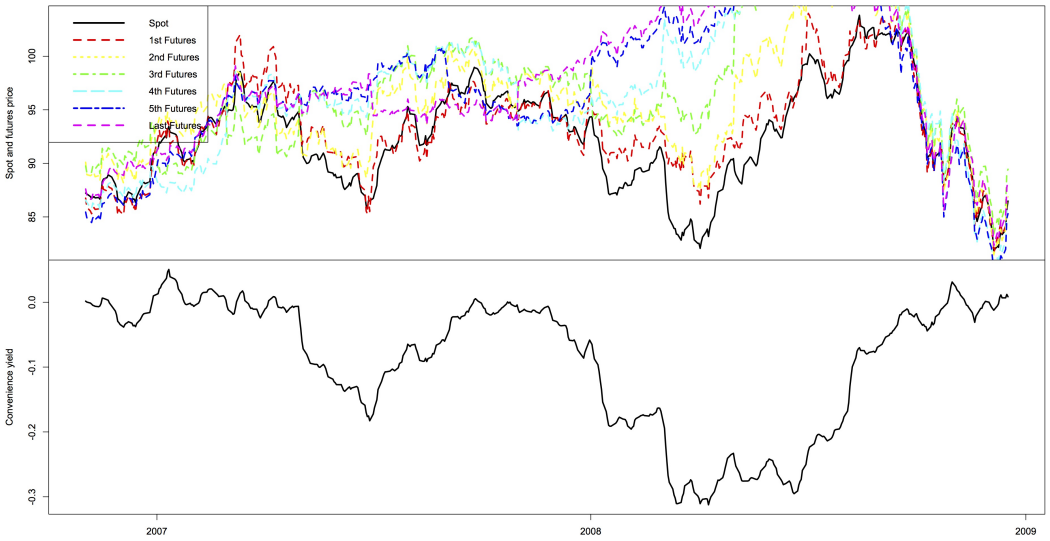

(c) $Data_3$

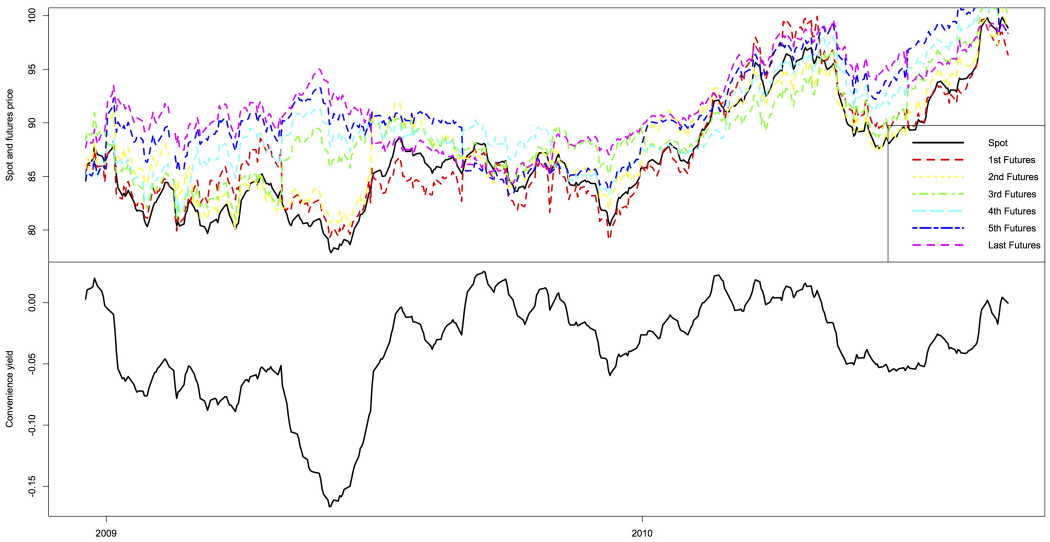

Figure 2.10. State variable for Panel A in cattle contracts

Note: Spot and futures prices are on the top of convenience yield; C1, C2, C3, C4, C5 and C6 correspond to the 1st Futures, 2nd Futures, 3rd Futures, 4th Futures, 5th Futures and Last Futures in the figure.

(a) $Data_1$

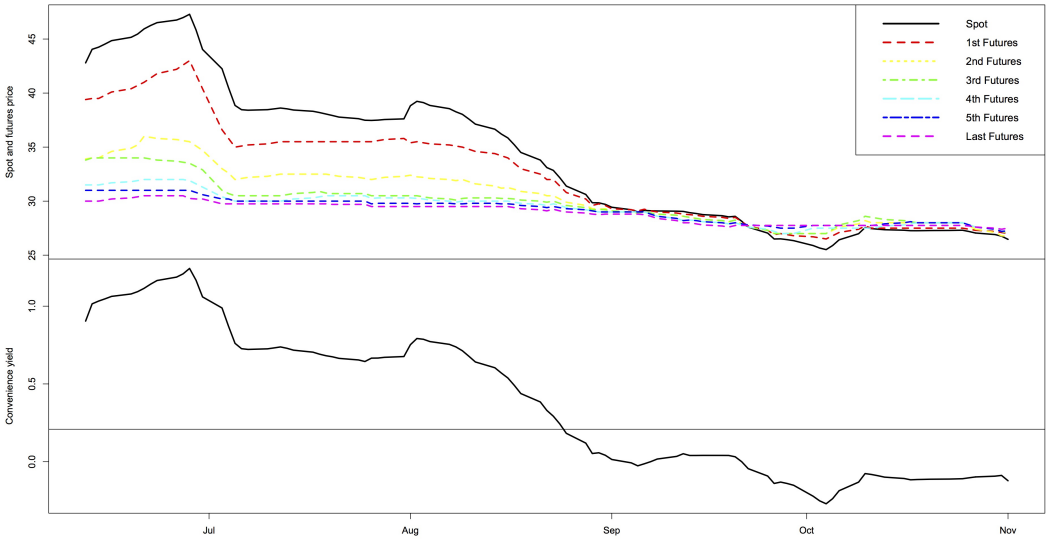

(b) $Data_2$

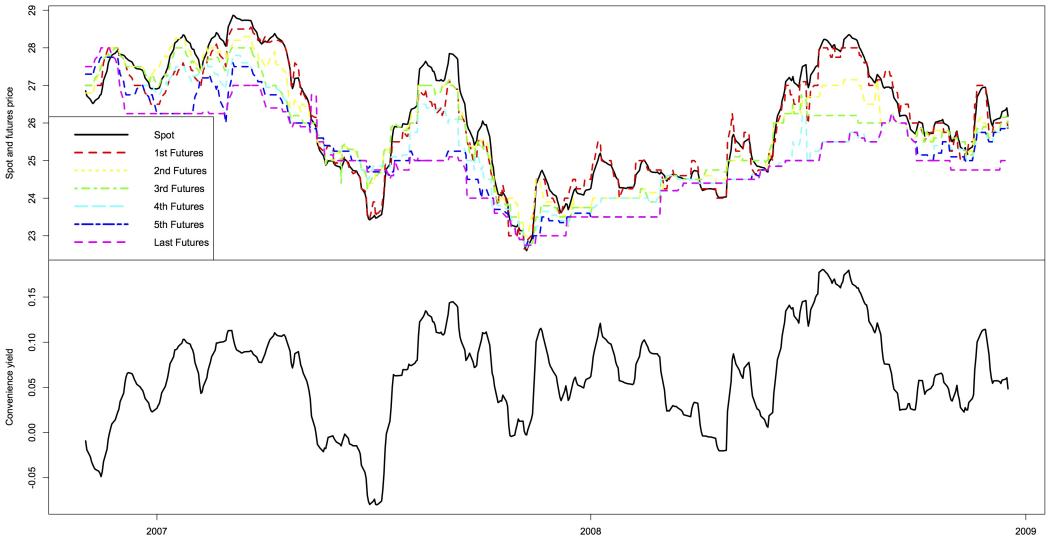

(c) $Data_3$

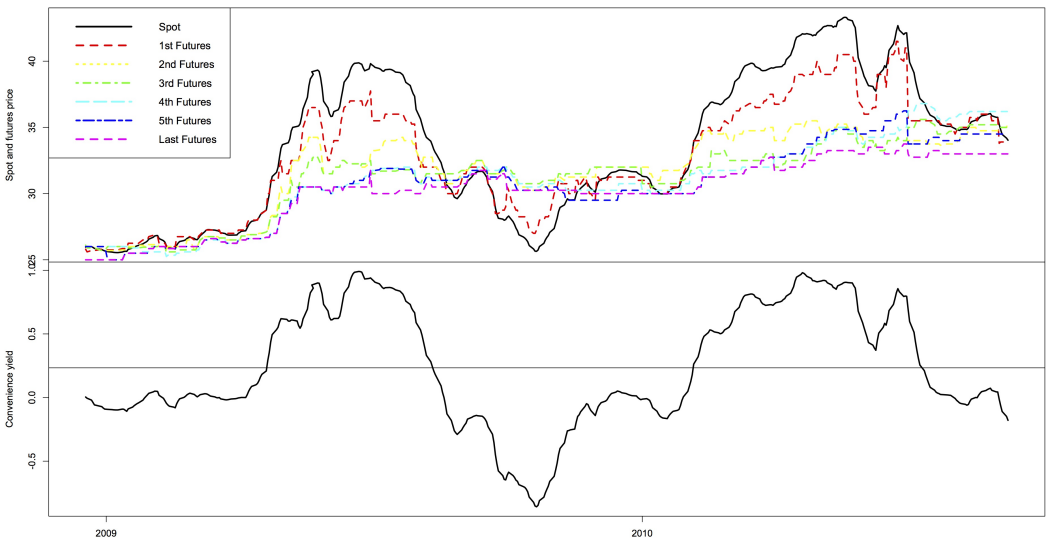

Figure 2.11. State variable for Panel A in salmon contracts

Note: Spot and futures prices are on the top of convenience yield; F2, F5, F7, F10, F13 and F16 correspond to the 1st Futures, 2nd Futures, 3rd Futures, 4th Futures, 5th Futures and Last Futures in the figure.

(a) $Data_1$

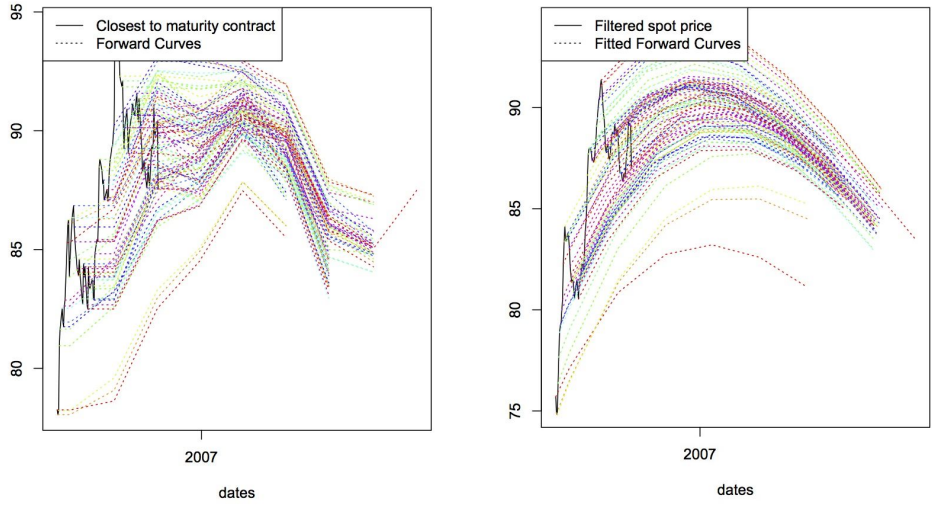

(b) $Data_2$

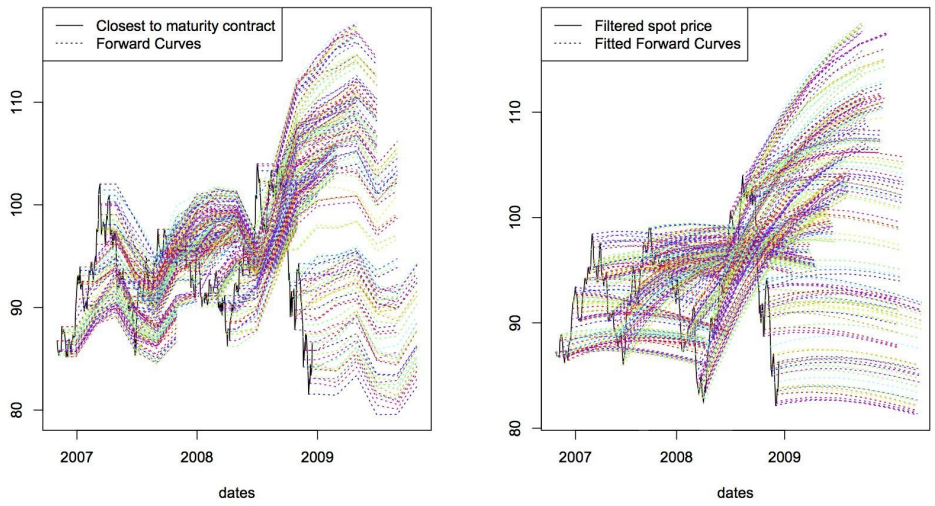

(c) $Data_3$

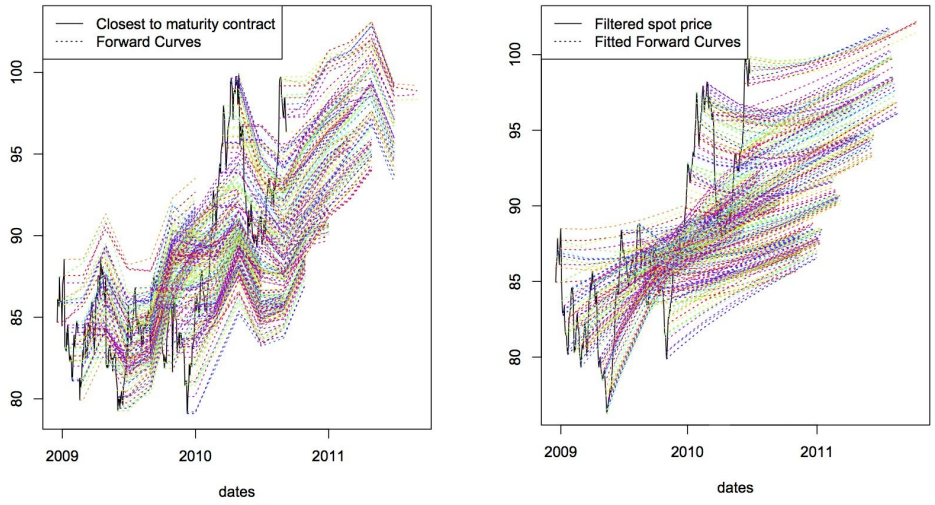

Figure 2.12. Term structures for Panel A in cattle contracts: actual forward curves on the left; model generated forward curves on the right

(a) $Data_1$

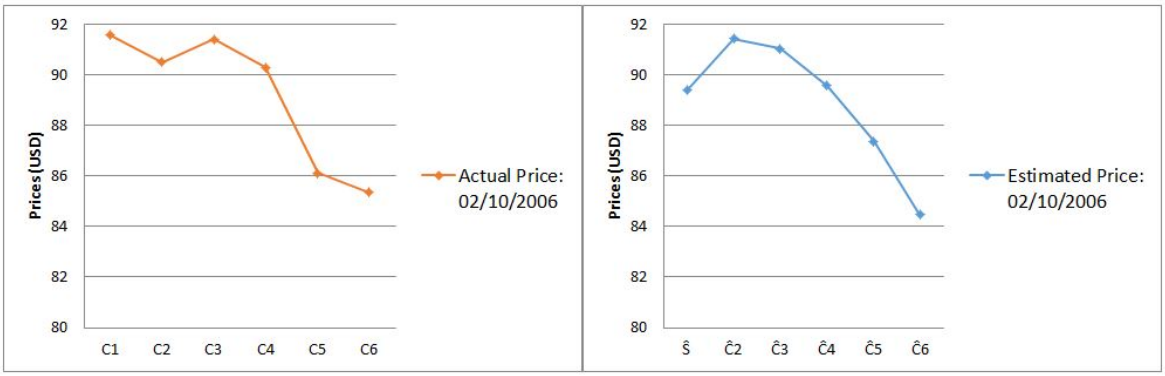

(b) $Data_2$

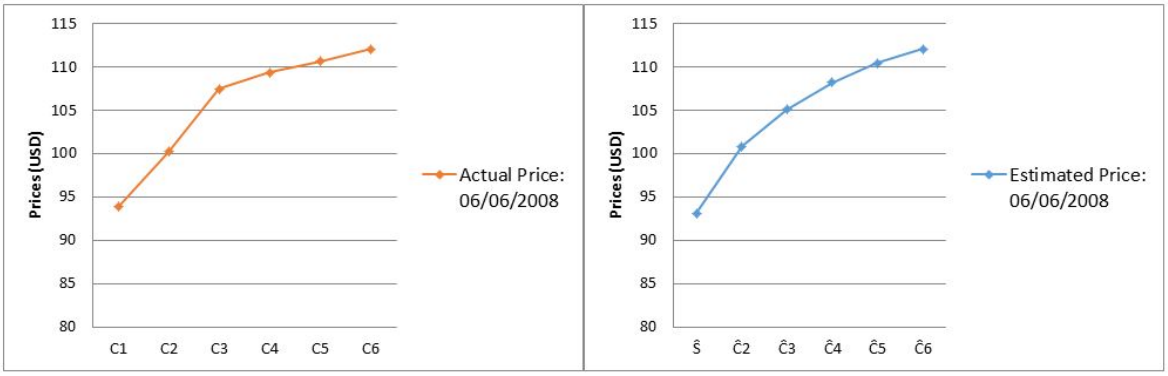

(c) $Data_3$

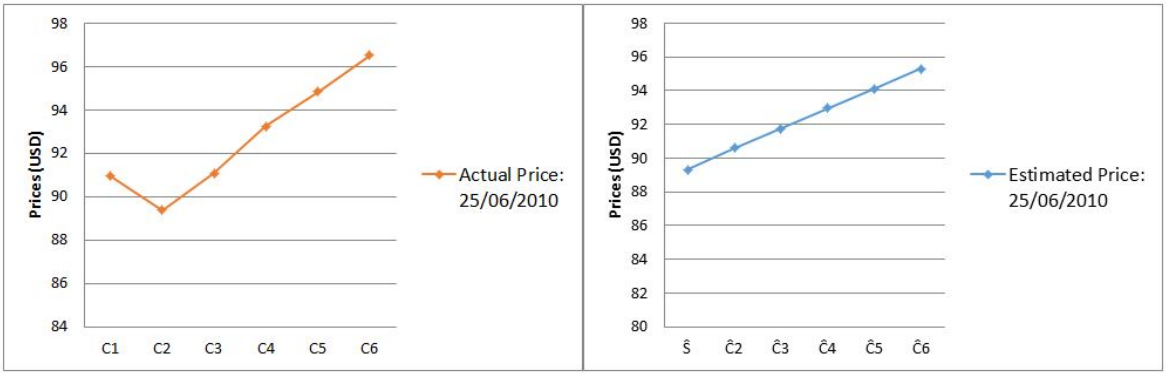

Figure 2.13. Term structures of cattle contracts on specific days: (a) $Data_1$; (b) $Data_2$; (c) $Data_3$; actual forward curves on the left, model generated forward curves on the right

Note: This figure shows the term structures on specific days. Each line corresponds to one colored line in Figure 2.12 on the same side. The observed term structures of live cattle prices are on the left; while the estimated term structures are on the right. C1 - C6 denote the actual futures prices with different maturities of live cattle. $\hat{S}$ is the filtered spot price on that day, and $\hat{C}2$ - $\hat{C}6$ represent the estimated futures prices.

(a) $Data_1$

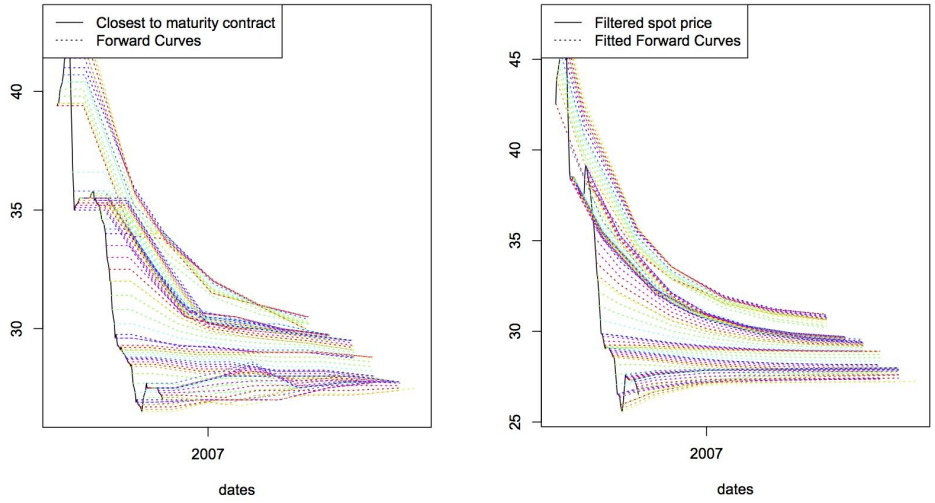

(b) $Data_2$

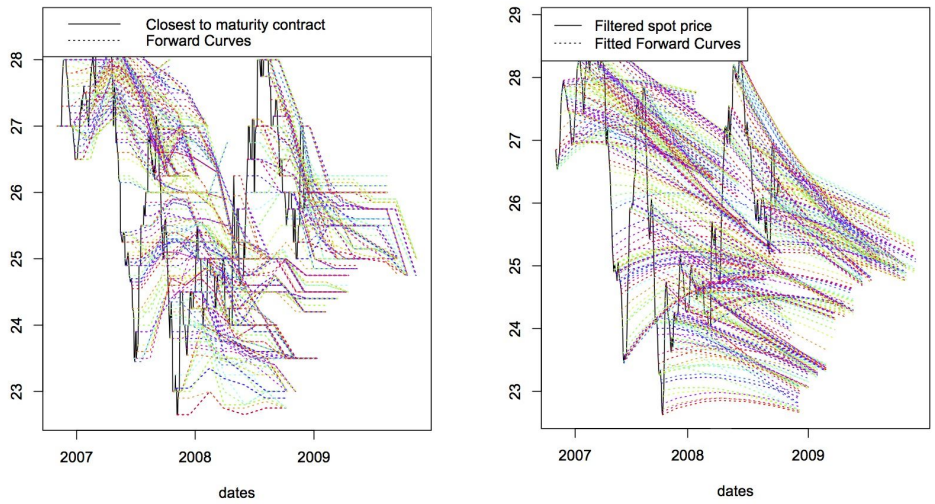

(c) $Data_3$

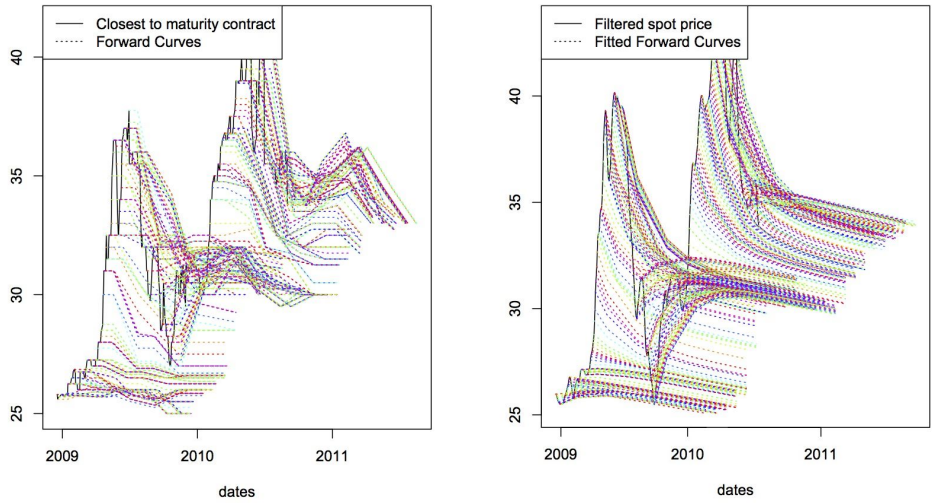

Figure 2.14. Term structures for Panel A in salmon contracts: actual forward curves on the left; model generated forward curves on the right

(a) $Data_1$

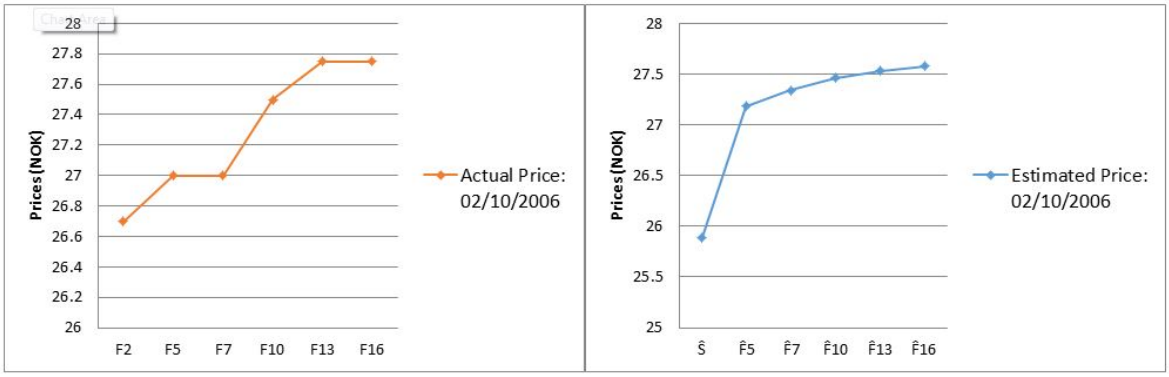

(b) $Data_2$

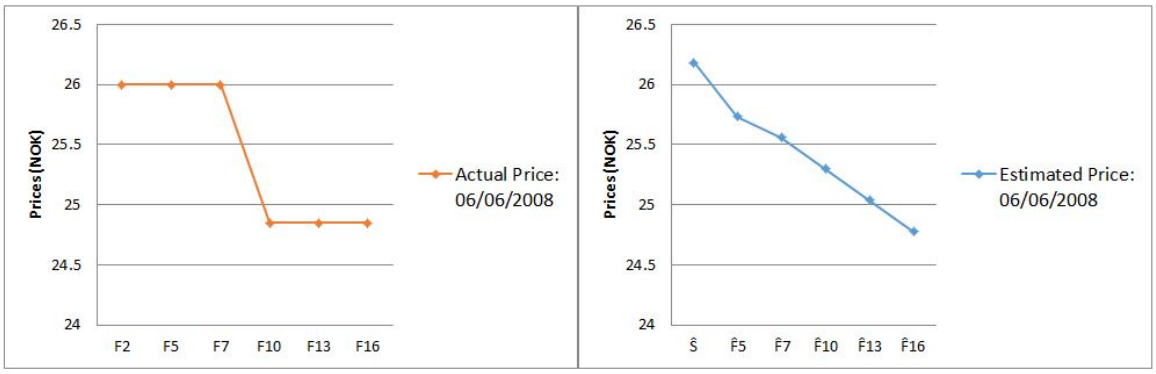

(c) $Data_3$

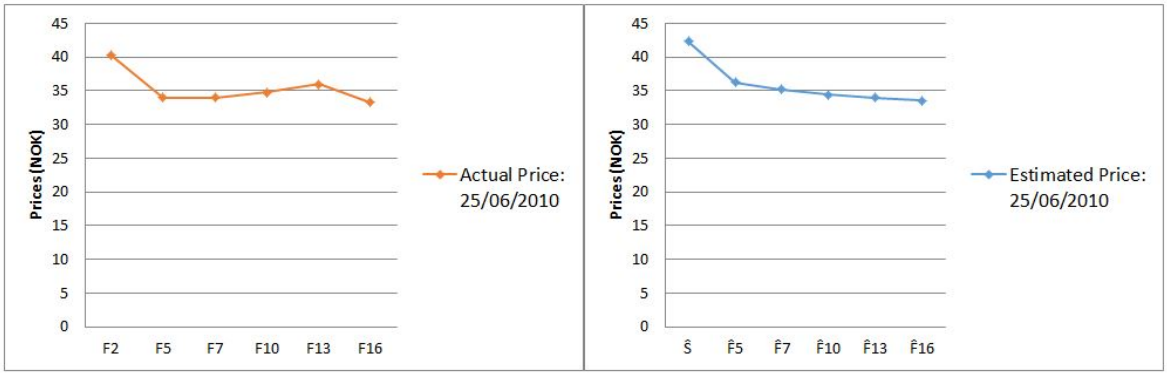

Figure 2.15. Term structures of salmon contracts on specific days: (a) $Data_1$; (b) $Data_2$; (c) $Data_3$; actual forward curves on the left, model generated forward curves on the right

Note: This figure shows the term structures on specific days. Each line corresponds to one colored line in Figure 2.14 on the same side. The observed term structures of salmon prices are on the left; while the estimated term structures are on the right. F2 - F16 denote the actual futures prices with different maturities of salmon. $\hat{S}$ is the filtered spot price on that day, and $\hat{F}5$ - $\hat{F}16$ represent the estimated futures prices.

Table 2.6. Estimation Results: Comparison between Cattle and Salmon

Parameter	$Data_1$		$Data_2$		$Data_3$	
	Cattle	Salmon	Cattle	Salmon	Cattle	Salmon
μ	0.224 (0.250)	0.241 (0.608)	0.108 (0.108)	0.195 (0.085)**	0.103 (0.106)	0.570 (0.121)***
κ	0.770 (0.179)***	2.844 (0.059)***	0.975 (0.082)***	1.139 (0.133)***	0.444 (0.180)***	4.257 (0.135)***
α	1.488 (0.934)	0.209 (0.667)	0.191 (0.143)	0.289 (0.120)**	0.060 (0.232)	0.233 (0.099)**
σ_1	0.145 (0.019)***	0.292 (0.023)***	0.149 (0.010)***	0.116 (0.006)***	0.136 (0.009)***	0.152 (0.007)***
σ_2	0.426 (0.054)***	1.595 (0.085)***	0.188 (0.018)***	0.174 (0.017)***	0.130 (0.018)***	0.527 (0.032)***
ρ	0.505 (0.107)***	0.636 (0.172)***	0.797 (0.034)***	0.884 (0.019)***	0.889 (0.021)***	0.864 (0.030)***
λ	0.819 (0.793)	0.368 (1.782)	0.113 (0.139)	0.247 (0.127)**	0.056 (0.102)	0.787 (0.419)*
Log-Likelihood	-1574.8	-1806	-8112.1	-10098	-6670.9	-6642

Note: Standard errors in parentheses. [***] Significant at 1% level; [**] Significant at 5% level; [*] Significant at 10% level. μ is the expected return on the spot commodity; κ is the speed of mean-reversion of the convenience yield; α is the mean level of the convenience yield; σ_1 is the volatility of the spot price; σ_2 is the volatility of the convenience yield; ρ is the correlation coefficient of spot price and convenience yield; λ is the market price of the convenience yield risk.

We observe from Figures 2.10 and 2.11 that the convenience yields are notably different in cattle than in salmon. While the convenience yield for cattle is negative almost all of the time, the convenience yield for salmon changes signs relatively frequently and is relatively equally balanced between positive and negative. This maybe attributed to storage issues and costs reflecting that fresh salmon is a highly perishable good, more so than cattle. It may also point towards liquidity issues and the fact that salmon farming is still far less developed than cattle farming, which may affect supply. In this case, the benefits for holding salmon in storage in the short term and hence being able to provide liquidity are higher than for cattle. Looking at the term structures in Figures 2.12 and Figure 2.14, it appears that the model captures the salmon contracts much better than the cattle contracts. This fact is confirmed numerically by Tables A.9 and A.10 in Appendix C, which show the root-mean-square errors (RMSE) and mean-absolute errors (MAE). Term structures on some specific days are further given as examples in Figure 2.13 and Figure 2.15.

2.6 Conclusion

In this paper we established a link between the popular Schwartz (1997) multifactor models used for the pricing of commodity derivatives and classical models originating from the aquaculture/fish farming literature. Specifically we looked at future contracts written on fresh farmed salmon, which have been actively traded at the Fish Pool Market in Norway since 2006. The link with the fish farming literature, has been established following first principles, starting by modeling the aggregate salmon farming production as well as modeling salmon demand using a Cobb-Douglas utility function for a representative consumer. We estimated our model using a rich data set of futures contracts with different maturities traded at Fish Pool between 12/06/2006 and 22/03/2012 by means of Kalman filter. Our results show that the framework presented is able to produce an excellent fit to the actual term structure of salmon futures. A comparison with live cattle futures traded within the same period reveals subtle difference, for example within the level of the convenience yield, the speed of mean reversion of the convenience yield and the convenience yield risk premium. Overall, the Schwartz (1997) multifactor approach appears to fit the salmon data better than the live cattle data.

Bibliography

Alvarez, L. H. (1998). Optimal harvesting under stochastic fluctuations and critical depensation. *Mathematical Biosciences*, *152*(1), 63–85.

Alvarez, L. H., & Shepp, L. A. (1998). Optimal harvesting of stochastically fluctuating populations. *Journal of Mathematical Biology*, *37*(2), 155–177.

Arnason, R. (1992). Optimal feeding schedules and harvesting time in aquaculture. *Marine Resource Economics*, 15–35.

Asche, F., Bjørndal, T., & Young, J. A. (2001). Market interactions for aquaculture products. *Aquaculture Economics & Management*, *5*(5-6), 303–318.

Asche, F., Bremnes, H., & Wessells, C. R. (1999). Product aggregation, market integration, and relationships between prices: an application to world salmon markets. *American Journal of Agricultural Economics*, *81*(3), 568–581.

Beddington, J. R., & May, R. M. (1977). Harvesting natural populations in a randomly fluctuating environment. *Science*, *197*(4302), 463–465.

Bjerksund, P. (1991). *Contingent claims evaluation when the convenience yield is stochastic: analytical results*. Institutt for foretaksøkonomi, Institute of Finance and Management Science.

Bjørndal, T. (1988). Optimal harvesting of farmed fish. *Marine Resource Economics*, 139–159.

Cacho, O. J. (1997). Systems modelling and bioeconomic modelling in aquaculture. *Aquaculture Economics & Management*, *1*(1-2), 45–64.

Erb, P., Lüthi, D., & Otziger, S. (2014). Schwartz 1997 two-factor model technical document.

Ewald, C.-O. (2013). Derivatives on nonstorable renewable resources: Fish futures and options, not so fishy after all. *Natural Resource Modeling*, *26*(2), 215–236.

Ewald, C.-O., & Wang, W.-K. (2010). Sustainable yields in fisheries: Uncertainty, risk-aversion, and mean-variance analysis. *Natural Resource Modeling*, *23*(3), 303–323.

Guttormsen, A. G. (2008). Faustmann in the sea: optimal rotation in aquaculture. *Marine Resource Economics*, 401–410.

Heaps, T. (1995). Density dependent growth and the culling of farmed fish. *Marine Resource Economics*, 285–298.

Jamshidian, F., & Fein, M. (1990). Closed-form solutions for oil futures and european options in the gibson-schwartz model: A note. *Merril Lynch Capital Markets*.

Lande, R., Engen, S., & Saether, B.-E. (1995). Optimal harvesting of fluctuating populations with a risk of extinction. *American naturalist*, 728–745.

May, R. M. (1973). Stability in randomly fluctuating versus deterministic environments. *American Naturalist*, 621–650.

Schwartz, E. S. (1997). The stochastic behavior of commodity prices: Implications for valuation and hedging. *The Journal of Finance*, *52*(3), 923–973.

Solibakke, P. B. (2012). Scientific stochastic volatility models for the salmon forward market: forecasting (un-) conditional moments. *Aquaculture Economics & Management*, *16*(3), 222–249.

Yu, R., & Leung, P. (2006). Optimal partial harvesting schedule for aquaculture operations. *Marine Resource Economics*, 301–315.

Appendix A: Data Description

Table A.1. Contracts in $Data_1$, 12/06/2006-1/11/2006

Contract	Mean Price (Standard Deviation)	Mean Maturity (Standard Deviation)
	Panel A: From 12/06/2006 to 1/11/2006: 103 Daily Observations	
F1	33.86 (5.32) *NOK*	0.040 (0.025) *years*
F3	31.68 (4.02)	0.212 (0.025)
F5	30.53 (2.68)	0.382 (0.025)
F7	29.82 (2.03)	0.551 (0.025)
F9	29.45 (1.51)	0.717 (0.025)
	Panel B: From 12/06/2006 to 1/11/2006: 103 Daily Observations	
F12	29.20 (1.25) *NOK*	0.968 (0.025) *years*
F14	29.05 (1.05)	1.141 (0.025)
F16	28.91 (0.98)	1.315 (0.025)
F18	28.74 (0.89)	1.485 (0.025)
F20	28.57 (0.79)	1.650 (0.025)
	Panel C: From 12/06/2006 to 1/11/2006: 103 Daily Observations	
F24	28.53 (0.80) *NOK*	1.984 (0.025) *years*
F25	28.53 (0.78)	2.072 (0.025)
F26	28.53 (0.78)	2.158 (0.025)
F28	28.53 (0.78)	2.327 (0.025)
F29	28.53 (0.78)	2.410 (0.025)

Note: We use a similar notation as in Schwartz (1997) and denote with F1 the contract closest to maturity counting up to F29 which represents the contract farthest to maturity.

Table A.2. Contracts in $Data_2$, 2/11/2006-17/12/2008

Contract	Mean Price (Standard Deviation)	Mean Maturity (Standard Deviation)
	Panel A: From 2/11/2006 to 17/12/2008: 545 Daily Observations	
F1	25.96 (1.59) *NOK*	0.041 (0.025) *year*
F3	25.92 (1.42)	0.210 (0.025)
F5	25.85 (1.39)	0.378 (0.026)
F7	25.71 (1.33)	0.547 (0.026)
F9	25.53 (1.28)	0.717 (0.025)
	Panel B: From 2/11/2006 to 17/12/2008: 545 Daily Observations	
F12	25.30 (1.24) *NOK*	0.973 (0.025) *years*
F14	25.12 (1.18)	1.143 (0.026)
F16	25.04 (1.18)	1.312 (0.026)
F18	24.94 (1.12)	1.483 (0.026)
F20	24.90 (1.10)	1.654 (0.027)
	Panel C: From 2/11/2006 to 17/12/2008: 545 Daily Observations	
F24	24.89 (1.12) *NOK*	1.997 (0.027) *years*
F25	24.89 (1.12)	2.083 (0.028)
F26	24.88 (1.13)	2.169 (0.028)
F28	24.86 (1.14)	2.341 (0.029)
F29	24.86 (1.14)	2.427 (0.028)

Note: We use a similar notation as in Schwartz (1997) and denote with F1 the contract closest to maturity counting up to F29 which represents the contract farthest to maturity.

Table A.3. Contracts in $Data_3$, 18/12/2008-22/03/2012

Contract	Mean Price (Standard Deviation)	Mean Maturity (Standard Deviation)
Panel A: From 18/12/2008 to 22/03/2012: 849 Daily Observations		
F1	32.93 (6.28) *NOK*	0.041 (0.025) *year*
F3	32.47 (5.53)	0.213 (0.025)
F5	32.01 (4.99)	0.386 (0.025)
F7	31.51 (4.66)	0.558 (0.026)
F9	31.07 (4.31)	0.729 (0.026)
Panel B: From 18/12/2008 to 22/03/2012: 849 Daily Observations		
F12	30.77 (3.91) *NOK*	0.986 (0.026) *years*
F14	30.45 (3.59)	1.157 (0.027)
F16	30.15 (3.16)	1.328 (0.028)
F18	30.12 (2.97)	1.498 (0.029)
F20	30.00 (2.81)	1.668 (0.031)
Panel C: From 18/12/2008 to 22/03/2012: 849 Daily Observations		
F24	29.29 (2.38) *NOK*	2.007 (0.033) *years*
F25	29.17 (2.26)	2.092 (0.034)
F26	29.08 (2.15)	2.176 (0.035)
F28	28.99 (1.90)	2.345 (0.036)
F29	28.89 (1.82)	2.430 (0.037)

Note: We use a similar notation as in Schwartz (1997) and denote with F1 the contract closest to maturity counting up to F29 which represents the contract farthest to maturity.

Table A.4. Live-Cattle Contracts, 12/06/2006-07/09/2010

Contract	Mean Price (Standard Deviation)	Mean Maturity (Standard Deviation)
	$Data_1$: From 12/06/2006 to 01/11/2006: 101 Daily Observations	
C1	87.16 (3.60) *USD*	0.101 (0.069) *years*
C2	88.79 (3.00)	0.333 (0.068)
C3	89.88 (1.98)	0.565 (0.067)
C4	90.22 (1.52)	0.798 (0.068)
C5	88.10 (1.91)	1.031 (0.068)
C6	85.40 (1.46)	1.268 (0.069)
	$Data_2$: From 02/11/2006 to 17/12/2008: 536 Daily Observations	
C1	93.36 (4.54) *USD*	0.114 (0.067) *years*
C2	95.69 (5.41)	0.349 (0.067)
C3	97.18 (6.22)	0.583 (0.067)
C4	97.39 (7.24)	0.817 (0.067)
C5	97.79 (7.62)	1.052 (0.067)
C6	98.29 (7.13)	1.286 (0.067)
	$Data_3$: From 18/12/2008 to 07/09/2010: 433 Daily Observations	
C1	87.46 (5.32) *USD*	0.112 (0.068) *years*
C2	88.23 (4.56)	0.346 (0.069)
C3	88.99 (4.19)	0.580 (0.069)
C4	89.96 (4.43)	0.814 (0.069)
C5	91.10 (4.65)	1.047 (0.069)
C6	91.58 (3.95)	1.281 (0.069)

Note: We use a similar notation as in Schwartz (1997) and denote with C1 the contract closest to maturity of live cattle, counting up to C6 which represents the contract farthest to maturity.

Appendix B: Additional Figures

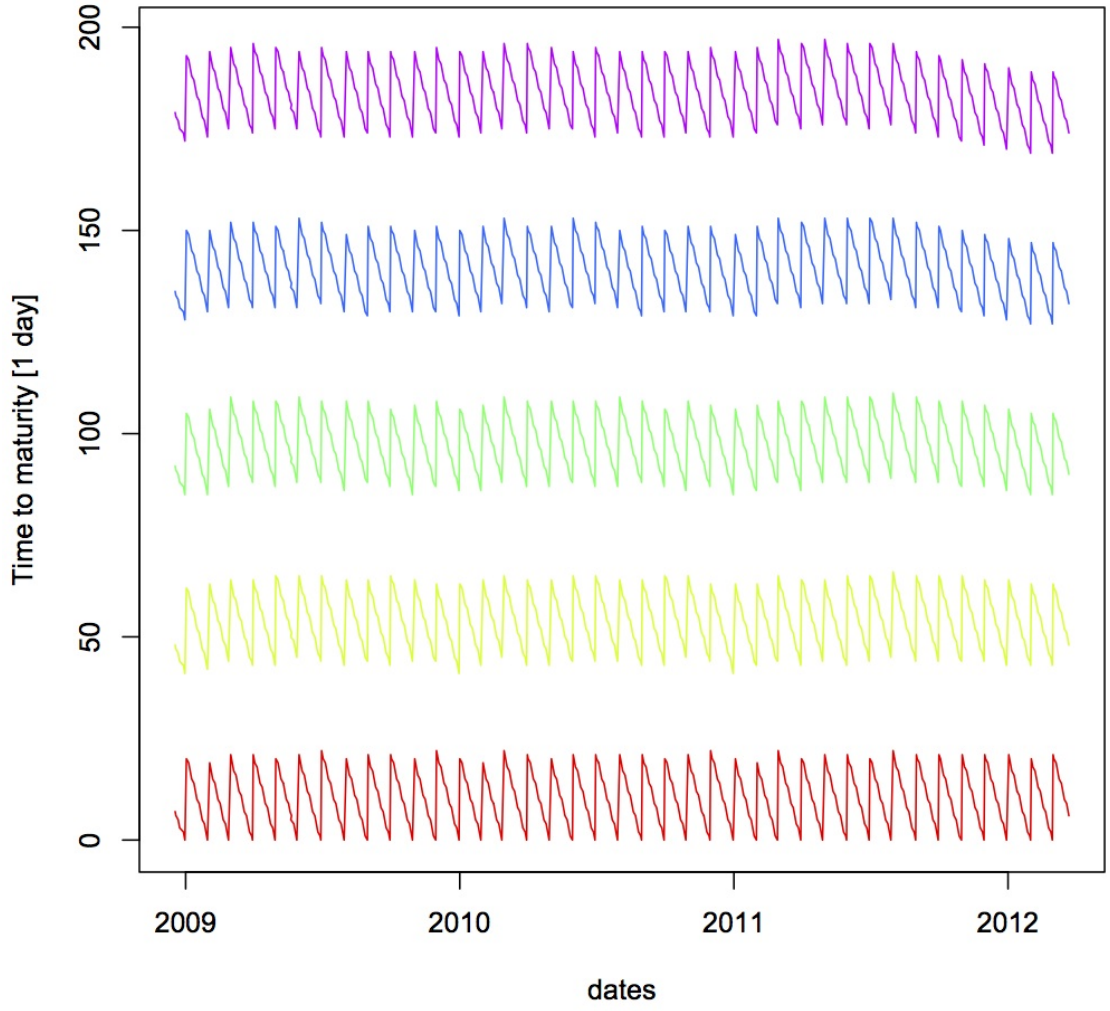

Figure A.1. Time-to-maturity pattern: Panel A of $Data_3$

Note: The figure shows the time-to-maturity pattern for each contract used in Panel A of $Data_3$, which fluctuates but remains within a narrow range during the sample period. This pattern of time-to-maturity is representative of all the data used in this study.

(a) Panel A

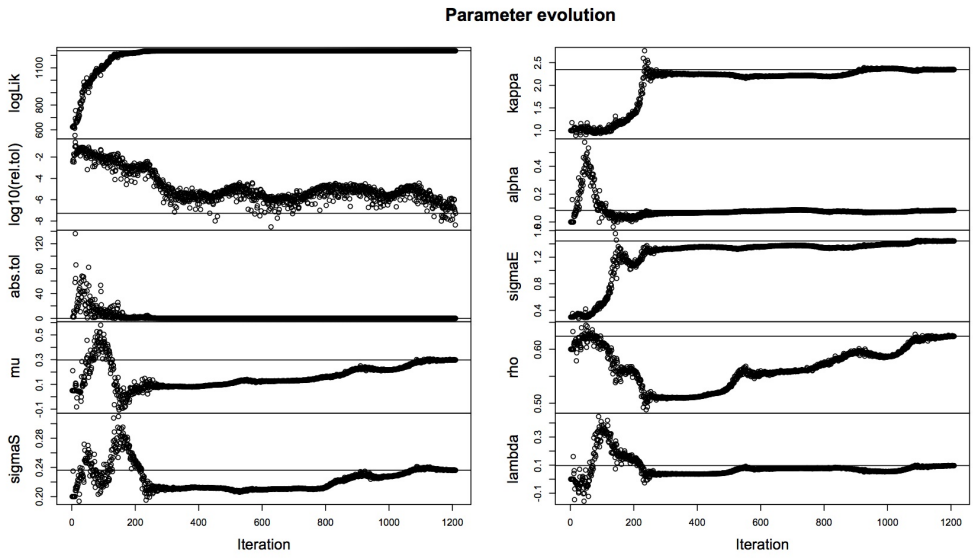

(b) Panel B

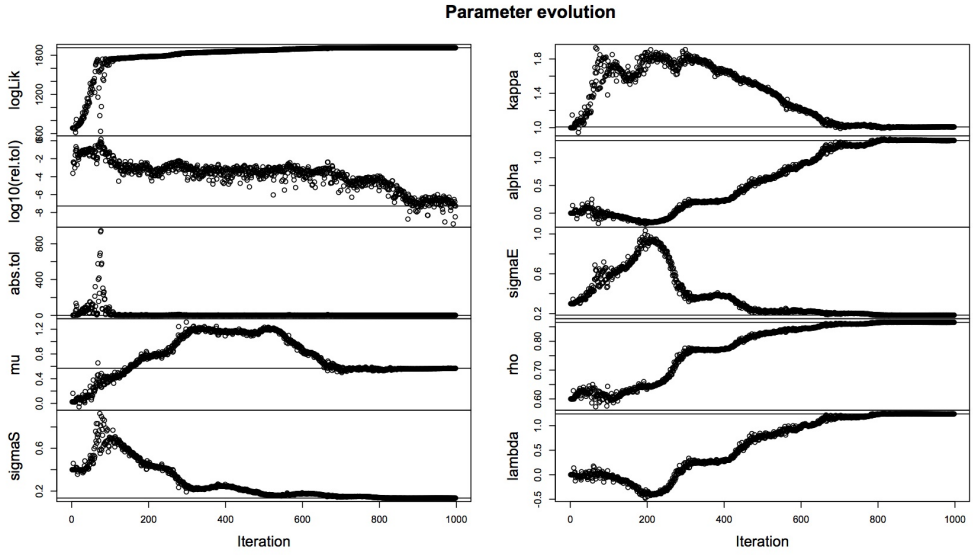

(c) Panel C

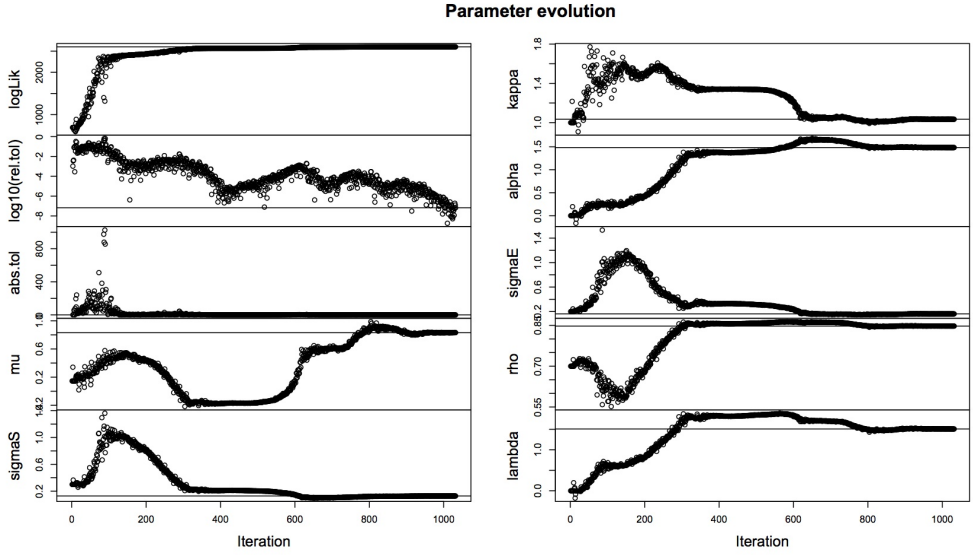

Figure A.2. Parameter evolution in $Data_1$, 12/06/2006-1/11/2006

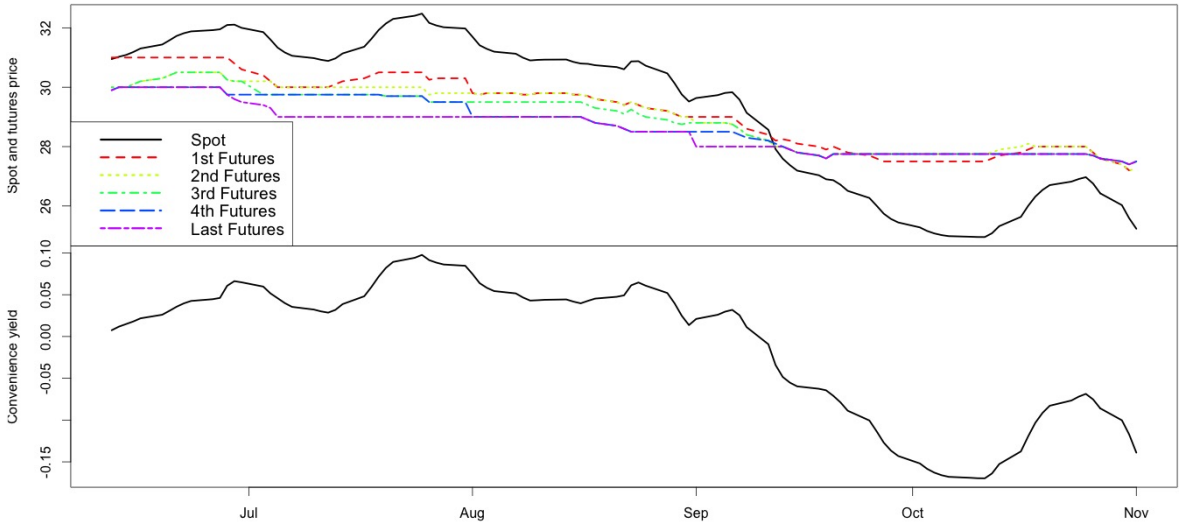

Figure A.3. State variables for Panel B in $Data_1$, 12/06/2006-1/11/2006

Note: Spot and futures prices are on the top of convenience yield; F12, F14, F16, F18 and F20 correspond to the 1st Futures, 2nd Futures, 3rd Futures, 4th Futures and Last Futures in the figure.

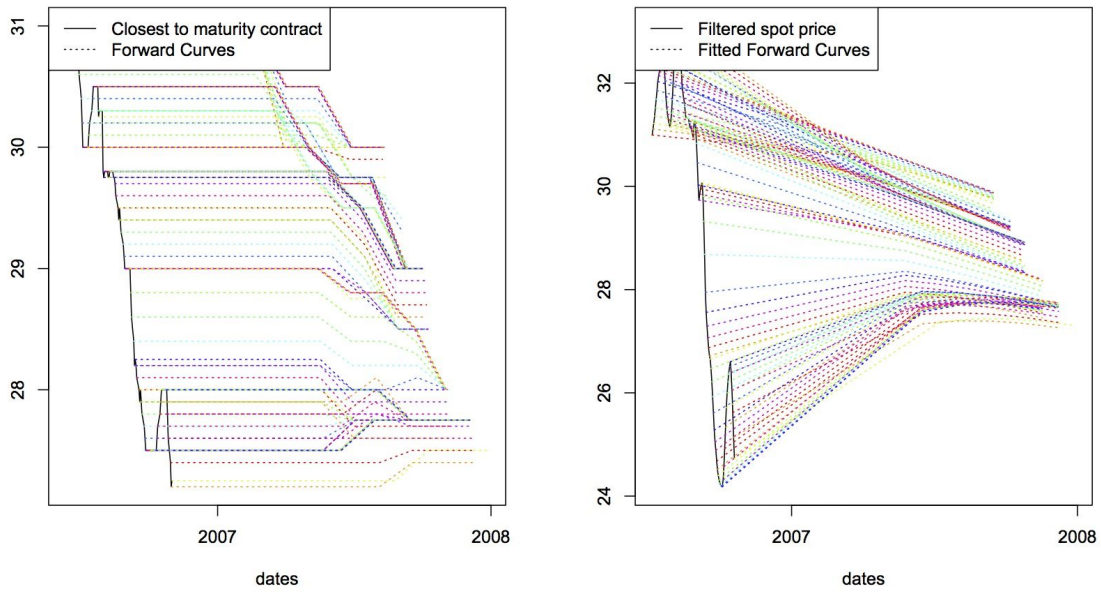

Figure A.4. Term structures for Panel B in $Data_1$: actual forward curves on the left; model generated forward curves on the right

Note: Each colored curve is a static picture of futures prices (y-axis) against contract maturities (x-axis), which is analogous to a plot of the term structure of interest rates. On the left side of the figure, the solid line represents the price of the closest-to-maturity futures contract, i.e., $F12$ in this case; while the dashed line consists of the actual prices of other futures contracts with different maturities in this panel. On the right side of the figure, the solid line is the filtered spot price obtained through the estimation procedure; while the dashed line consists of the estimated futures prices given by the pricing formula.

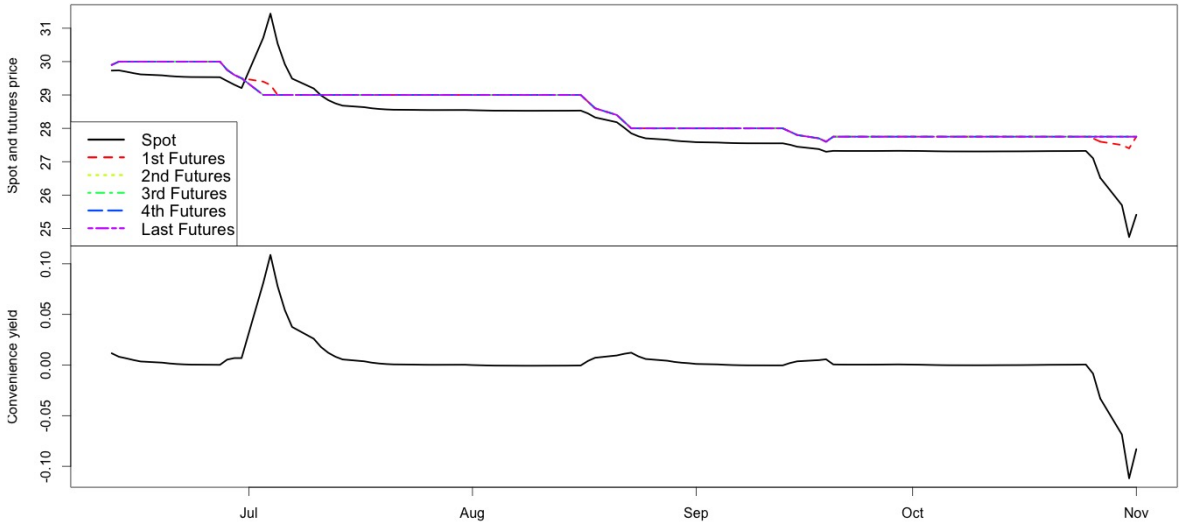

Figure A.5. State variables for Panel C in $Data_1$, 12/06/2006-1/11/2006

Note: Spot and futures prices are on the top of convenience yield; F24, F25, F26, F28 and F29 correspond to the 1st Futures, 2nd Futures, 3rd Futures, 4th Futures and Last Futures in the figure.

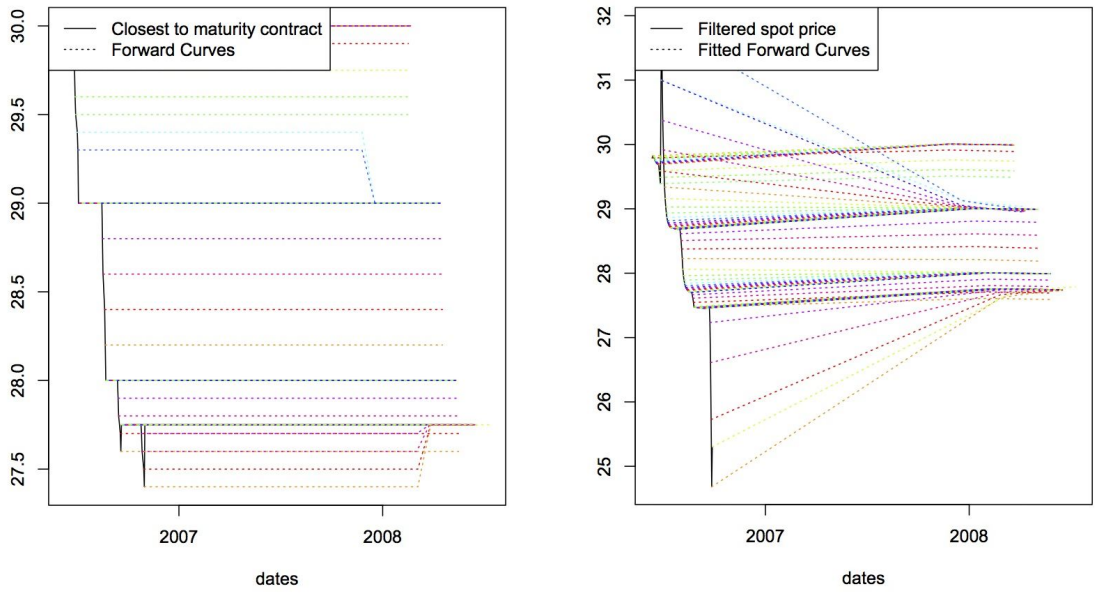

Figure A.6. Term structures for Panel C in $Data_1$: actual forward curves on the left; model generated forward curves on the right

Note: Each colored curve is a static picture of futures prices (y-axis) against contract maturities (x-axis), which is analogous to a plot of the term structure of interest rates. On the left side of the figure, the solid line represents the price of the closest-to-maturity futures contract, i.e., $F24$ in this case; while the dashed line consists of the actual prices of other futures contracts with different maturities in this panel. On the right side of the figure, the solid line is the filtered spot price obtained through the estimation procedure; while the dashed line consists of the estimated futures prices given by the pricing formula.

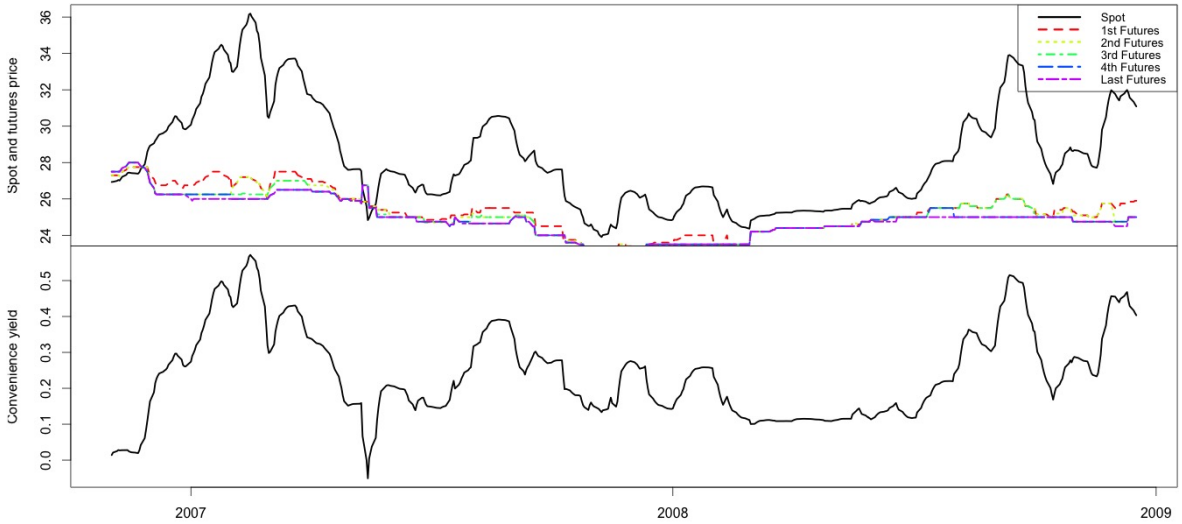

Figure A.7. State variables for Panel B in $Data_2$, 2/11/2006-17/12/2008

Note: Spot and futures prices are on the top of convenience yield; F12, F14, F16, F18 and F20 correspond to the 1st Futures, 2nd Futures, 3rd Futures, 4th Futures and Last Futures in the figure.

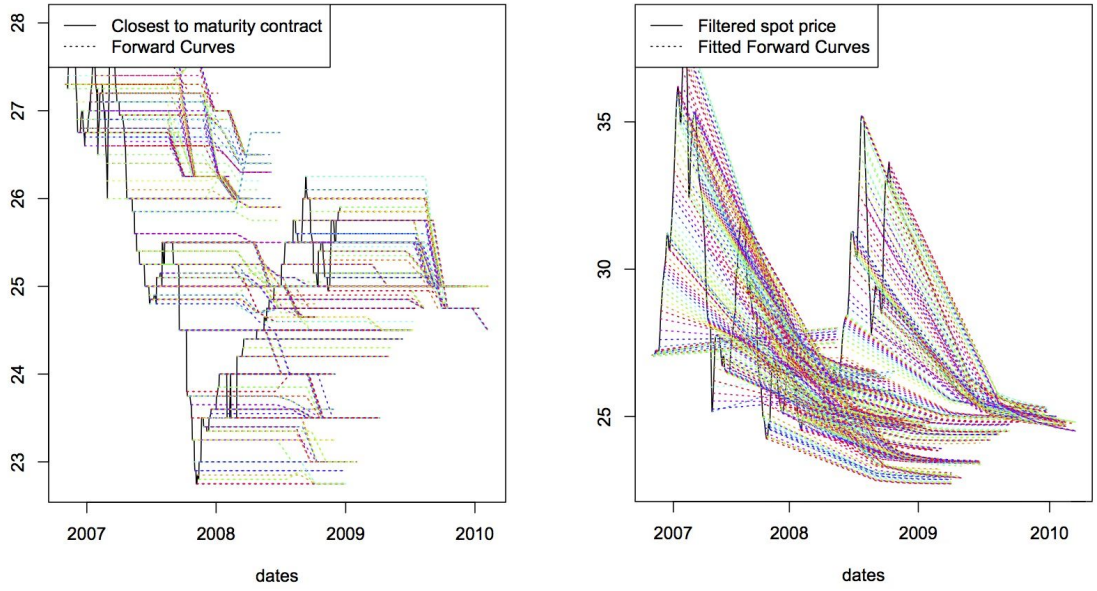

Figure A.8. Term structures for Panel B in $Data_2$: actual forward curves on the left; model generated forward curves on the right

Note: Each colored curve is a static picture of futures prices (y-axis) against contract maturities (x-axis), which is analogous to a plot of the term structure of interest rates. On the left side of the figure, the solid line represents the price of the closest-to-maturity futures contract, i.e., $F12$ in this case; while the dashed line consists of the actual prices of other futures contracts with different maturities in this panel. On the right side of the figure, the solid line is the filtered spot price obtained through the estimation procedure; while the dashed line consists of the estimated futures prices given by the pricing formula.

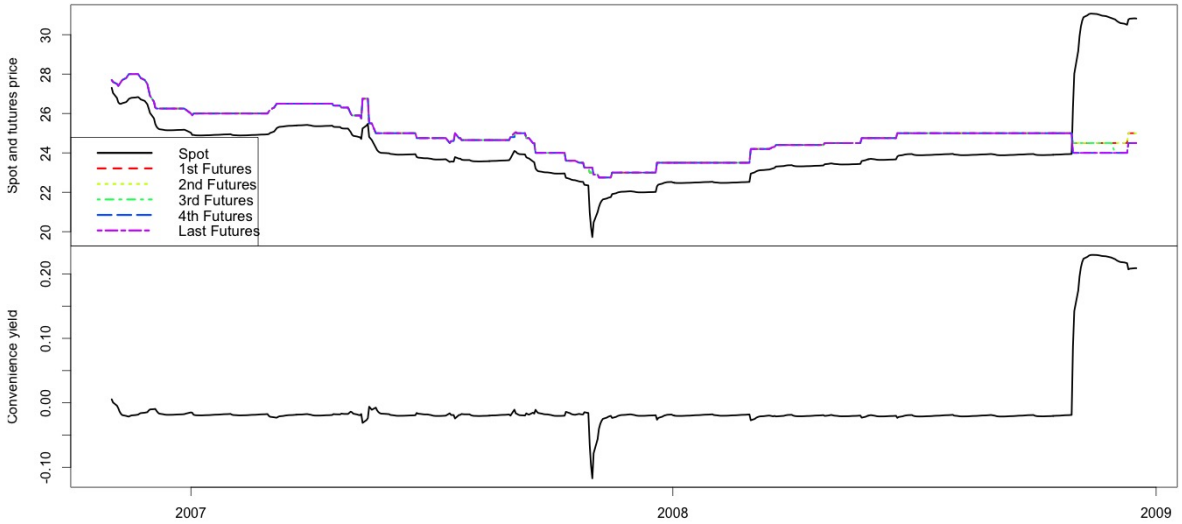

Figure A.9. State variables for Panel C in $Data_2$, 2/11/2006-17/12/2008

Note: Spot and futures prices are on the top of convenience yield; F24, F25, F26, F28 and F29 correspond to the 1st Futures, 2nd Futures, 3rd Futures, 4th Futures and Last Futures in the figure.

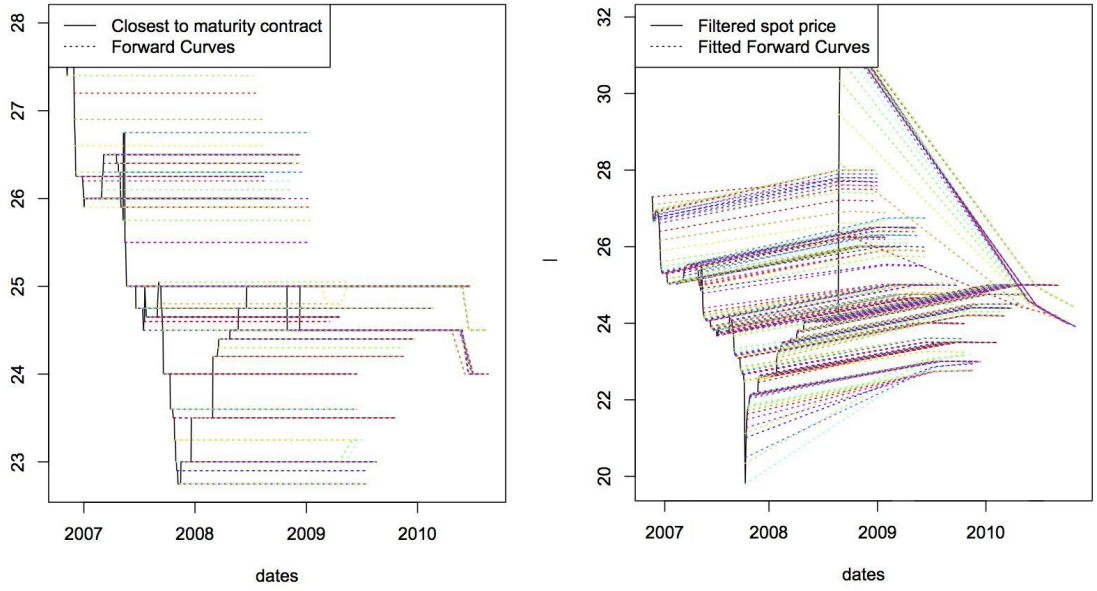

Figure A.10. Term structures for Panel C in $Data_2$: actual forward curves on the left; model generated forward curves on the right

Note: Each colored curve is a static picture of futures prices (y-axis) against contract maturities (x-axis), which is analogous to a plot of the term structure of interest rates. On the left side of the figure, the solid line represents the price of the closest-to-maturity futures contract, i.e., $F24$ in this case; while the dashed line consists of the actual prices of other futures contracts with different maturities in this panel. On the right side of the figure, the solid line is the filtered spot price obtained through the estimation procedure; while the dashed line consists of the estimated futures prices given by the pricing formula.

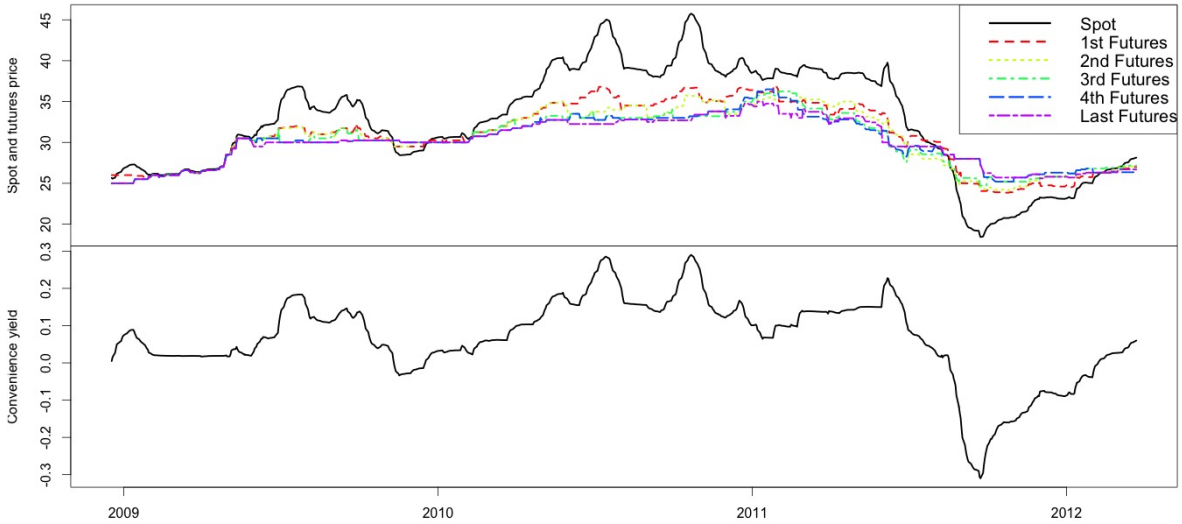

Figure A.11. State variables for Panel B in $Data_3$, 18/12/2008-22/03/2012

Note: Spot and futures prices are on the top of convenience yield; F12, F14, F16, F18 and F20 correspond to the 1st Futures, 2nd Futures, 3rd Futures, 4th Futures and Last Futures in the figure.

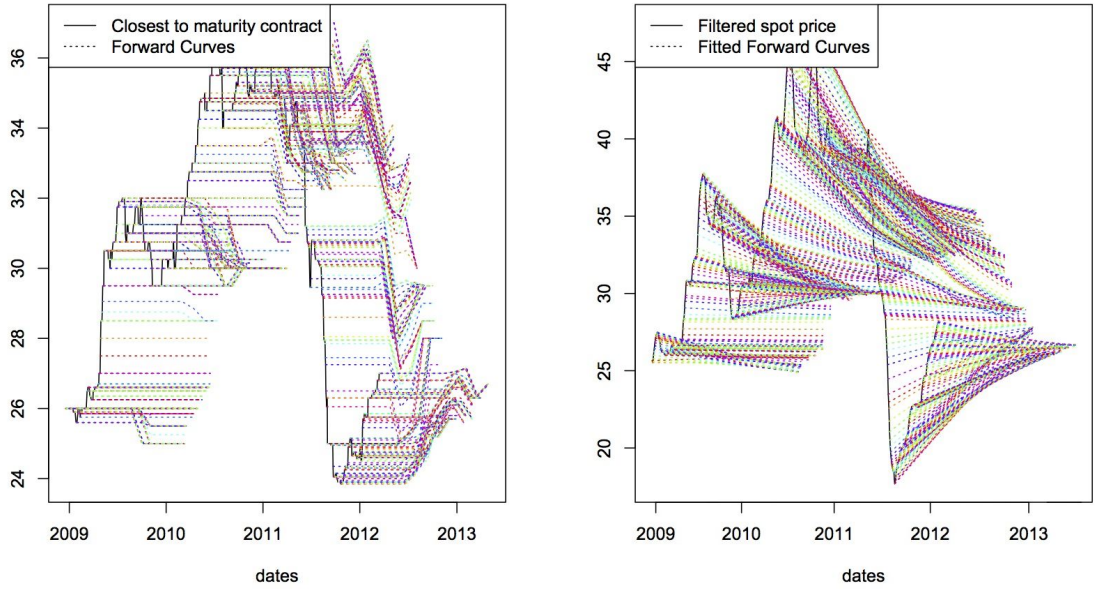

Figure A.12. Term structures for Panel B in $Data_3$: actual forward curves on the left; model generated forward curves on the right

Note: Each colored curve is a static picture of futures prices (y-axis) against contract maturities (x-axis), which is analogous to a plot of the term structure of interest rates. On the left side of the figure, the solid line represents the price of the closest-to-maturity futures contract, i.e., $F12$ in this case; while the dashed line consists of the actual prices of other futures contracts with different maturities in this panel. On the right side of the figure, the solid line is the filtered spot price obtained through the estimation procedure; while the dashed line consists of the estimated futures prices given by the pricing formula.

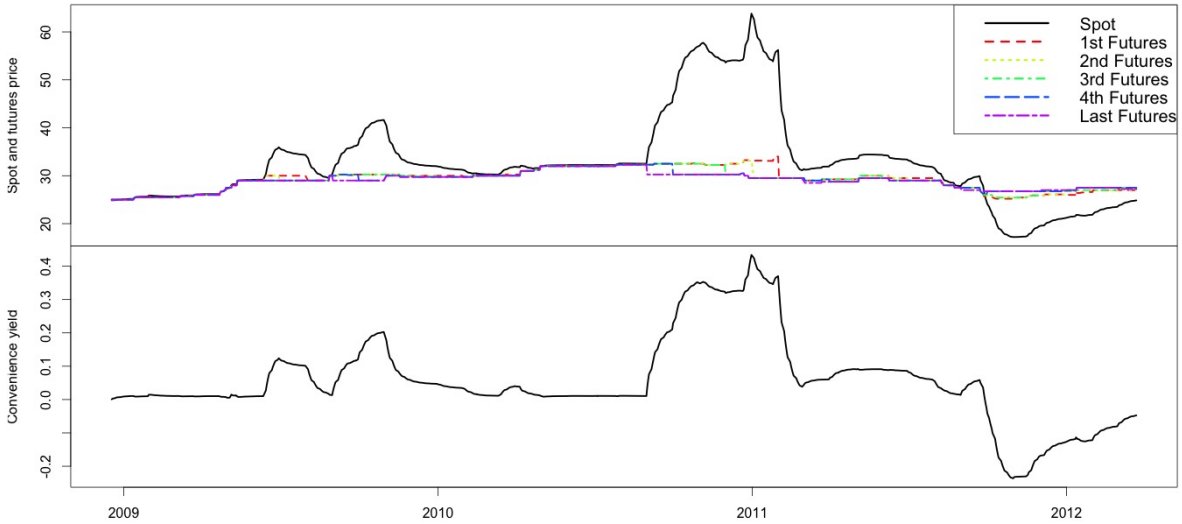

Figure A.13. State variables for Panel C in $Data_3$, 18/12/2008-22/03/2012

Note: Spot and futures prices are on the top of convenience yield; F24, F25, F26, F28 and F29 correspond to the 1st Futures, 2nd Futures, 3rd Futures, 4th Futures and Last Futures in the figure.

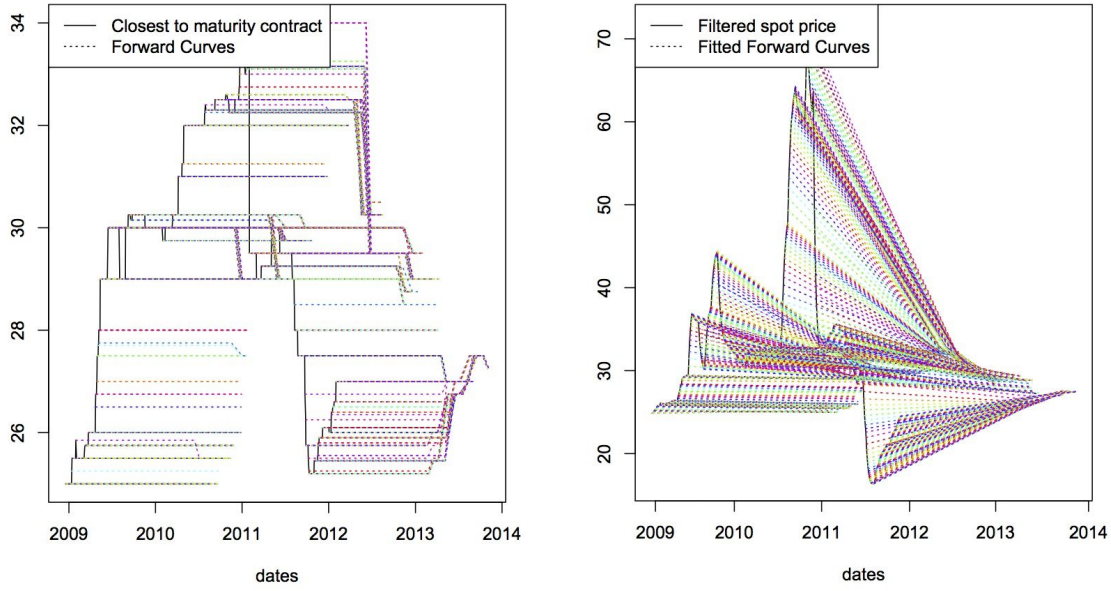

Figure A.14. Term structures for Panel C in $Data_3$: actual forward curves on the left; model generated forward curves on the right

Note: Each colored curve is a static picture of futures prices (y-axis) against contract maturities (x-axis), which is analogous to a plot of the term structure of interest rates. On the left side of the figure, the solid line represents the price of the closest-to-maturity futures contract, i.e., $F24$ in this case; while the dashed line consists of the actual prices of other futures contracts with different maturities in this panel. On the right side of the figure, the solid line is the filtered spot price obtained through the estimation procedure; while the dashed line consists of the estimated futures prices given by the pricing formula.

Appendix C: RMSE and MAE

Table A.5. RMSE and MAE of Log Price: $Data_1$, 12/06/2006-01/11/2006

	F1	F3	F5	F7	F9	ALL
RMSE	0.0148	0.0216	0.0095	0.0099	0.0134	0.0145
MAE	0.0100	0.0159	0.0073	0.0079	0.0097	0.0101
	F12	F14	F16	F18	F20	ALL
RMSE	0.0047	0.0049	0.0032	0.0049	0.0046	0.0045
MAE	0.0040	0.0040	0.0026	0.0039	0.0041	0.0037
	F24	F25	F26	F28	F29	ALL
RMSE	0.0015	0.0007	0.0005	0.0003	0.0004	0.0008
MAE	0.0006	0.0003	0.0002	0.0002	0.0004	0.0003

Note: The root-mean-square error (RMSE) and mean-absolute error (MAE) are used to evaluate the model fit.

Table A.6. RMSE and MAE of Log Price: $Data_2$, 02/11/2006-17/12/2008

	F1	F3	F5	F7	F9	ALL
RMSE	0.0095	0.0121	0.0073	0.0065	0.0093	0.0091
MAE	0.0070	0.0102	0.0055	0.0050	0.0074	0.0070
	F12	F14	F16	F18	F20	ALL
RMSE	0.0053	0.0060	0.0055	0.0041	0.0037	0.0050
MAE	0.0040	0.0043	0.0037	0.0028	0.0027	0.0035
	F24	F25	F26	F28	F29	ALL
RMSE	0.0008	0.0011	0.0021	0.0011	0.0008	0.0013
MAE	0.0003	0.0004	0.0007	0.0004	0.0005	0.0005

Note: The root-mean-square error (RMSE) and mean-absolute error (MAE) are used to evaluate the model fit.

Table A.7. RMSE and MAE of Log Price: $Data_3$, 18/12/2008-22/03/2012

	F1	F3	F5	F7	F9	ALL
RMSE	0.0237	0.0288	0.0207	0.0170	0.0257	0.0235
MAE	0.0186	0.0227	0.0159	0.0129	0.0205	0.0181
	F12	F14	F16	F18	F20	ALL
RMSE	0.0123	0.0154	0.0151	0.0107	0.0113	0.0131
MAE	0.0088	0.0114	0.0112	0.0078	0.0085	0.0096
	F24	F25	F26	F28	F29	ALL
RMSE	0.0107	0.0105	0.0115	0.0079	0.0096	0.0101
MAE	0.0061	0.0054	0.0071	0.0050	0.0058	0.0059

Note: The root-mean-square error (RMSE) and mean-absolute error (MAE) are used to evaluate the model fit.

Table A.8. RMSE and MAE of Log Price: Three-Factor Model (Panel A)

Contracts	$Data_1$		$Data_2$		$Data_3$	
	RMSE	MAE	RMSE	MAE	RMSE	MAE
F1	0.0146	0.0101	0.0076	0.0057	0.0221	0.0174
F3	0.0217	0.0160	0.0121	0.0102	0.0287	0.0226
F5	0.0100	0.0076	0.0074	0.0055	0.0209	0.0161
F7	0.0101	0.0082	0.0065	0.0050	0.0170	0.0130
F9	0.0131	0.0093	0.0093	0.0074	0.0258	0.0205
ALL	0.0145	0.0102	0.0088	0.0068	0.0232	0.0179

Note: The root-mean-square error (RMSE) and mean-absolute error (MAE) are used to evaluate the model fit.

Table A.9. RMSE and MAE of Log Price: Cattle, 12/06/2006-07/09/2010

Contracts	$Data_1$		$Data_2$		$Data_3$	
	RMSE	MAE	RMSE	MAE	RMSE	MAE
C1	0.0124	0.0102	0.0150	0.0128	0.0175	0.0141
C2	0.0144	0.0123	0.0149	0.0123	0.0169	0.0141
C3	0.0054	0.0042	0.0208	0.0181	0.0196	0.0165
C4	0.0133	0.0114	0.0170	0.0139	0.0149	0.0119
C5	0.0140	0.0129	0.0144	0.0123	0.0126	0.0110
C6	0.0164	0.0134	0.0191	0.0164	0.0164	0.0137
ALL	0.0131	0.0107	0.0170	0.0143	0.0165	0.0136

Note: The root-mean-square error (RMSE) and mean-absolute error (MAE) are used to evaluate the model fit.

Table A.10. RMSE and MAE of Log Price: Salmon, 12/06/2006-07/09/2010

Contracts	$Data_1$		$Data_2$		$Data_3$	
	RMSE	MAE	RMSE	MAE	RMSE	MAE
F2	0.0043	0.0033	0.0107	0.0087	0.0174	0.0131
F5	0.0059	0.0048	0.0095	0.0073	0.0231	0.0187
F7	0.0134	0.0106	0.0104	0.0083	0.0166	0.0129
F10	0.0047	0.0036	0.0085	0.0068	0.0190	0.0135
F13	0.0051	0.0044	0.0078	0.0056	0.0177	0.0132
F16	0.0078	0.0060	0.0090	0.0072	0.0144	0.0110
ALL	0.0075	0.0054	0.0094	0.0073	0.0182	0.0137

Note: The root-mean-square error (RMSE) and mean-absolute error (MAE) are used to evaluate the model fit.

Chapter 3

An Analysis of the Fish Pool Market in the Context of Seasonality and Stochastic Convenient Yield

Abstract

Based on the popular Schwartz 97 two-factor approach, we develop a model featuring seasonality and study future contracts written on fresh farmed salmon, which have been actively traded at the Fish Pool Market in Norway since 2006. The model is estimated by means of Kalman filter, using a rich data set of contracts with different maturities traded at Fish Pool between 01/01/2010 and 24/04/2014. The results are then discussed in the context of other commodity markets, specifically live cattle which acts as a substitute.

Keywords: Futures, Commodities, Seasonality, Aquaculture, Fisheries Economics, Agricultural Economics

3.1 Introduction

In this chapter we analyse the futures on fresh farmed salmon traded on the Fish Pool exchange, in the context of seasonality and stochastic convenience yield. Nowadays, about 70% of the world's salmon production is farmed and most of the cultured salmon comes from Norway, Chile, Scotland and Canada (Marine Harvest, 2016). According to the Global Aquaculture Production (2015), "aquaculture is understood to mean the farming of aquatic organisms including fish, molluscs, crustaceans and aquatic plants. Farming implies some form of intervention in the rearing process to enhance production, such as regular stocking, feeding, protection from predators, etc. Farming also implies individual or corporate ownership of the stock being cultivated." In the aquaculture industry, regardless of different species of fish and different farms' technologies, the general process is similar: the farmer releases juvenile fish (recruits) into pens or ponds, feeds them until they reach a certain level, and then harvests for sale; after that, pens or ponds become available for a new generation and a new rotation may begin. These features make aquaculture share lots of common characteristics with agriculture.

Similar to many agricultural commodities, salmon prices show seasonal pattern.[1] As discussed in Bjørndal, Knapp, and Lem (2003), Asche and Bjørndal (2011) and Asche, Misund, and Oglend (2016), the seasonal behaviour of salmon spot price is due to several factors. Generally speaking, on one hand, the availability of different weight classes of salmon for market follows a seasonal pattern because the salmon growth can be affected by the water temperature; on the other hand, the major social events or holidays and changes in salmon's quality can cause seasonal fluctuation in salmon consumption. Considering the front-month futures price as a proxy of spot price, Figure 3.1 plots the average price for each month over the years 2007-2013,[2] from which we can observe that the price peaks in May and hits bottom in October and a lower peak occurs in July. It's also worthwhile to find out the effects of seasonality on futures prices. We obtain the pattern of futures contracts by grouping data into expiration

[1] Seasonality of many agricultural commodities prices can be naturally caused by the market supply, e.g., harvesting pattern, and demand, e.g., consumer preferences. See Brennan (1958), Fama and French (1987), Milonas (1991), Sørensen (2002) and Richter and Sørensen (2002).

[2] We first transform the observed daily prices into the monthly data, then standardize the data by the annual mean value, and finally take the average of each month over the time period.

months,[3] see Figure A.1 in Appendix B. Although patterns are similar, futures prices (Figure A.1) fluctuate within a relatively narrow range, compared to the spot/front-month-futures prices (Figure 3.1).

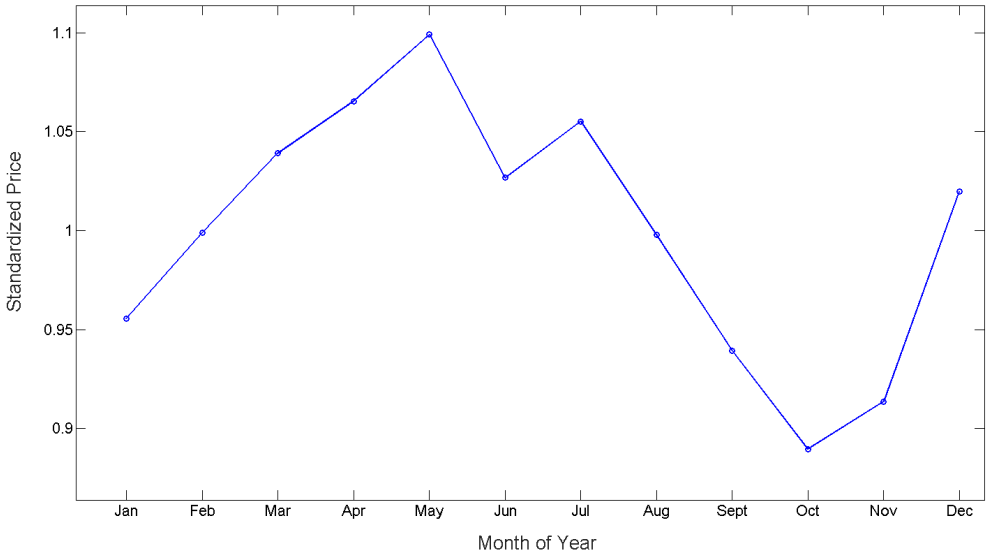

Figure 3.1. Pattern of spot price: the line is obtained by using the front-month futures price as a proxy of spot price, Jan 2007 - Dec 2013.

How to model the seasonality of commodity prices has been addressed in several literature. Inspired by Schwartz and Smith (2000), Sørensen (2002) include the seasonality by modelling the dynamics of the spot price as the sum of a deterministic seasonal component, a non-stationary state-variable, and a stationary state-variable. West (2012) adopted a multifactor seasonal Nelson-Siegel model to obtain seasonal commodity price estimates. Mirantes, Población, and Serna (2013) mainly focus on the convenience yield and use the four-factor model proposed by Mirantes, Población, and Serna (2012) to capture mean-reversion and stochastic seasonality of convenience yield. In our model, the seasonality factor is embedded in the drift term of convenience yield as a function of calendar time. Convenience yield can be understood as the benefit or premium associated with holding an underlying product or physical good, rather than the contract or derivative product. Several papers have indicated that the convenience yield is economically significant, e.g., Brennan (1958), Deaton and Laroque (1992), Routledge, Seppi, and Spatt (2000), Casassus and Collin-Dufresne (2005) and

[3]Unlike plotting time-series data of the spot/front-month-futures prices, the seasonal pattern of futures is investigated via term structure.

Wei and Zhu (2006). They point out that the convenience yield arises endogenously as a result of the interaction among supply, demand, and storage decisions. According to the theory of storage (see Brennan (1958)), there is a negative relationship between supply/inventories and convenience yields. Fama and French (1987) also finds reliable seasonals in the basis for most agricultural and animal products.[4] These previous studies provide some economic rationale for allowing the drift term of convenience yield to capture the seasonality as in our model.

The rest of the paper is structured as follows. In section 2, we give a description of models. In section 3, data and empirical study will be discussed. Following that, in section 4, we draw a comparison between the futures contracts written on live cattle and salmon. Our conclusions are summarised in the final section.

[4]As mentioned in Fama and French (1987), under the theory of storage, inventory seasonals generate seasonals in the marginal convenience yield and in the basis.

3.2 Models

In this section, we demonstrate a valuation model of commodity price and derive the corresponding formula of futures price. Further, by putting the valuation model into the state space form, the empirical model is presented.

3.2.1 Valuation Model

The valuation model is based on the Schwartz (1997) two-factor model, by adding a seasonality feature to the mean-level of convenience yield (α). The spot price of the commodity (P) and the instantaneous convenience yield (δ) are assumed to follow the joint stochastic process:

$$dP(t) = (\mu - \delta(t))P(t)dt + \sigma_1 P(t)dZ_1(t) \tag{3.1}$$

$$d\delta(t) = \kappa(\alpha(t) - \delta(t))dt + \sigma_2 dZ_2(t) \tag{3.2}$$

where

$$\alpha(t) = \alpha_0 + \sum_{k=1}^{N} (\gamma_k \cos(2k\pi \cdot t) + \gamma_k^* \sin(2k\pi \cdot t)) \tag{3.3}$$

$Z_1(t)$ and $Z_2(t)$ are Brownian motions under the real world probability $\mathbb{P}$ and $dZ_1(t)dZ_2(t) = \rho dt$. α_0, γ_k and γ_k^* are constant parameters while N determines the number of trigonometric coefficients. Fackler and Roberts (1999), Sørensen (2002), Richter and Sørensen (2002), Lin and Roberts (2006) use a similar trigonometric function as (3.3) to describe seasonality.

The stochastic convenience yield described in (3.2) reflects the benefits received by agents who hold commodities or physical goods other than derivative contracts. It follows a mean-reverting Ornstein-Uhlenbeck process, where $\alpha(t)$ represents the mean reversion level and $\kappa > 0$ represents the mean reversion speed. The seasonality feature embedded in the convenience yield process by a truncated Fourier series can further influence the price dynamics, for $P(t)$ would be positively correlated with $\delta(t)$ and have implicit mean reversion feature if $\rho > 0$. Specifically, $P(t)$ is likely to be large when

$\delta(t)$ is large and $\delta(t)$ could be larger than μ. In this case, the drift term in (3.1) would push $P(t)$ downwards. The opposite happens if $P(t)$ is small, pushing $P(t)$ upwards.[5]

Under the pricing measure $\mathbb{Q}$ which takes the market price of convenience yield risk (λ) into account, the dynamics are in the form of

$$dP(t) = (r - \delta(t))P(t)dt + \sigma_1 P(t)d\widetilde{Z}_1(t) \tag{3.4}$$

$$d\delta(t) = [\kappa(\alpha(t) - \delta(t)) - \lambda]dt + \sigma_2 d\widetilde{Z}_2(t) \tag{3.5}$$

where $\widetilde{Z}_1(t)$ and $\widetilde{Z}_2(t)$ are $\mathbb{Q}$-Brownian motions and $d\widetilde{Z}_1(t)d\widetilde{Z}_2(t) = \rho dt$. The mean-level of convenience yield under $\mathbb{Q}$ can be defined as

$$\tilde{\alpha}(t) = \alpha(t) - \lambda/\kappa \tag{3.6}$$

which leads to the dynamics

$$dP(t) = (r - \delta(t))P(t)dt + \sigma_1 P(t)d\widetilde{Z}_1(t) \tag{3.7}$$

$$d\delta(t) = \kappa(\tilde{\alpha}(t) - \delta(t))dt + \sigma_2 d\widetilde{Z}_2(t) \tag{3.8}$$

(3.6) can also be expressed as

$$\tilde{\alpha}(t) = \bar{\alpha} + \sum_{k=1}^{N} (\gamma_k \cos(2k\pi \cdot t) + \gamma_k^* \sin(2k\pi \cdot t)) \tag{3.9}$$

where

$$\bar{\alpha} = \alpha_0 - \lambda/\kappa \tag{3.10}$$

3.2.2 Futures Price

Since the interest rate is constant in our model, so the futures and forward price coincide. Therefore, the statements made about futures contracts also hold for forward

[5] Schwartz (1997) illustrates that in an equilibrium setting, supply will increase when prices are relatively high, since higher cost producers of the commodity will enter the market putting a downward pressure on prices and vice versa. This is known as the mean reversion in commodity prices.

contracts and we do not distinguish between them in this paper. Let the futures price at time t with the given and fixed expiration date of contract T be $F(P, \delta, t; T)$. Under the no-arbitrage condition, the futures price satisfies the partial differential equation:

$$\frac{1}{2}\sigma_1^2 P^2 F_{PP} + \sigma_1\sigma_2\rho P F_{P\delta} + \frac{1}{2}\sigma_2^2 F_{\delta\delta} + (r-\delta)PF_P + (\kappa(\tilde{\alpha}(t)-\delta))F_\delta + F_t = 0 \tag{3.11}$$

subject to the terminal boundary condition $F(P, \delta, T; T) = P(T)$. Note, $\tilde{\alpha}(t)$ in (3.11) is the mean-level of convenience yield defined in (3.9). Let $A(t;T) = A_1(t;T) + A_2(t;T)$ and the solution can be verified as follows:

$$\begin{aligned} F(P, \delta, t; T) &= \mathbb{E}_{\mathbb{Q}}\left(P(T)|\mathcal{F}_t\right). && (3.12)\\ &= P(t)e^{A(t;T)+B(t;T)\delta(t)} && (3.13)\\ &= P(t)e^{A_1(t;T)+A_2(t;T)+B(t;T)\delta(t)} && (3.14) \end{aligned}$$

with

$$\begin{aligned} A_1(t;T) &= \left(r - \tilde{\alpha} + \frac{1}{2}\frac{\sigma_2^2}{\kappa^2} - \frac{\sigma_1\sigma_2\rho}{\kappa}\right)(T-t) + \frac{1}{4}\sigma_2^2\frac{1-e^{-2\kappa(T-t)}}{\kappa^3} \\ &\quad + \left(\kappa\tilde{\alpha} + \sigma_1\sigma_2\rho - \frac{\sigma_2^2}{\kappa}\right)\frac{1-e^{-\kappa(T-t)}}{\kappa^2} && (3.15)\\ A_2(t;T) &= \sum_{k=1}^{N}\gamma_k\left(\frac{\sin(2k\pi\cdot t) - \sin(2k\pi\cdot T)}{2k\pi} - \frac{\kappa e^{-\kappa(T-t)}\cos(2k\pi\cdot t) - \kappa\cos(2k\pi\cdot T)}{\kappa^2 + (2k\pi)^2}\right. \\ &\quad \left. - \frac{2k\pi e^{-\kappa(T-t)}\sin(2k\pi\cdot t) - 2k\pi\sin(2k\pi\cdot T)}{\kappa^2 + (2k\pi)^2}\right) \\ &\quad + \sum_{k=1}^{N}\gamma_k^*\left(\frac{\cos(2k\pi\cdot T) - \cos(2k\pi\cdot t)}{2k\pi} - \frac{\kappa e^{-\kappa(T-t)}\sin(2k\pi\cdot t) - \kappa\sin(2k\pi\cdot T)}{\kappa^2 + (2k\pi)^2}\right. \\ &\quad \left. + \frac{2k\pi e^{-\kappa(T-t)}\cos(2k\pi\cdot t) - 2k\pi\cos(2k\pi\cdot T)}{\kappa^2 + (2k\pi)^2}\right) && (3.16)\\ B(t;T) &= -\frac{1-e^{-\kappa(T-t)}}{\kappa} && (3.17) \end{aligned}$$

where the symbol $\mathcal{F}_t$ denotes the information available at time t and $(T-t)$ is the time-to-maturity. Without $A_2(t;T)$, the solution is the same as the solution of classic Schwartz (1997) two-factor model.

3.2.3 Empirical Model

In our model, both the commodity price (P) and the convenience yield (δ) are assumed to be unobservable, and only the futures price (F) can be observed.[6] Once the model has been cast in the state space form, model parameters can be estimated by the Kalman filter. Let $\mathbf{y}_t$ denote a $(n \times 1)$ vector of futures prices observed at time t and $\mathbf{\Phi}_t$ denote a (2×1) vector of state variables, i.e., the log spot price (X) and the convenience yield (δ). The state space representation can be written as

$$\mathbf{y}_t = \mathbf{d}_t + Z_t \mathbf{\Phi}_t + \boldsymbol{\epsilon}_t \tag{3.18}$$

$$\mathbf{\Phi}_{t+1} = \mathbf{c}_t + Q_t \mathbf{\Phi}_t + \boldsymbol{\eta}_t, \tag{3.19}$$

(3.18) is the measurement equation with components

$$\mathbf{y}_t = \begin{pmatrix} \ln F(t;T_1) \\ \vdots \\ \ln F(t;T_n) \end{pmatrix}, \qquad \mathbf{d}_t = \begin{pmatrix} A(t;T_1) \\ \vdots \\ A(t;T_n) \end{pmatrix}, \qquad \mathbf{Z}_t = \begin{pmatrix} 1 & B(t;T_1) \\ \vdots & \vdots \\ 1 & B(t;T_n) \end{pmatrix} \tag{3.20}$$

and $\boldsymbol{\epsilon}_t$ is a $(n \times 1)$ vector of serially uncorrelated disturbance with

$$\mathrm{E}(\boldsymbol{\epsilon}_t) = 0, \qquad \mathrm{Var}(\boldsymbol{\epsilon}_t) = H \tag{3.21}$$

(3.19) is the transition equation with components

$$\mathbf{\Phi}_t = \begin{pmatrix} X(t) \\ \delta(t) \end{pmatrix} \tag{3.22}$$

$$\mathbf{c}_t = \begin{pmatrix} \left(\mu - \frac{1}{2}\sigma_1^2 - \alpha_0\right)\Delta t + \frac{1-e^{-\kappa\Delta t}}{\kappa}\left(\alpha_0 + L(t)\right) - \left(M(t+\Delta t) - M(t)\right) \\ \alpha_0\left(1 - e^{-\kappa\Delta t}\right) + \left(L(t+\Delta t) - e^{-\kappa\Delta t}L(t)\right) \end{pmatrix} \tag{3.23}$$

$$\mathbf{Q}_t = \begin{pmatrix} 1 & \frac{1}{\kappa}\left(e^{-\kappa\Delta t} - 1\right) \\ 0 & e^{-\kappa\Delta t} \end{pmatrix} \tag{3.24}$$

[6] As indicated by Schwartz (1997), one major difficulty in the implementation of commodity price models arises from the indirectly observable state variables. In most cases, the spot price is quite uncertain and the instantaneous convenience yield is hardly estimated, but the futures contracts traded on exchanges are more attainable.

and $\boldsymbol{\eta}_t$ is serially uncorrelated disturbance with

$$\mathrm{E}(\boldsymbol{\eta}_t) = 0, \qquad \mathrm{Var}(\boldsymbol{\eta}_t) = \begin{pmatrix} \sigma_X^2(\Delta t) & \sigma_{X\delta}(\Delta t) \\ \sigma_{X\delta}(\Delta t) & \sigma_\delta^2(\Delta t) \end{pmatrix} \tag{3.25}$$

where $\Delta t = t_{k+1} - t_k$ represents the time interval and T_i denotes the given and fixed maturity of the i-th closest-to-maturity futures contract. The functions $A(\cdot)$ and $B(\cdot)$ are defined in (3.15) - (3.17); while $L(\cdot)$ and $M(\cdot)$ are defined in (31) and (36) respectively in Appendix A. Moreover, the derivation of the joint distribution of $X(t)$ and $\delta(t)$ can be found in Appendix A.

3.3 Data and Empirical Results

In this section, salmon futures prices used for the empirical test will be described and the empirical results will be given and analysed.

3.3.1 Data

Our data set consists of 1126 daily observations of futures prices on Fish Pool ASA from 01/01/2010 to 24/04/2014. We use a similar notation as in Schwartz (1997) and denote with F1 the contract closest to maturity (with average maturity of 0.040 year) counting up to F29 which represents the contract farthest to maturity (with average maturity of 2.389 years). Table 3.1 describes the data features of sample contracts. Unlike Ewald, Ouyang, and Siu (2016) use different combinations of contracts, i.e., short-term, medium-term, long-term and mixed-term, to emphasize different parts of the forward curve, we would not consider the medium-term and long-term contracts individually in this paper. We would expect that on top of lower liquidity of these contracts, over the long time that it takes until these contracts mature, seasonal effects average out and become blurred in a way, which also negatively effects the filter process. Therefore, taking factors as liquidity and representativeness into consideration, two panels with 5 contracts in each are considered in the empirical study.[7] More precisely, Panel A consists of F1, F3, F5, F7 and F9, having relatively short and narrow range of maturities; Panel B contains F1, F7, F14, F20, and F25, having longer and a wider range of maturities. The *last trading day* of contract is chosen to represent the expiration date, for the reason that it is actually the final day that a contract can be traded or closed out at the market without physical delivery.[8] For each contract, its time-to-maturity fluctuates within a certain narrow range as time progress during the sample period.

3.3.2 Empirical Results

Once the model has been cast in the state space form as introduced in Section 3.2.3, the Kalman filter can be applied to estimate parameters in the model. We compare

[7]Comparison can be made between different selection of futures contracts.
[8]No physical delivery but only financial settlement occurs at the Fish Pool.

Table 3.1. Contracts Features, 01/01/2010-24/04/2014

Contract	Mean Price (Standard Deviation)	Mean Maturity (Standard Deviation)
F1	34.67 (7.58) *NOK*	0.040 (0.024) *year*
F3	33.76 (6.27)	0.208 (0.025)
F5	33.27 (5.51)	0.376 (0.025)
F7	32.79 (5.03)	0.543 (0.025)
F9	32.49 (4.50)	0.711 (0.026)
F12	32.24 (4.14)	0.963 (0.026)
F14	31.91 (3.81)	1.131 (0.026)
F16	31.56 (3.50)	1.298 (0.026)
F18	31.38 (3.15)	1.466 (0.026)
F20	31.27 (2.95)	1.634 (0.026)
F24	30.76 (2.73)	1.969 (0.026)
F25	30.56 (2.56)	2.053 (0.026)
F26	30.40 (2.43)	2.137 (0.026)
F28	30.20 (2.19)	2.305 (0.026)
F29	30.08 (2.07)	2.389 (0.026)

Note: We use a similar notation as in Schwartz (1997) and denote with F1 the contract closest to maturity counting up to F29 which represents the contract farthest to maturity.

the estimates with different value of N in (3.3), i.e., the number of trigonometric terms describing seasonality in the model, and select $N = 2$ based on the log-likelihood ratio test,[9] which leads to

$$\alpha(t) = \alpha_0 + [\gamma_1 \cos(2\pi \cdot t) + \gamma_1^* \sin(2\pi \cdot t) + \gamma_2 \cos(4\pi \cdot t) + \gamma_2^* \sin(4\pi \cdot t)] \tag{3.26}$$

By using sample data ranging from 01/01/2010 to 24/04/2014 and choosing the average rate of 3-month Norwegian Treasury Bill as the risk-free rate r (1.81%), the estimates are obtained as shown in Table 3.2. In each panel, parameters are all highly significant at 1% level, except γ_2 in Panel A and γ_2^* in Panel B; the correlation coefficient ρ is positive and large as expected; the expected return on the spot price μ, the mean-reversion speed κ and the market price of convenience yield risk λ are all positive and reasonable. In both cases, one of the standard deviations of the measurement errors goes to zero, which is a common phenomenon in this type of analysis (Schwartz, 1997). Due to containing contracts with relatively short term, Panel A

[9]The test includes a penalty that is an increasing function of the number of estimated parameters.

has lower expected return on spot commodity μ but higher mean-reversion speed κ, compared to Panel B. It's also worth to note that the volatility of convenience yield σ_2 decreases as the term of contracts increases while the volatility of spot price σ_1 is relatively stable, which implies the convenience yield is more sensitive to changes in maturities. The estimates are generally good in both panels as indicated by Table 3.3. Particularly, F7 in Panel A and F20 in Panel B are nearly perfectly fitted by the model.

Table 3.2. Results of Whole Sample, Avg. Rate 1.81%, 01/01/2010-24/04/2014

Parameter	Panel A F1, F3, F5, F7, F9	Panel B F1, F7, F14, F20, F25
μ	0.419 (0.150)***	0.528 (0.173)***
κ	2.885 (0.128)***	0.958 (0.046)***
α_0	0.801 (0.257)***	0.742 (0.217)***
σ_1	0.299 (0.019)***	0.236 (0.016)***
σ_2	1.228 (0.094)***	0.290 (0.023)***
ρ	0.855 (0.026)***	0.908 (0.020)***
λ	1.286 (0.620)**	0.676 (0.222)***
γ_1	0.332 (0.128)***	0.837 (0.121)***
γ_2	-0.215 (0.133)	-1.024 (0.180)***
γ_1^*	-0.586 (0.218)***	-0.425 (0.054)***
γ_2^*	-0.562 (0.179)***	0.143 (0.137)
ξ_1	0.009 (0.001)***	0.009 (0.001)***
ξ_2	0.057 (0.001)***	0.082 (0.002)***
ξ_3	0.049 (0.001)***	0.033 (0.001)***
ξ_4	0	0
ξ_5	0.055 (0.001)***	0.039 (0.001)***
Log-Likelihood	-11409.86	-12452.29

Note: Standard errors in parentheses. [***] Significant at 1% level; [**] Significant at 5% level; [*] Significant at 10% level. μ is the expected return on the spot commodity; κ is the speed of mean-reversion of the convenience yield; α_0 is the constant term in the mean level of the convenience yield; σ_1 is the volatility of the spot price; σ_2 is the volatility of the convenience yield; ρ is the correlation coefficient of spot price and convenience yield; λ is the market price of the convenience yield risk; γ_1, γ_2, γ_1^* and γ_2^* are the coefficients of trigonometric terms in the mean level of the convenience yield; ξ_1 - ξ_5 are the measurement errors.

Figure 3.2 depicts the state variables, i.e., spot price (P) and convenience yield (δ), filtered by the model, from which we can observe a strong positive correlation

Table 3.3. RMSE and MAE of Log Price: Salmon, 01/01/2010-24/04/2014

			Panel A			
	F1	F3	F5	F7	F9	ALL
RMSE	0.0046	0.0575	0.0496	0.0000	0.0552	0.0420
MAE	0.0020	0.0458	0.0375	0.0000	0.0400	0.0251
			Panel B			
	F1	F7	F14	F20	F25	ALL
RMSE	0.0050	0.0817	0.0336	0.0000	0.0410	0.0436
MAE	0.0021	0.0664	0.0248	0.0000	0.0294	0.0246

Note: The root-mean-square error (RMSE) and mean-absolute error (MAE) are used to evaluate the model fit.

not only between state variables but also between spot price and futures price. As we could expected, the ability of futures contracts to proxy spot prices becomes weaker when maturity increases. It is also clear to see a seasonal pattern of each variable, which is consistent with the pattern shown in Figure 3.1 and Figure A.1. Moreover, as shown in Figure 3.3 and Figure 3.4, the spot prices filtered from Panel A and Panel B are almost the same; while the filtered convenience yields share similar pattern but have different bounds due to different selection of futures contracts. Figure 3.5 shows the term structures for each panel, where in each sub-figure, the left part displays the actual term structures and the right part displays the model generated term structures. Moreover, Figure 3.6 displays the term structures on a randomly picked day under both panels. Overall, the model makes a good prediction for each panel, namely the model generated forward curves match the actual forward curves and the filtered spot price is near the price of closest-to-maturity futures. It is obvious that term structures of Panel A and Panel B are different, for they consist of different futures contracts, but as mentioned before, the plots of filtered spot price are nearly the same. Since Kalman filter based estimation is an iterative procedure, we also include the figure of parameter evolution in Appendix B. Figure A.2 shows that the convergence is good in all cases.

(a) Panel A

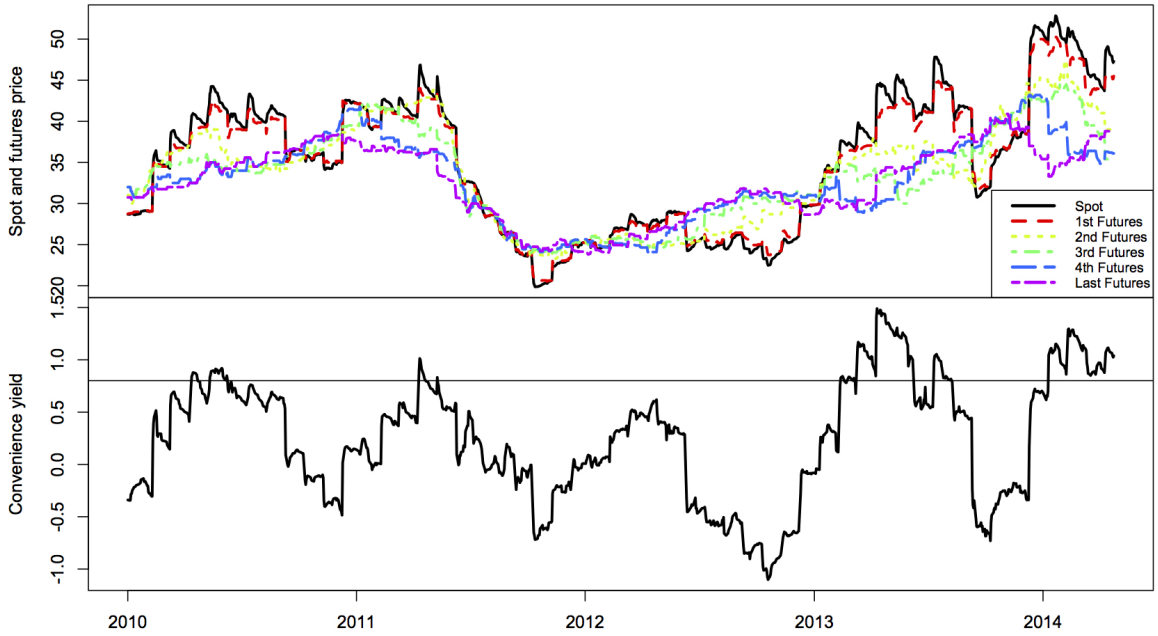

(b) Panel B

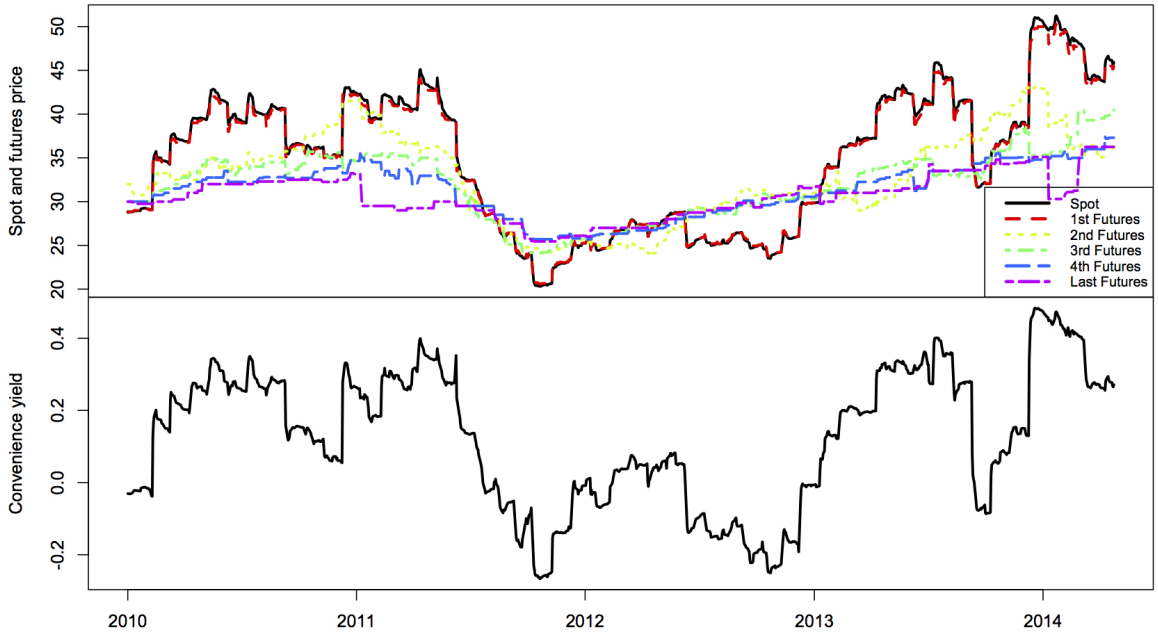

Figure 3.2. State variables: (a) Panel A; (b) Panel B

Note: In each plot, spot and futures prices are on the top of convenience yield. In Panel A, F1, F3, F5, F7 and F9 correspond to the 1st Futures, 2nd Futures, 3rd Futures, 4th Futures and Last Futures in the figure; while in Panel B, F1, F7, F14, F20 and F25 correspond to the 1st Futures, 2nd Futures, 3rd Futures, 4th Futures and Last Futures in the figure.

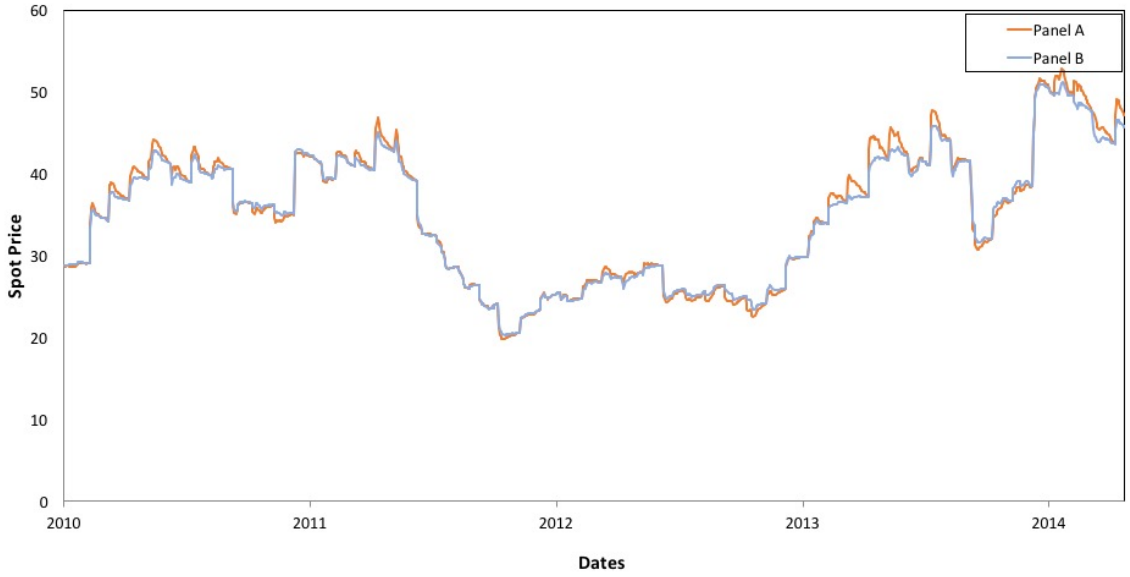

Figure 3.3. Filtered spot prices: Panel A and Panel B

Figure 3.4. Filtered convenience yields: Panel A and Panel B

(a) Panel A

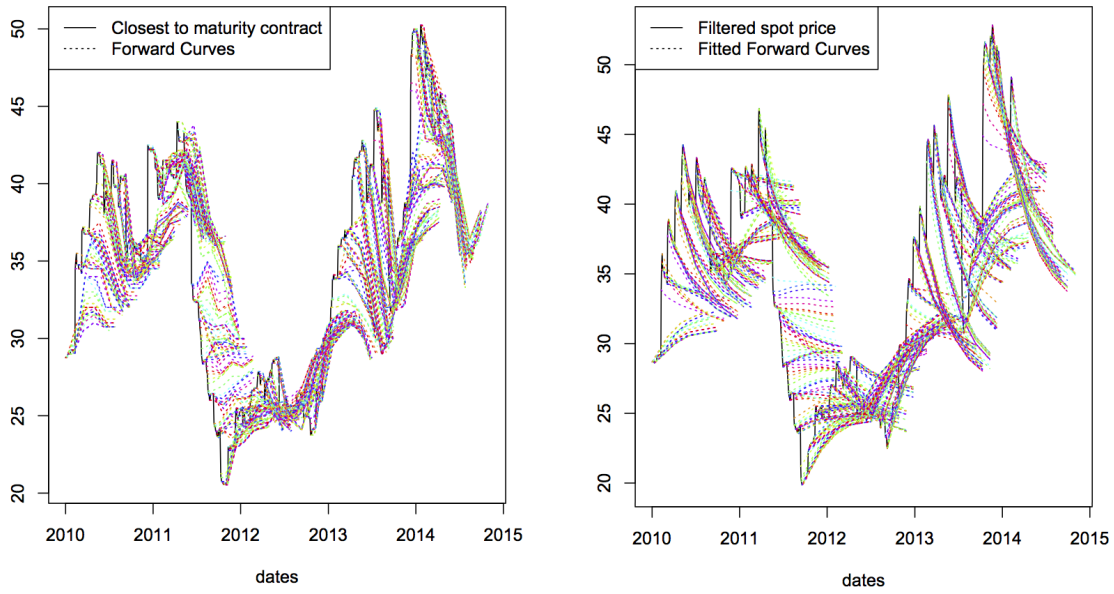

(b) Panel B

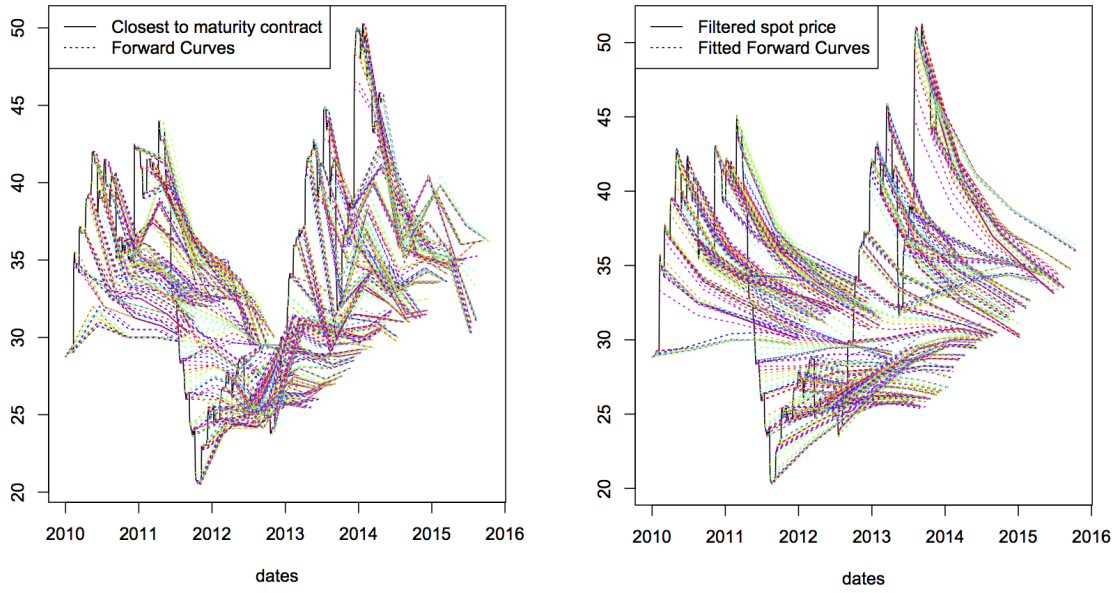

Figure 3.5. Term structures: (a) Panel A; (b) Panel B; actual forward curves on the left, model generated forward curves on the right

Note: Each colored curve is a static picture of futures prices (y-axis) against contract maturities (x-axis), which is analogous to a plot of the term structure of interest rates. On the left side of the figure, the solid line represents the price of the closest-to-maturity futures contract, i.e., $F1$ in this case; while the dashed line consists of the actual prices of other futures contracts with different maturities in this panel. On the right side of the figure, the solid line is the filtered spot price obtained through the estimation procedure; while the dashed line consists of the estimated futures prices given by the pricing formula.

(a) Panel A

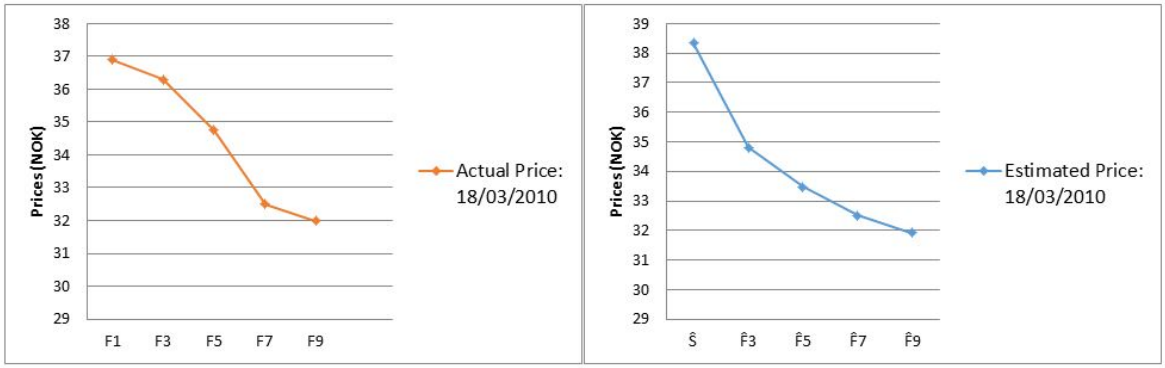

(b) Panel B

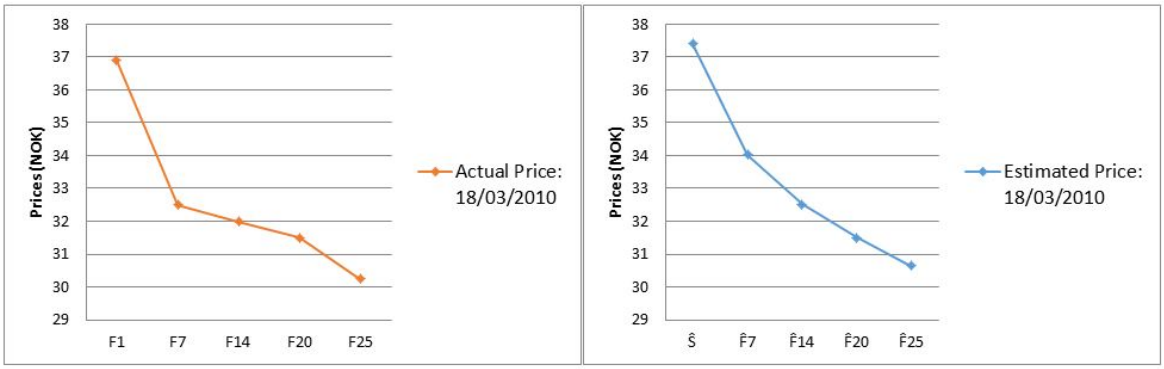

Figure 3.6. Term structures on 18/03/2010: (a) Panel A; (b) Panel B; actual forward curves on the left, model generated forward curves on the right

Note: This figure shows the term structures on a specific day. Each line corresponds to one colored line in Figure 3.5 on the same side of same panel. The observed term structure of salmon prices is on the left; while the estimated term structure is on the right. F1 - F25 denote the actual futures prices with different maturities on 18/03/2010. $\hat{S}$ is the filtered spot price on that day and $\hat{F}3$ - $\hat{F}25$ represent the estimated futures prices.

3.4 Comparison between Cattle and Salmon

How do the salmon futures compare to futures traded on other related commodities? Live cattle seems to reflect some of the properties of farmed salmon as a commodity. Futures on live cattle are the first livestock contracts traded at the Chicago Mercantile Exchange (CME) and have been traded in high volume since 1964. As before, we consider the front-month futures price as a proxy of spot price and check the price pattern of the live cattle. Figure 3.7 plots the average price for each month over the years 2007-2013,[10] from which we can observe that the price peaks in September and hits bottom in June and a lower peak occurs in April. Similar to salmon, the seasonal behaviour of cattle prices is mainly caused by the biological processes and the consumer's demand for beef, which can be largely affected by weather and disease. Based on data availability for both the Fish Pool market and the live-cattle futures market, we have chosen 6 cattle contracts covering almost the same period as for the salmon contracts, i.e., from 04/01/2010 to 24/04/2014. With regard to the risk-free rate, we use the average rate of 3-month Norwegian Treasury Bill rates and 3-month U.S. Treasury Bill rates during the sample period for the salmon and cattle contracts accordingly, i.e., 1.81% and 0.08%, based on the place they traded. Six salmon contracts S2, S4, S6, S8, S10 and S12 [11] as listed in Table 3.1 are chosen for they have similar maturities as the first six cattle contracts, where the closest-to-maturity contract is referred to as C1 and the farthest-to-maturity contract as C6. Table 3.4 illustrates some data features of the cattle contracts. The empirical results of our analysis are shown in Table 3.5. We observe that in general, cattle has higher expected returns on the spot commodity μ and mean-reversion speed κ, but lower volatilities of both spot price and convenience yield, compared to salmon. In addition, the market price of convenience yield risk in the case of cattle is notably higher during the sample period. Some parameters related to seasonality, as γ_2 and γ_2^* for the cattle and γ_1 and γ_1^* for the salmon, are not statistically significant.

[10] We first transform the observed daily prices into the monthly data, then standardize the data by the annual mean value, and finally take the average of each month over the time period.

[11] S- instead of F- is used as the prefix to represent the salmon futures contract in this section. The average maturities of these contracts are 0.124 year, 0.292 year, 0.460 year, 0.627 year, 0.795 year and 0.963 year respectively.

Table 3.4. Contracts Features: Live Cattle, 01/01/2010-24/04/2014

Contract	Mean Price (Standard Deviation)	Mean Maturity (Standard Deviation)
C1	116.73 (14.55) *USD*	0.081 (0.048) *year*
C2	117.68 (14.22)	0.249 (0.048)
C3	118.95 (13.97)	0.416 (0.048)
C4	120.31 (13.96)	0.583 (0.048)
C5	121.05 (13.82)	0.751 (0.048)
C6	121.33 (13.89)	0.918 (0.048)

Note: We use a similar notation as in Schwartz (1997) and denote with C1 the contract closest to maturity of live cattle, counting up to C6 which represents the contract farthest to maturity.

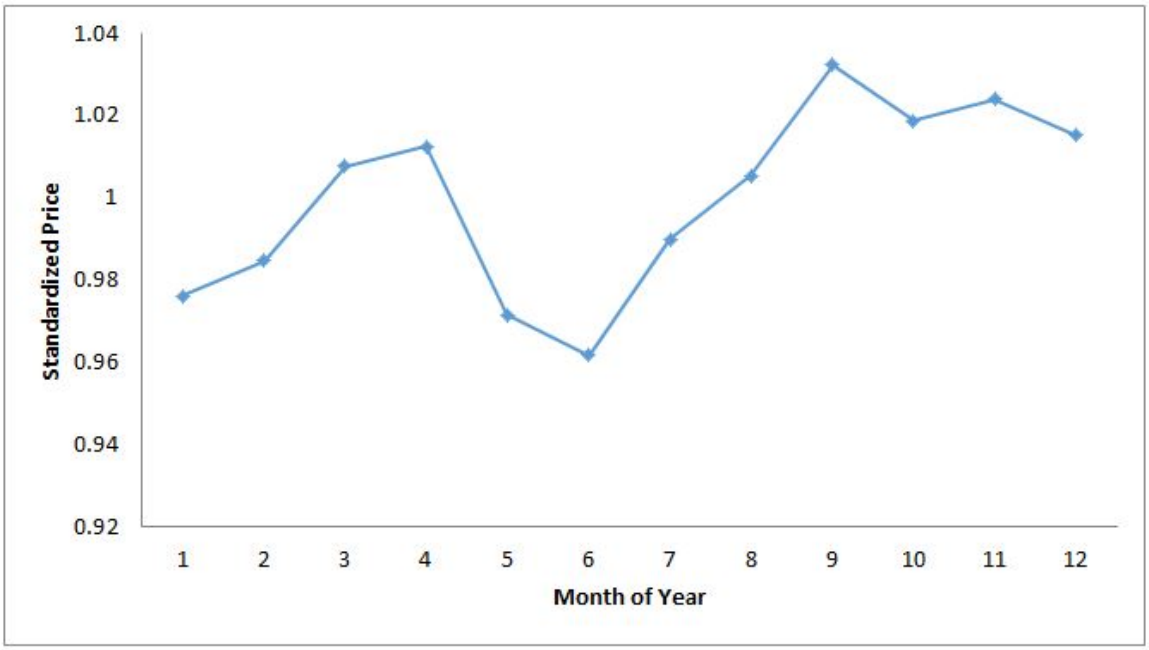

Figure 3.7. Spot price pattern of cattle: the line is obtained by using the front-month futures price as a proxy of spot price, Jan 2007 - Dec 2013.

Table 3.5. Estimation Results: Comparison between Live Cattle and Salmon, 01/01/2010-24/04/2014

Parameter	Live Cattle C1, C2, C3, C4, C5, C6	Salmon S2, S4, S6, S8, S10, S12
μ	0.992 (0.106)***	0.447 (0.141)***
κ	1.988 (0.120)***	1.000 (0.131)***
α_0	1.058 (0.117)***	0.988 (0.291)***
σ_1	0.162 (0.006)***	0.258 (0.016)***
σ_2	0.347 (0.020)***	0.582 (0.054)***
ρ	0.784 (0.021)***	0.902 (0.015)***
λ	2.211 (0.251)***	1.037 (0.333)***
γ_1	0.025 (0.009)***	-0.007 (0.036)
γ_2	-0.010 (0.033)	-0.175 (0.083)**
γ_1^*	-0.126 (0.013)***	0.041 (0.036)
γ_2^*	0.028 (0.020)	0.244 (0.111)**
ξ_1	0.003 (0.000)***	0.078 (0.002)***
ξ_2	0.022 (0.000)***	0.003 (0.000)***
ξ_3	0.028 (0.001)***	0.043 (0.001)***
ξ_4	0.018 (0.000)***	0.044 (0.001)***
ξ_5	0.002 (0.000)***	0.001 (0.001)**
ξ_6	0.019 (0.000)***	0.053 (0.001)***
Log-Likelihood	-18153.09	-14243.34

Note: Standard errors in parentheses. [***] Significant at 1% level; [**] Significant at 5% level; [*] Significant at 10% level. μ is the expected return on the spot commodity; κ is the speed of mean-reversion of the convenience yield; α_0 is the constant term in the mean level of the convenience yield; σ_1 is the volatility of the spot price; σ_2 is the volatility of the convenience yield; ρ is the correlation coefficient of spot price and convenience yield; λ is the market price of the convenience yield risk; γ_1, γ_2, γ_1^* and γ_2^* are the coefficients of trigonometric terms in the mean level of the convenience yield; ξ_1 - ξ_6 are the measurement errors.

Figure 3.8 shows the filtered state variables, i.e. the spot price and the instantaneous convenience yield, along with selected futures prices. We observe from Figure 3.8 that the convenience yields are notably different in cattle than in salmon. To have a better view of the results, we also plot the filtered spot prices and convenience yields separately in Figure 3.9 and Figure 3.10. Not surprisingly, the spot price and convenience yield obtained from the live cattle and salmon are quite different. While the convenience yield for cattle fluctuates in a relatively narrow range than salmon, see Figure 3.10. This may be attributed to storage issues and costs reflecting that fresh salmon is a highly perishable good, more so than cattle. It may also point towards liquidity issues and the fact that salmon farming is still far less developed than cattle farming, which

Table 3.6. RMSE and MAE of Log Price: Cattle and Salmon, 01/01/2010-24/04/2014

				Live Cattle			
	C1	C2	C3	C4	C5	C6	ALL
RMSE	0.0010	0.0232	0.0269	0.01789	0.0009	0.0182	0.0179
MAE	0.0007	0.0199	0.0214	0.01357	0.0006	0.0139	0.0117
				Salmon			
	S2	S4	S6	S8	S10	S12	ALL
RMSE	0.0754	0.0010	0.0438	0.0448	0.0002	0.0529	0.0455
MAE	0.0589	0.0005	0.0332	0.0320	0.0001	0.0406	0.0276

Note: The root-mean-square error (RMSE) and mean-absolute error (MAE) are used to evaluate the model fit.

may affect supply. In this case, the benefits for holding salmon in storage in the short term and hence being able to provide liquidity are higher than for cattle. Looking at the term structures in Figure 3.11 as well as root-mean-square-errors (RMSE) and mean-absolute-errors (MAE) in Table 3.6, it appears that the model captures both the salmon and the cattle contracts well but slightly better for the cattle. Term structures of both cattle and salmon on a randomly picked day are shown in Figure 3.12.

(a) Live Cattle

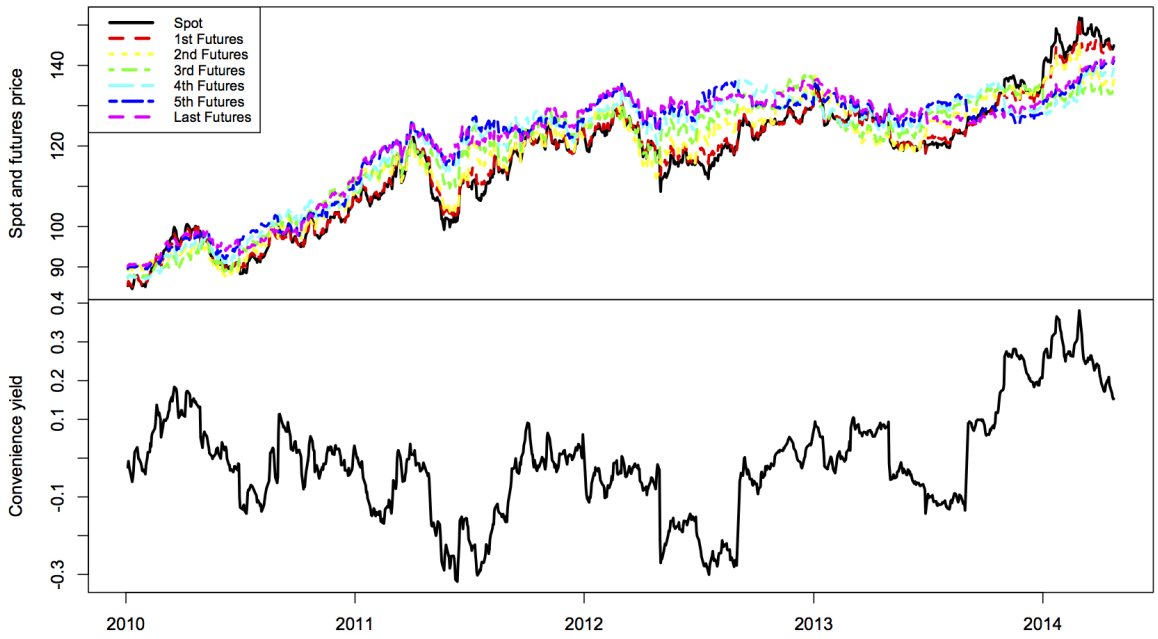

(b) Salmon

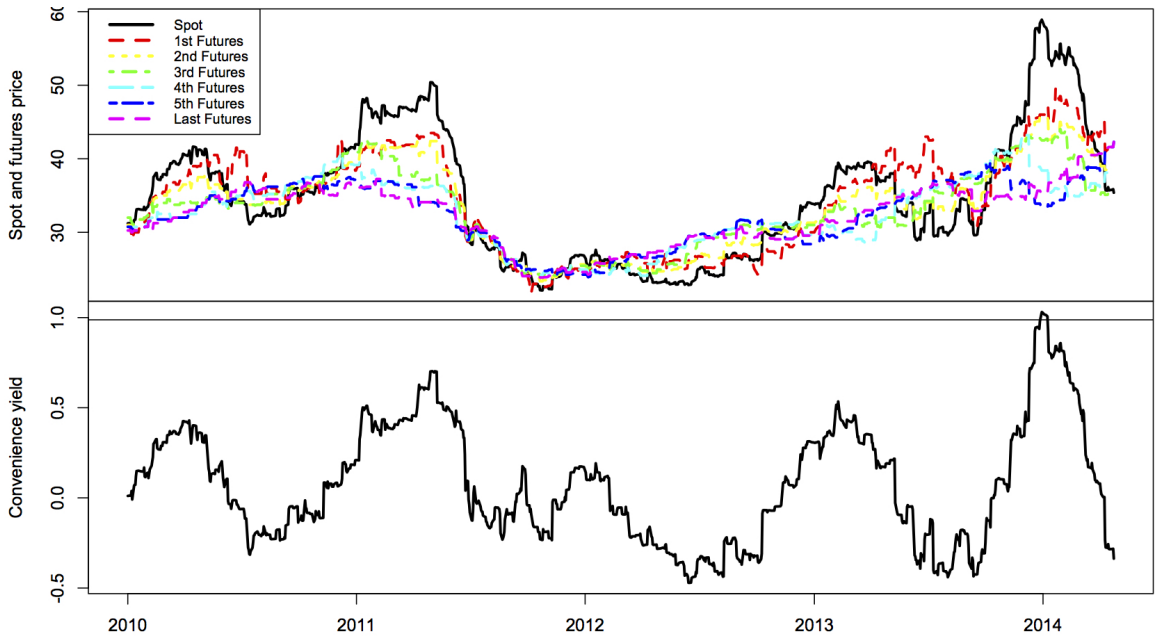

Figure 3.8. State variables: (a) live cattle; (b) salmon

Note: In each plot, spot and futures prices are on the top of convenience yield. In the plot of Cattle, C1, C2, C3, C4, C5 and C6 correspond to the 1st Futures, 2nd Futures, 3rd Futures, 4th Futures, 5th Futures and Last Futures in the figure; while in the plot of Salmon, S2, S4, S6, S8, S10 and S12 correspond to the 1st Futures, 2nd Futures, 3rd Futures, 4th Futures, 5th Futures and Last Futures in the figure.

Figure 3.9. Filtered spot prices: live cattle and salmon

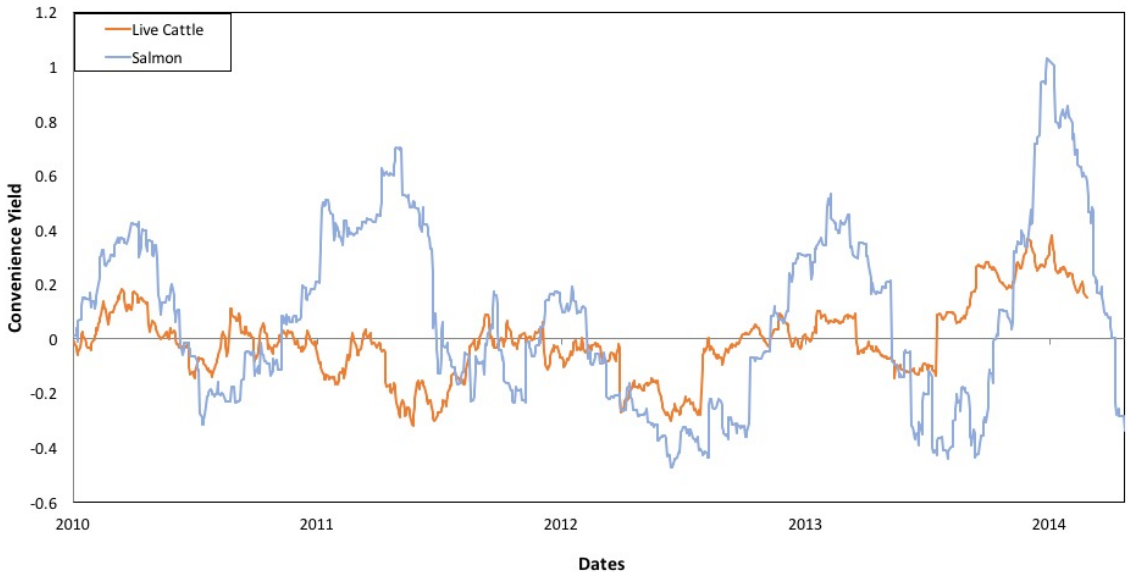

Figure 3.10. Filtered convenience yields: live cattle and salmon

(a) Live Cattle

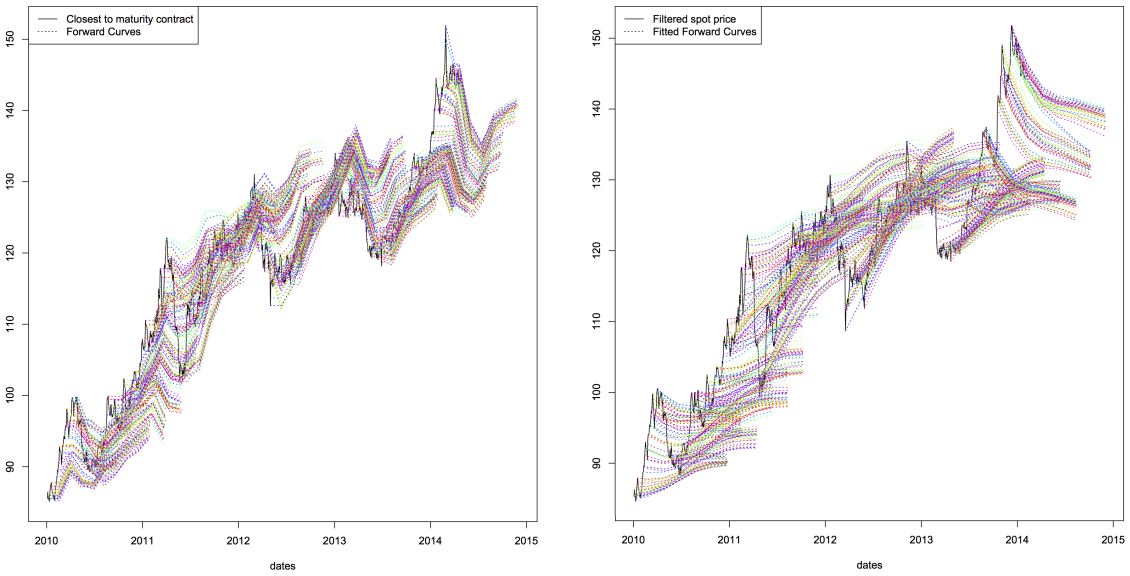

(b) Salmon

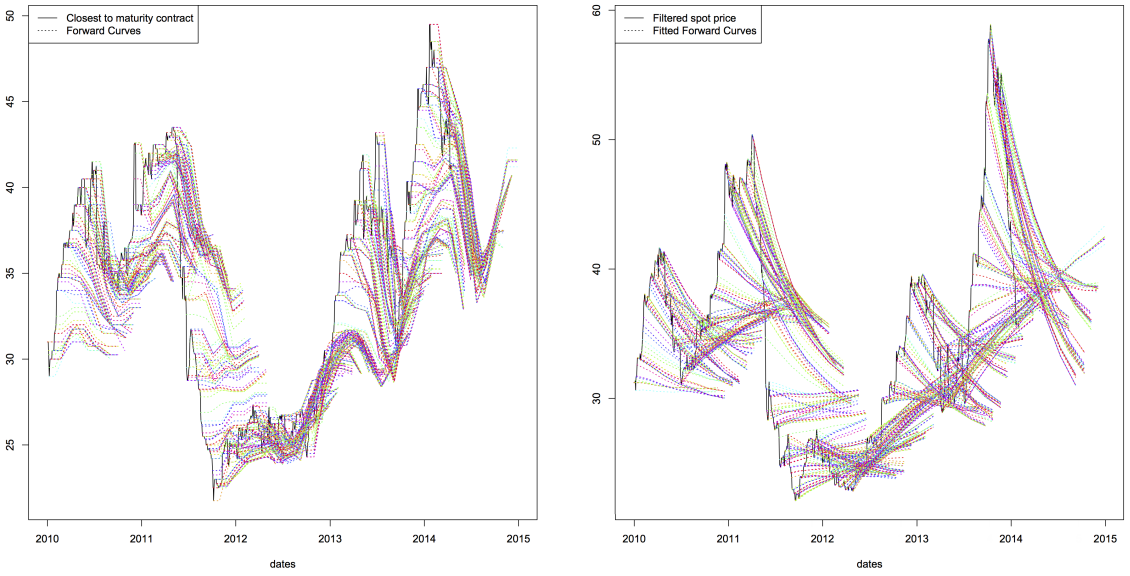

Figure 3.11. Term structures: (a) live cattle; (b) salmon; actual forward curves on the left, model generated forward curves on the right

Note: Each colored curve is a static picture of futures prices (y-axis) against contract maturities (x-axis), which is analogous to a plot of the term structure of interest rates. On the left side of the figure, the solid line represents the price of the closest-to-maturity futures contract, i.e., $C1$ and $S2$ in this case; while the dashed line consists of the actual prices of other futures contracts with different maturities in this panel. On the right side of the figure, the solid line is the filtered spot price obtained through the estimation procedure; while the dashed line consists of the estimated futures prices given by the pricing formula.

(a) Live Cattle

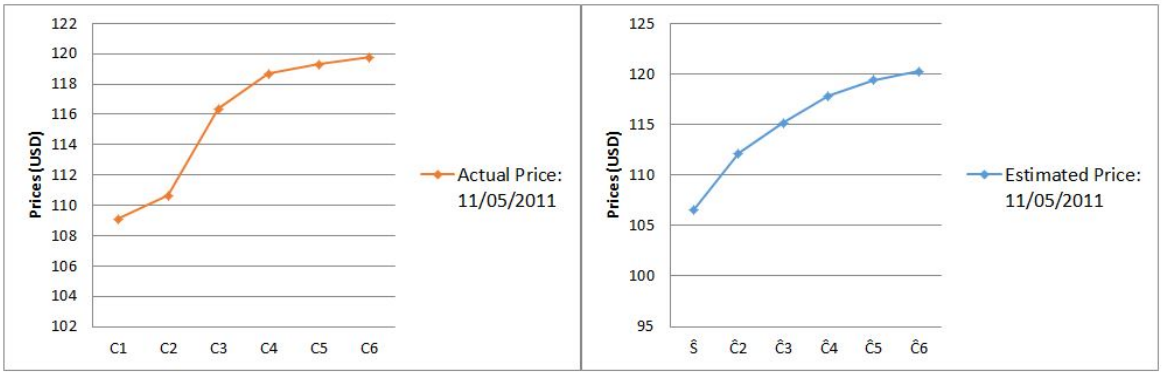

(b) Salmon

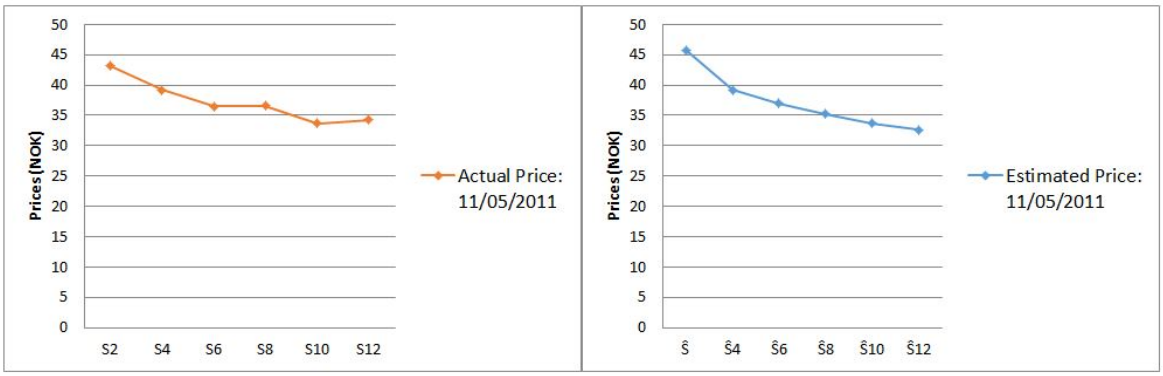

Figure 3.12. Term structures on 11/05/2011: (a) live cattle; (b) salmon; actual forward curves on the left; model generated forward curves on the right

Note: This figure shows the term structures on a specific day. Each line corresponds to one colored line in Figure 3.11 on the same side. The observed term structures of live cattle and salmon prices are on the left; while the estimated term structures are on the right. C1 - C6 and S2 - S12 denote the actual futures prices with different maturities of live cattle and salmon on 11/05/2011 respectively. $\hat{S}$ is the filtered spot price on that day, and $\hat{C}2$ - $\hat{C}6$ as well as $\hat{S}4$ - $\hat{S}12$ represent the estimated futures prices.

3.5 Conclusion

In this paper we set up a valuation model of commodity based on the Schwartz (1997) two-factor model, featuring a seasonality to the convenience yield, and estimate the model using salmon futures prices. Specifically, we add the seasonality factor as a truncated Fourier series to the mean-level of convenience yield (α_t) and derive a formula of the futures price. The empirical analysis is based on futures contracts of salmon with different maturities traded at Fish Pool between 01/01/2010 and 24/04/2014 and the means of Kalman filter. Our results show that the model proposed in this paper can describe the behavior of salmon prices well.

Bibliography

Global Aquaculture Production. (2015). *Food and agricultural organization of united nations.* Retrieved 2016-01-02, from http://www.fao.org/fishery/statistics/global-aquaculture-production/en

Asche, F., & Bjørndal, T. (2011). *The economics of salmon aquaculture* (Vol. 10). John Wiley & Sons.

Asche, F., Misund, B., & Oglend, A. (2016). Determinants of the atlantic salmon futures risk premium. *Journal of Commodity Markets*.

Bjørndal, T., Knapp, G. A., & Lem, A. (2003). *Salmon: a study of global supply and demand.* SNF/Centre for Fishery Economics.

Brennan, M. J. (1958). The supply of storage. *The American Economic Review*, *48*(1), 50–72.

Casassus, J., & Collin-Dufresne, P. (2005). Stochastic convenience yield implied from commodity futures and interest rates. *The Journal of Finance*, *60*(5), 2283–2331.

Deaton, A., & Laroque, G. (1992). On the behaviour of commodity prices. *The Review of Economic Studies*, *59*(1), 1–23.

Erb, P., Lüthi, D., & Otziger, S. (2014). Schwartz 1997 two-factor model technical document.

Ewald, C.-O., Ouyang, R., & Siu, T. K. (2016). On the market consistent valuation of fish farms: using the real option approach and salmon futures. *American Journal of Agricultural Economics*.

Fackler, P. L., & Roberts, M. C. (1999). A term structure model for agricultural futures. In *Selected paper presented at the annual meeting of the american agricultural economics association. nashville, usa.*

Fama, E. F., & French, K. R. (1987). Commodity futures prices: Some evidence on

forecast power, premiums, and the theory of storage. *Journal of Business*, 55–73.

Lin, C., & Roberts, M. C. (2006). A term structure model for commodity prices: Does storability matter? In *Proceedings of the 2006 ncc-134 conference on applied commodity price analysis, forecasting and market risk management.*

Marine Harvest. (2016). *Salmon farming industry handbook.* Retrieved 2016-07-19, from http://www.marineharvest.com/globalassets/investors/handbook/2016-salmon-industry-handbook-final.pdf

Milonas, N. T. (1991). Measuring seasonalities in commodity markets and the half-month effect. *Journal of Futures Markets*, *11*(3), 331–345.

Mirantes, A. G., Población, J., & Serna, G. (2012). The stochastic seasonal behaviour of natural gas prices. *European Financial Management*, *18*(3), 410–443.

Mirantes, A. G., Población, J., & Serna, G. (2013). The stochastic seasonal behavior of energy commodity convenience yields. *Energy Economics*, *40*, 155–166.

Richter, M., & Sørensen, C. (2002). Stochastic volatility and seasonality in commodity futures and options: The case of soybeans. *Journal of Futures Markets*.

Routledge, B. R., Seppi, D. J., & Spatt, C. S. (2000). Equilibrium forward curves for commodities. *The Journal of Finance*, *55*(3), 1297–1338.

Schwartz, E., & Smith, J. E. (2000). Short-term variations and long-term dynamics in commodity prices. *Management Science*, *46*(7), 893–911.

Schwartz, E. S. (1997). The stochastic behavior of commodity prices: Implications for valuation and hedging. *The Journal of Finance*, *52*(3), 923–973.

Sørensen, C. (2002). Modeling seasonality in agricultural commodity futures. *Journal of Futures Markets*, *22*(5), 393–426.

Wei, S. Z. C., & Zhu, Z. (2006). Commodity convenience yield and risk premium determination: The case of the us natural gas market. *Energy Economics*, *28*(4), 523–534.

West, J. (2012). Long-dated agricultural futures price estimates using the seasonal nelson-siegel model. *International Journal of Business and Management*, *7*(3), 78.

Appendix A:

Derivation of the Joint Distribution

The derivation follows the idea proposed by Erb, Lüthi, and Otziger (2014). The joint dynamics of the commodity log-price $X_t = \ln(P_t)$ and the spot convenience yield δ_t can be expressed as [12]

$$dX_t = \left(\mu - \delta_t - \frac{1}{2}\sigma_1^2\right)dt + \sigma_1\sqrt{1-\rho^2}dZ_t^1 + \sigma_1\rho dZ_t^2 \tag{27}$$

$$d\delta_t = \kappa(\alpha_t - \delta_t)dt + \sigma_2 dZ_t^2, \tag{28}$$

By using the substitution $\tilde{\delta}_t = e^{\kappa t}\delta_t$ and Itô's lemma, (28) can be solved

$$\delta_t = e^{-\kappa t}\delta_0 + \kappa e^{-\kappa t}\int_0^t e^{\kappa u}\alpha_u du + \sigma_2 e^{-\kappa t}\int_0^t e^{\kappa u}dZ_u^2 \tag{29}$$

with

$$\kappa e^{-\kappa t}\int_0^t e^{\kappa u}\alpha_u du = \alpha_0(1-e^{-\kappa t}) + L_t \tag{30}$$

where

$$\begin{aligned} L_t = \sum_{k=1}^{N}\frac{\kappa}{\kappa^2+(2k\pi)^2}\Big\{&\gamma_k\left[\kappa\cos(2k\pi\cdot t) + 2k\pi\sin(2k\pi\cdot t) - \kappa e^{-\kappa t}\right] \\ &+\gamma_k^*\left[\kappa\sin(2k\pi\cdot t) - 2k\pi\cos(2k\pi\cdot t) + 2k\pi e^{-\kappa t}\right]\Big\} \end{aligned} \tag{31}$$

Plugging (29) into (27) gives

$$X_t = X_0 + \int_0^t dX_u \tag{32}$$

$$= X_0 + \left(\mu - \frac{1}{2}\sigma_1^2\right)t - \int_0^t \delta_u du + \int_0^t \sigma_1\sqrt{1-\rho^2}dZ_u^1 + \int_0^t \sigma_1\rho dZ_u^2. \tag{33}$$

[12] We indicate time dependence via sub-indices here, e.g. $P_t = P(t)$, which is common in literature.

where

$$\int_0^t \delta_u du = \int_0^t e^{-\kappa u}\delta_0 du + \int_0^t \left(\alpha_0(1-e^{-\kappa u}) + L_u\right) du + \int_0^t \sigma_2 e^{-\kappa u}\left(\int_0^u e^{\kappa s} dZ_s^2\right) du \tag{34}$$

With regards to the integral $\int_0^t \left(\alpha_0(1-e^{-\kappa u}) + L_u\right) du$, we have

$$\int_0^t \left(\alpha_0(1-e^{-\kappa u}) + L_u\right) du = \alpha_0\left(t - \frac{1-e^{-\kappa t}}{\kappa}\right) + M_t \tag{35}$$

where

$$\begin{aligned} M_t = \sum_{k=1}^{N} \frac{\kappa}{\kappa^2 + (2k\pi)^2} \Bigg\{ & \gamma_k \left[\frac{\kappa \sin(2k\pi \cdot t)}{2k\pi} - \cos(2k\pi \cdot t) + e^{-\kappa t}\right] \\ & -\gamma_k^* \left[\frac{\kappa \cos(2k\pi \cdot t)}{2k\pi} + \sin(2k\pi \cdot t) - \frac{\kappa}{2k\pi} - \frac{2k\pi\left(1-e^{-\kappa t}\right)}{\kappa}\right] \Bigg\} \end{aligned} \tag{36}$$

According to Fubini's theorem, the order of integration of $\int_0^t e^{-\kappa u}\left(\int_0^u e^{\kappa s} dZ_s^2\right) du$ can be interchanged as

$$\int_0^t \left(\int_0^u e^{-\kappa u} e^{\kappa s} dZ_s^2\right) du = \int_0^t \left(\int_s^t e^{-\kappa u} e^{\kappa s} du\right) dZ_s^2 \tag{37}$$

$$= \int_0^t \frac{1}{\kappa}\left(1 - e^{-\kappa(t-s)}\right) dZ_s^2 \tag{38}$$

Plugging (35) and (38) into (34) and solving the integrals yields

$$\int_0^t \delta_u du = \frac{\delta_0}{\kappa}\left(1-e^{-\kappa t}\right) + \alpha_0\left(t - \frac{1-e^{-\kappa t}}{\kappa}\right) + M_t + \sigma_2 \int_0^t \frac{1}{\kappa}\left(1 - e^{-\kappa(t-s)}\right) dZ_s^2. \tag{39}$$

Therefore, X_t can be further expressed as:

$$\begin{aligned} X_t = X_0 + \left(\mu - \frac{1}{2}\sigma_1^2 - \alpha_0\right) t + (\alpha_0 - \delta_0)\frac{1-e^{-\kappa t}}{\kappa} - M_t \\ + \int_0^t \sigma_1 \sqrt{1-\rho^2} dZ_u^1 + \int_0^t \left\{\sigma_1 \rho + \frac{\sigma_2}{\kappa}\left(e^{-\kappa(t-u)} - 1\right)\right\} dZ_u^2. \end{aligned} \tag{40}$$

The log-price X_t and the convenience yield δ_t are jointly normally distributed with expectations

$$\begin{aligned} \mathrm{E}(X_t) &= \mu_X = X_0 + \left(\mu - \frac{1}{2}\sigma_1^2 - \alpha_0\right) t + (\alpha_0 - \delta_0)\,\frac{1 - e^{-\kappa t}}{\kappa} - M_t \qquad (41) \\ \mathrm{E}(\delta_t) &= \mu_\delta = e^{-\kappa t}\delta_0 + \alpha_0\left(1 - e^{-\kappa t}\right) + L_t. \qquad (42) \end{aligned}$$

and variances can be obtained by using expectation rules for Itô integrals and the Itô isometry.

$$\mathrm{Var}(X_t) = \sigma_X^2 = \frac{\sigma_2^2}{\kappa^2}\left\{\frac{1}{2\kappa}\left(1 - e^{-2\kappa t}\right) - \frac{2}{\kappa}\left(1 - e^{-\kappa t}\right) + t\right\} + 2\frac{\sigma_1\sigma_2\rho}{\kappa}\left(\frac{1 - e^{-\kappa t}}{\kappa} - t\right) + \sigma_1^2 t \quad (43)$$

$$\mathrm{Var}(\delta_t) = \sigma_\delta^2 = \frac{\sigma_2^2}{2\kappa}\left(1 - e^{-2\kappa t}\right) \quad (44)$$

$$\mathrm{Cov}(X_t, \delta_t) = \sigma_{X\delta} = \frac{1}{\kappa}\left[\left(\sigma_1\sigma_2\rho - \frac{\sigma_2^2}{\kappa}\right)\left(1 - e^{-\kappa t}\right) + \frac{\sigma_2^2}{2\kappa}\left(1 - e^{-2\kappa t}\right)\right] \quad (45)$$

The mean-parameters given in (41) and (42) refer to the $\mathbb{P}$-dynamics. To obtain the parameters under $\mathbb{Q}$ we can simply replace μ by r and α_0 by $\bar{\alpha}$ defined in (3.10).

Appendix B: Additional Figures

Figure A.1 plots the pattern of futures prices by grouping contracts into expiration months during the sample period, from which we can observe a similar pattern as shown in Figure 3.1 and due to the narrower range of maturity, red line has relatively wider bounds than blue line. Figure A.2 and Figure A.3 shows the parameter evolution, due to space limits, not all parameters are included. We can observe that the convergence of parameter is generally good.

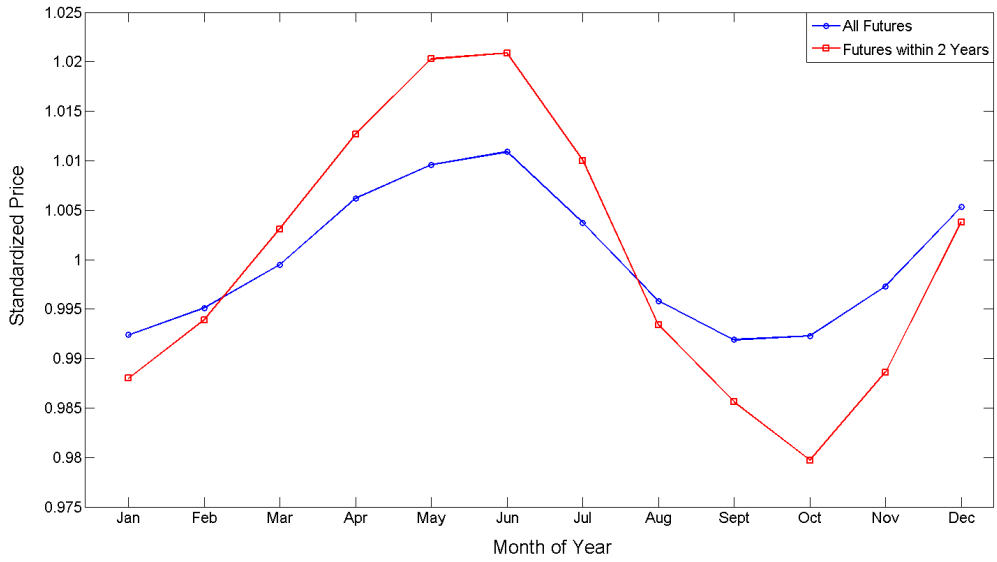

Figure A.1. Price pattern: futures price

Note: Blue line is obtained by grouping all available futures contracts into expiration months; red line is obtained by grouping futures contracts spanned no longer than 2 years into expiration months. The data ranges from Jan 2007 to Dec 2013.

(a) Panel A

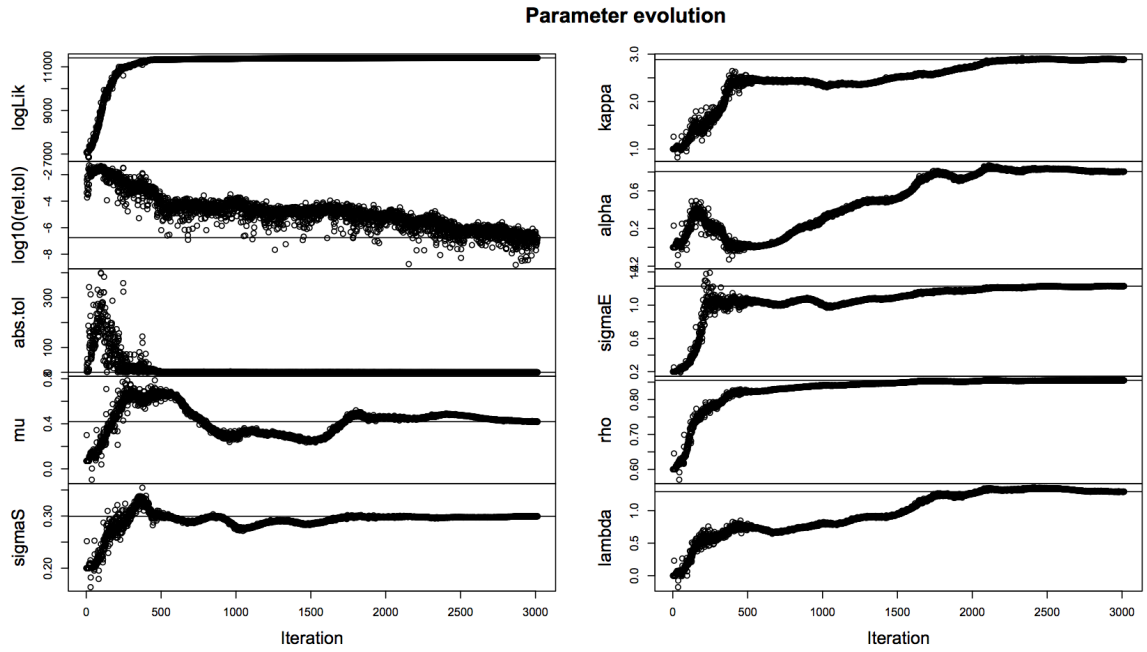

(b) Panel B

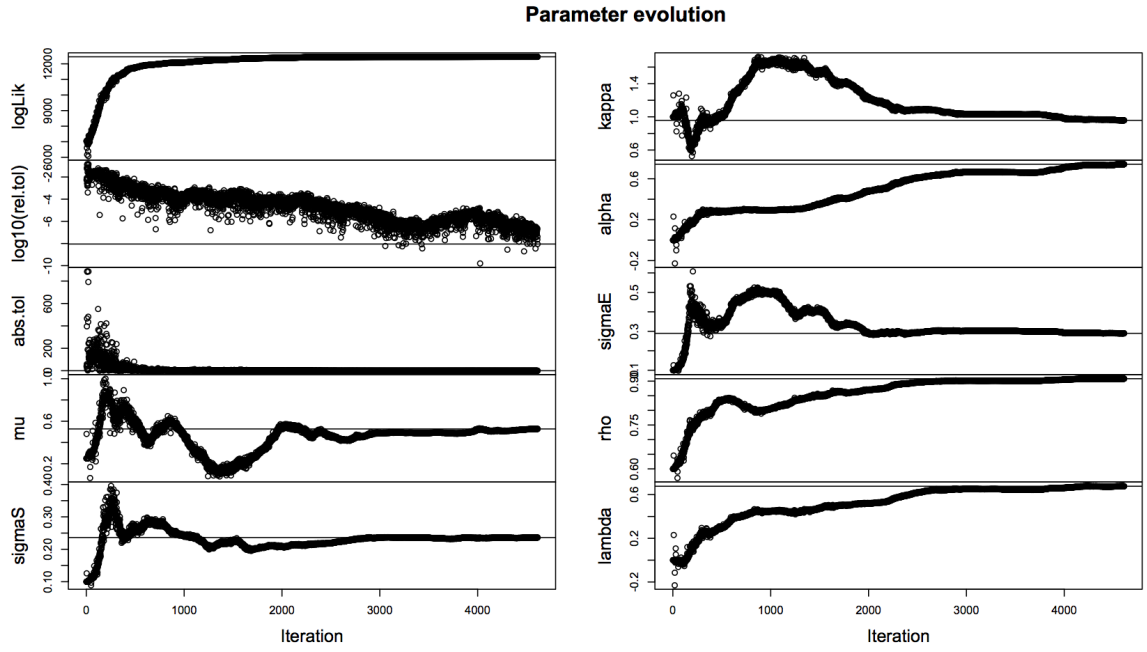

Figure A.2. Parameter evolution: (a) Panel A; (b) Panel B

(a) Live Cattle

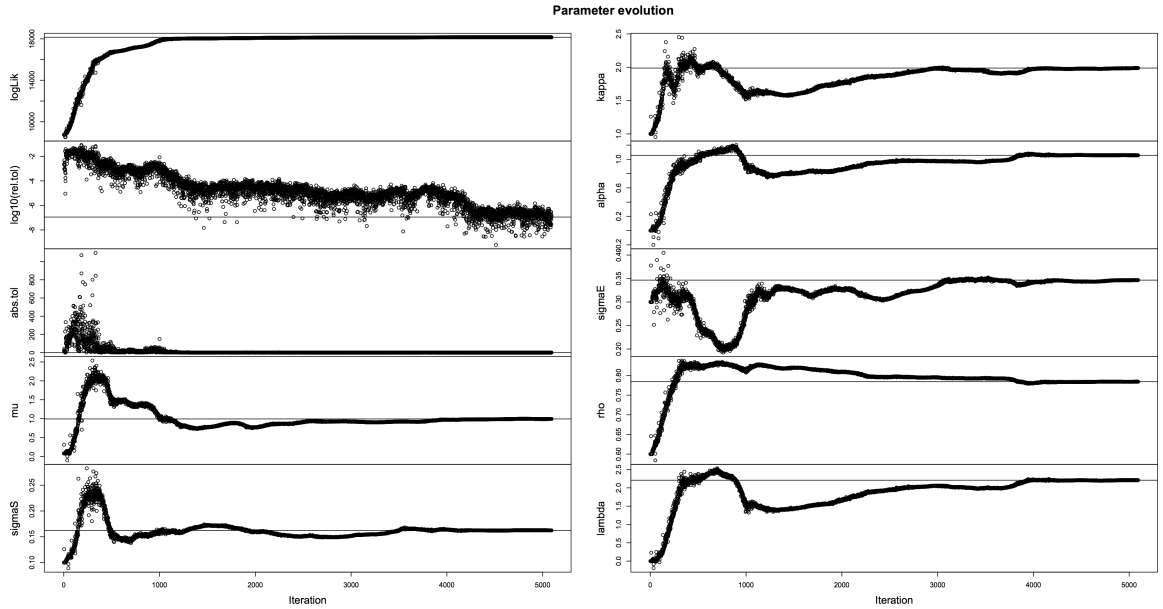

(b) Salmon

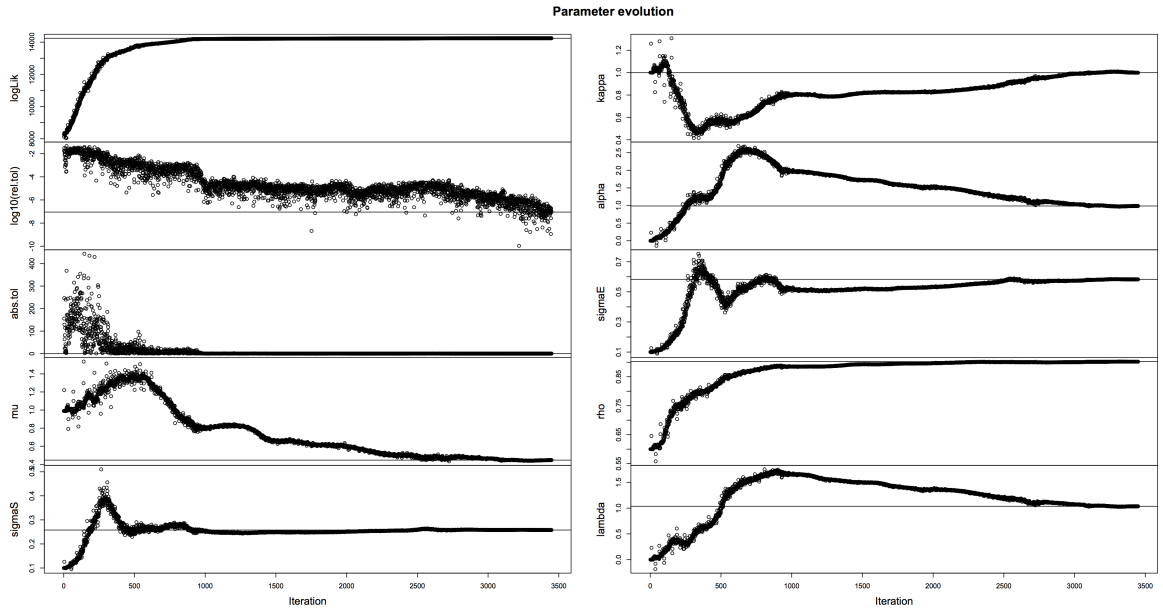

Figure A.3. Parameter evolution: (a) live cattle; (b) salmon

Chapter 4

On the Market Consistent Valuation of Fish Farms: Using the Real Option Approach and Salmon Futures

Abstract

We consider the optimal harvesting problem for a fish farmer in a model which accounts for stochastic prices featuring a Schwartz (1997) two-factor price dynamics. Unlike any other literature in this context, we take account of the existence of a newly established market in salmon futures, which determines risk premia and other relevant variables, that influence the fish farmer in his decision. We consider the cases of single and infinite rotations. The value function of the harvesting problem determined in our arbitrage free setup constitutes the fair values of lease and ownership of the fish farm when correctly accounting for price risk. The data set used for this analysis contains a large set of futures contracts with different maturities traded at the Fish Pool market between 12/06/2006 and 22/03/2012. We assess the optimal strategy, harvesting time and value against two alternative setups. The first alternative involves simple strategies which lack managerial flexibility, the second alternative allows for managerial flexibility and risk aversion as modeled by a constant relative risk aversion utility function, but without access to the salmon futures market. In both cases, the loss in project value

can be very significant, and in the second case is only negligible for extremely low levels of risk aversion. In consequence, for a risk averse fish farmer, the presence of a salmon futures market as well as managerial flexibility are highly important.

Keywords: Futures, Commodities, Aquaculture, Fisheries Economics, Renewable Resources, Real Option, Risk Management

4.1 Introduction

In this chapter we discuss how information reflected in the prices of contracts traded at a market such a Fish Pool can be used to compute fair (i.e. arbitrage free) prices for lease and ownership of fish farms. One of the most crucial elements in this process is to correctly account for risk premia persisting in the stochastically fluctuating salmon spot price and how these affect the harvesting decision of salmon farmers. The value function attached to the harvesting problem, obtained within a generally arbitrage free setting, will then provide the fair value of the salmon farm, either in terms of lease, when single rotation is considered, or in terms of ownership, when infinite rotation is considered. More specifically we are using the Schwartz (1997) two-factor approach to model the stochastic dynamics of the spot price. This approach features a stochastic convenience yield and is considered to be a benchmark in the pricing of commodity futures. It generally provides a good fit to various shapes of the forward curve corresponding to the associated futures prices and can realistically describe classical conditions such as market backwardation or contango.[1]

The salmon farming component of our model is constructed along the line of the classical models discussed in Cacho (1997), Yu and Leung (2006), Guttormsen (2008), Heaps (1995), Bjørndal (1988) and Arnason (1992) but with the added complexity of price uncertainty. Price uncertainty and the effect on harvesting behavior in the salmon context has been discussed in Forsberg and Guttormsen (2006), but in a very simplistic framework, one which is not able to realistically account for market data, such as provided by the Fish Pool market. The latter is also too disconnected from the existing financial literature on asset pricing. In contrast to this, our article is strongly linked to the Schwartz (1997) framework, which is considered to be a benchmark for commodity futures pricing. We estimate the parameters in our model on the basis of

[1] Solibakke (2012) presents an approach using stochastic volatility to model the Fish Pool market. However, only front months contracts are considered and the term structure, which can only be obtained from contracts with longer maturities, is not accounted for. In fact, it is well known that stochastic volatility alone cannot produce realistic term structures. While Solibakke (2012) makes excellent contributions to the understanding of the dynamics of short term contracts at the Fish Pool market, our analysis, which looks at the valuation of lease and ownership of fish farms, looks further ahead into the future and requires information from contracts with longer maturities and the forward curves in particular. We recognize that stochastic volatility on top of stochastic convenience yield would be a desirable feature, but this would lead to a model too complex to handle efficiently.

an extensive data-set obtained from the Fish Pool market covering the period from 12/06/2006 until 22/03/2012. Then, by looking at the optimal stopping problem of an individual fish farmer, we use real option theory to determine the monetary values for lease and ownership for a model fish farm. A related approach has been used to price forestry resources by Chen, Insley, and Wirjanto (2011) based on lumber futures traded on the Chicago Mercantile Exchange. However these authors use a simplification of the Schwartz (1997) two-factor model, the so called "long-term model", which only features one stochastic state variable (a combination of spot price and stochastic convenience yield). This model leads to good approximations of the results that would be produced by the actual two-factor model if rotation periods are sufficiently long. In reality the rotation periods and harvesting cycles in salmon farming are however significantly shorter than for forestry resources, which is why we used the actual two-factor model from Schwartz (1997). We solve this more complex problem by appropriately adjusting the Longstaff and Schwartz (2001) least squares Monte Carlo approach, rather than using the long term approximation.

The existing literature on the economics of salmon farming and aquaculture can broadly be classified into two categories. The first category focuses on models, where salmon prices are assumed to be deterministic. Representative examples are Bjørndal (1988), Arnason (1992), Cacho (1997) who also provides a good survey about general work that falls in this category, Yu and Leung (2006) as well as Guttormsen (2008). Some of these outputs emphasize additional important issues such as optimal feeding schedules or partial harvesting plans. The second category involves models where prices are assumed to follow a stochastic process. Forsberg and Guttormsen (2006) present a simplistic framework in discrete time, where the price process is specified without reflection on actual market prices. The harvesting decision is made on the basis of the agents subjective assessment on the distribution of prices without accounting for risk aversion. More sophisticated models have been developed in the related context of forestry management. Insley (2002) and Insley and Rollins (2003) present continuous time models, with general stochastic price dynamics, emphasizing the effect of mean

reversion.[2] Here, the specification of the dynamic model is informed by historical data on timber prices (no derivatives). The harvesting decision is then based on the expected profits under the empirical distribution of prices. This approach ignores relevant risk premia that reflect the risk aversion of a representative agent. This shortcoming has been corrected in Chen et al. (2011) to which we will refer further below. In general, while adding the important feature of price uncertainty, the literature in the second category is still too disconnected from the existing financial literature on asset pricing. In contrast to this literature, our article is strongly linked to the Schwartz (1997) framework, which is considered to be a benchmark for commodity futures pricing. We estimate the parameters in our model on the basis of an extensive data-set of futures prices obtained from the Fish Pool market, covering the period from 12/06/2006 until 22/03/2012. Futures prices, as opposed to spot prices, allow us to determine the market measure that is used to price contingent claims. They are also far more abundant, spot prices are often only published irregularly and infrequently. By looking at the optimal stopping problem of an individual fish farmer, we then use real option theory to determine the monetary values for lease and ownership for a model fish farm. This analysis is undertaken under the market measure and hence reflects relevant risk premia and the risk aversion of a representative agent who is able to hedge risk exposure through salmon futures.[3] A related approach has been used to price forestry resources by Chen et al. (2011) based on lumber futures traded on the Chicago Mercantile Exchange. However these authors use a simplification of the Schwartz (1997) two-factor model, the so called "long-term model", which only features one stochastic state variable (a combination of spot price and stochastic convenience yield). This model leads to good approximations of the results that would be produced by the actual two-factor model if rotation periods are sufficiently long. In reality the rotation periods and harvesting

[2]The models presented in Insley (2002) and Insley and Rollins (2003) are single-factor models and hence feature significantly reduced mathematical complexity as compared to the model discussed in our article.

[3]This is the only way to price the fish farm in a market consistent way, so as to not introduce arbitrage. Application of the CAPM to price the fish farm is problematic from a number of aspects. As Dusak (1973), Carter, Rausser, and Schmitz (1983) and Baxter, Conine, and Tamarkin (1985) highlight, zero net-supply of futures contract (there is a long position for every short position) make it difficult to account for these assets in the market portfolio. Additionally, as Ewald and Salehi (2015) have demonstrated, correlation from returns in futures position with the returns of the market portfolio is close to zero. Further note that Bessembinder (1992) as well as Xu and Malkiel (2004) confirmed that idiosyncratic risk is priced in agricultural futures markets.

cycles in salmon farming are however significantly shorter than for forestry resources, which is why we used the actual two-factor model from Schwartz (1997). We solve this more complex problem by appropriately adjusting the Longstaff and Schwartz (2001) least squares Monte Carlo approach, rather than using the long term approximation.

The methodology presented is applied to determine value of lease and ownership of a model fish farm. It is important to emphasize that this is for illustrative purposes, as some of the relevant costs are implicit or omitted. Our analysis has been guided by a number of practitioners from salmon farming businesses in Norway and Scotland and we would like to thank those involved for their contributions. Real option theory is applied in aquaculture management, but the financial models currently used do not seem to go beyond Black (1976), which is obtained from our set-up by fixing the convenience yield to a constant level. To further investigate the value of managerial flexibility, we assessed our harvesting strategy against simple ones, taking a similar line as in Mcdonald (2000). We show that our harvesting strategy adds approximately an extra 10% to the farm's value.

Finally, but perhaps most importantly, we look at the impact that the existence of a salmon futures market has on the harvesting decision of an individual fish farmer, depending on the level of risk aversion that this fish farmer exhibits. In order to do this, we assume that the fish farmer's preferences are modeled by a constant relative risk aversion (CRRA) utility function and that the fish farmer does not have access to the salmon futures market. We observe that the loss due to no access to the salmon futures market is only negligible for extremely low levels of risk aversion, but can be very substantial (more than 10%) for reasonable levels of risk aversion. We further observe that the average harvesting time is decreasing with the level of risk aversion, but can be higher or lower without access to the salmon futures market than it is with access. As such our conclusion is that the salmon futures market provides a highly valuable service for risk averse fish farmers. These results are also relevant and related to literature in the context of real options under risk aversion, which includes Hugonnier and Morellec (2007), Henderson (2007) and Ewald and Yang (2008).

The rest of the chapter is structured as follows. In the next section we will briefly review the Schwartz (1997) two-factor approach, while in the following section we summarize the results of our empirical estimation of the model. The optimal harvesting and rotation problem of an individual fish farmer and in consequence the valuation for lease and ownership of a model fish farm are discussed in detail in the penultimate section. The final section contains our main conclusions.

4.2 The Schwartz (1997) Two-Factor Model

Although we have introduced the Schwartz (1997) multifactor framework in Chapter 2, it is worthwhile to have a review of the two-factor model here. Let us denote with $P(t)$ the salmon spot price at time t. This can be identified with the Fish Pool Index against which future contracts are settled at the Fish Pool market. In the Schwartz (1997) two-factor framework the dynamics of $P(t)$ is given by

$$dP(t) = (\mu - \delta(t))P(t)dt + \sigma_1 P(t)dZ_1(t) \tag{4.1}$$

$$d\delta(t) = \kappa(\alpha - \delta(t))dt + \sigma_2 dZ_2(t), \tag{4.2}$$

with constants μ, κ, α, σ_1 and σ_2 under the real world probability $\mathbb{P}$. The two Brownian motions $Z_1(t)$ and $Z_2(t)$ are assumed to be correlated, i.e.

$$dZ_1(t)dZ_2(t) = \rho dt. \tag{4.3}$$

The process $\delta(t)$ represents the stochastic convenience yield and can be recognized as a mean reverting Ornstein Uhlenbeck process, where α represents the mean reversion level and $\kappa > 0$ the mean reversion speed. It reflects the benefits and costs that an agent receives when holding the salmon, such as liquidity and storage/maintenance costs. The price dynamics (4.1) has an implicit mean reversion feature. If $\rho > 0$, then the instantaneous correlation between $P(t)$ and $\delta(t)$ is positive. Hence $P(t)$ is likely to be large when $\delta(t)$ is large and in this case $\delta(t)$ is likely to be larger than μ. The drift term in (4.1) will then push $P(t)$ downwards. The opposite happens if $P(t)$ is small, pushing $P(t)$ upwards. If in fact one chooses $\delta(t) = \kappa \ln(P(t))$, one obtains the dynamics of a geometric Ornstein-Uhlenbeck process in (4.1), and $\delta(t)$ defined in this way satisfies (4.2) with $\rho = 1$. In this case we obtain the so called Schwartz (1997) one-factor model.

A forward contract in this context is an agreement established at a time $s < T$ to deliver or receive the salmon at time T for a price K, which is specified at time s. In

financial terms, the payoff at time of maturity T of such a forward contract is

$$H = P(T) - K. \tag{4.4}$$

We assume here and in the following that the interest rate r is constant. The value K that makes this contract have a value of zero under a no-arbitrage assumption is then given by

$$F_P(s,T) = \mathbb{E}_{\mathbb{Q}}\left(P(T)|\mathcal{F}_s\right). \tag{4.5}$$

This is called the forward price at time s. The symbol $\mathcal{F}_s$ denotes the information available at time s and we denote in the following with $\mathbb{F} = (\mathcal{F}_s)$ the associated filtration which represents the information flow.[4] The expectation in (4.5) is taken with respect to the pricing measure $\mathbb{Q}$, which takes into account a market price of convenience yield risk λ, i.e.

$$dP(t) = (r - \delta(t))P(t)dt + \sigma_1 P(t)d\tilde{Z}_1(t) \tag{4.6}$$

$$d\delta(t) = (\kappa(\alpha - \delta(t)) - \lambda)dt + \sigma_2 d\tilde{Z}_2(t), \tag{4.7}$$

with $\tilde{Z}_1(t)$ and $\tilde{Z}_2(t)$ Brownian motions under $\mathbb{Q}$ and $d\tilde{Z}_1(t)d\tilde{Z}_2(t) = \rho dt$. We assume here and in the following that the interest rate is constant and equal to r. In this case, we do not need to distinguish between forwards and futures.[5]

For convenience, we can always assume that current time is normalized to 0 and that the time of maturity T is relative to this, hence the same as the time to maturity. Since our model is Markovian, we can then denote the futures price in (4.5) as $F(P, \delta, T)$ depending on current spot price, level of convenience yield and time-to-maturity T. With this notation, Schwartz (1997) refers to Jamshidian and Fein (1990)

[4] More precisely, $\mathbb{F} = (\mathcal{F}_s)$ denotes the augmented and completed filtration generated by the Brownian motions $Z_1(s)$ and $Z_2(s)$.

[5] The difference between futures and forwards is that the former are exchange traded, while the latter are mostly traded over the counter (OTC). The exchange usually requires the agent to set up a margin account, the amount held reflecting price movements in the market, protecting buyer and seller from possible default of the other party. The mechanism of the margin account can in principle affect the futures price, but under the assumption of constant rates, it is well known that both futures and forward price coincide.

and Bjerksund (1991) for an explicit expression for (4.5):

$$F(P,\delta,T) = P\cdot\exp\left(-\delta\cdot\left(\frac{1-e^{-\kappa T}}{\kappa}\right)+A(T)\right) \tag{4.8}$$

$$\begin{aligned} A(T) = &\left(r-\alpha+\frac{\lambda}{\kappa}+\frac{1}{2}\frac{\sigma_2^2}{\kappa^2}-\frac{\sigma_1\sigma_2\rho}{\kappa}\right)T+\frac{1}{4}\sigma_2^2\left(\frac{1-e^{-2\kappa T}}{\kappa^3}\right) \\ &+\left(\alpha\kappa-\lambda+\sigma_1\sigma_2\rho-\frac{\sigma_2^2}{\kappa}\right)\left(\frac{1-e^{-\kappa T}}{\kappa^2}\right). \end{aligned} \tag{4.9}$$

Note, that the futures price (4.8) has a log-normal distribution, which makes the analytical pricing of options in this framework possible. On the other hand note that at least one of the state variables, the convenience yield $\delta(t)$ is unobservable. In fact Schwartz (1997) assumes in general that both the commodity price $P(t)$ and the convenience yield $\delta(t)$ are unobservable, and only the future prices (4.8) are observable. In order to estimate the model, Schwartz (1997) then applies Kalman filter techniques.

4.3 Data and Empirical Estimates

Our data set consists of 1496 daily observations of futures prices on Fish Pool ASA from 12/06/2006 to 22/03/2012. For the whole sample period, complete data on the first 29 futures contracts sorted by different maturities are available. We use a similar notation as in Schwartz (1997) and denote with F1 the contract closest to maturity (with average maturity of 0.040 year) counting up to F29 which represents the contract farthest to maturity (with average maturity of 2.382 years).[6] Despite of dividing the whole sample into a number of sub-panels in Chapter 2, we use the whole sample data to do estimation. Contracts in Panel A, Panel B, Panel C and Panel D are chosen as proxies for short-term, medium-term, long-term and mixed-term futures contracts respectively.[7] In each panel, five contracts (i.e., N=5) are used for the estimation. More precisely, Panel A contains F1, F3, F5, F7 and F9; Panel B contains F12, F14, F16, F18, F20; Panel C contains F24, F25, F26, F28 and F29 and Panel D contains F1, F7, F14, F20, F25. Note that Panel D is a combination of two short-term contracts, two medium-term contracts and one long-term contract. Table 4.1 describes the data features.[8]

In this article we use an approach proposed by Schwartz (1997), which is based on Kalman filter, to estimate the parameters in the model. The estimates are shown in Table 4.2, and the root-mean-square deviation (RMSE) and the mean-absolute error (MAE) of each panel are shown in Table 4.3. The risk-free rate r (3.03%) is chosen as the average Norwegian interest rate over the sample period. It can be observed that for each panel, all coefficients are significant at the 1% level; the correlation coefficient ρ is large; the speed of mean-reversion of the convenience yield κ, the expected return on the spot commodity μ, the mean-level of convenience yield α and the market

[6] Contracts expire at the end of each months and over the course of the month time-to-maturity decreases before rollover at the end of the month. F1 is a contract with a notional one month maturity, but because of the time-to-maturity decreasing over the month, the average maturity is just about half a month, which is 0.040 year. In the same way, F2 is a contract which has an average maturity of one and a half month and so on.

[7] The Schwartz (1997) model is able to capture a variety of shapes for the forward curves, but not all. Different time horizons and combinations of contracts in the different panel emphasize different parts of the forward curve. The nature and in particular the time horizon of the problem motivate the choice of a specific panel.

[8] Panel D is a combination of contracts from the other panels and is therefore not displayed in Table 4.1.

Table 4.1. Contracts Features, 12/06/2006 - 22/03/2012

Contract	Mean Price (Standard Deviation)	Mean Maturity (Standard Deviation)
	Panel A	
F1	30.55 (6.14) *NOK*	0.040 (0.024) *year*
F3	30.08 (5.42)	0.207 (0.024)
F5	29.71 (4.92)	0.374 (0.024)
F7	29.33 (4.59)	0.542 (0.024)
F9	28.97 (4.29)	0.709 (0.024)
	Panel B	
F12	28.71 (4.03) *NOK*	0.960 (0.024) *years*
F14	28.45 (3.81)	1.127 (0.024)
F16	28.23 (3.51)	1.295 (0.024)
F18	28.15 (3.40)	1.462 (0.024)
F20	28.07 (3.29)	1.629 (0.024)
	Panel C	
F24	27.67 (2.88) *NOK*	1.964 (0.024) *years*
F25	27.59 (2.77)	2.047 (0.024)
F26	27.53 (2.68)	2.131 (0.024)
F28	27.47 (2.56)	2.299 (0.025)
F29	27.42 (2.49)	2.382 (0.025)

Note: We use a similar notation as in Schwartz (1997) and denote with F1 the contract closest to maturity counting up to F29 which represents the contract farthest to maturity.

price of convenience yield risk λ are all positive and reasonable. The volatility of the spot price σ_1 is relatively stable compared to the volatility of the convenience yield σ_2. Besides, it is also worth to note that the expected return on the spot commodity μ increases while the speed of mean-reversion κ decreases as the term of the contracts increases. The parameters obtained from Panel D seem to reflect and moderate the corresponding parameters from Panels A, B and C. This is intuitive as Panel D is a mixture of contracts from these panels. According to Table 4.3, the estimates are generally good. In addition we have assessed the parameter estimates against possible seasonal effects and found that seasonality only marginally affects the fish farm valuation problem discussed in the later sections. These results are available in Appendix A.

Table 4.2. Estimation Results for Whole Sample, Avg. Rate 3.03%, 12/06/2006-22/03/2012

Parameter	Panel A F1, F3, F5, F7, F9 (Short Term)	Panel B F12, F14, F16, F18, F20 (Medium Term)	Panel C F24, F25, F26, F28, F29 (Long Term)	Panel D F1, F7, F14, F20, F25 (Mixed Term)
μ	0.364 (0.102)***	0.692 (0.078)***	0.818 (0.136)***	0.520 (0.108)***
κ	4.342 (0.110)***	1.092 (0.058)***	0.495 (0.045)***	1.664 (0.054)***
α	0.493 (0.126)***	1.034 (0.117)***	1.286 (0.178)***	0.460 (0.143)***
σ_1	0.236 (0.009)***	0.158 (0.001)***	0.219 (0.003)***	0.214 (0.011)***
σ_2	1.270 (0.062)***	0.221 (0.006)***	0.163 (0.008)***	0.448 (0.026)***
ρ	0.892 (0.011)***	0.803 (0.014)***	0.921 (0.005)***	0.806 (0.029)***
λ	1.799 (0.554)***	1.131 (0.172)***	0.630 (0.132)***	0.690 (0.230)***
Log-Likelihood	-17344.3	-22184.1	-24116.7	-15995

Note: Standard errors in parentheses. [***] Significant at 1% level; [**] Significant at 5% level; [*] Significant at 10% level. μ is the expected return on the spot commodity; κ is the speed of mean-reversion of the convenience yield; α is the mean level of the convenience yield; σ_1 is the volatility of the spot price; σ_2 is the volatility of the convenience yield; ρ is the correlation coefficient of spot price and convenience yield; λ is the market price of the convenience yield risk.

Figure 4.1 below displays the term structure (real and model generated) for Panel A, where the left part shows the actual term structures and the right part shows the model generated term structures, showing that both contango and backwardation are present in the market at different times. Besides, Figure 4.2 gives a view of the term structures on one single day. Term structures for Panel B, Panel C and Panel D are included in Appendix B. In general, the model makes a good prediction for the short-term panel (filtered spot is near closest to maturity future and model generated forward curves match the shape of the actual forward curves) but finds it more difficult to capture the shapes of the forward curves corresponding to longer-term panels, where the actual term structure appears to be rather unconventional, see Figure A.5 - Figure

Table 4.3. RMSE and MAE of Log Prices: Salmon, 12/06/2006-22/03/2012

			Panel A			
	F1	F3	F5	F7	F9	ALL
RMSE	0.0177	0.0269	0.0173	0.0140	0.0228	0.0203
MAE	0.0131	0.0208	0.0125	0.0098	0.0168	0.0146
			Panel B			
	F12	F14	F16	F18	F20	ALL
RMSE	0.0097	0.0128	0.0116	0.0088	0.0094	0.0106
MAE	0.0072	0.0088	0.0078	0.0059	0.0064	0.0072
			Panel C			
	F24	F25	F26	F28	F29	ALL
RMSE	0.0085	0.0085	0.0090	0.0061	0.0076	0.0080
MAE	0.0040	0.0035	0.0043	0.0033	0.0039	0.0038
			Panel D			
	F1	F7	F14	F20	F25	ALL
RMSE	0.0198	0.0350	0.0220	0.0152	0.0265	0.0246
MAE	0.0150	0.0280	0.0158	0.0105	0.0167	0.0172

Note: The root-mean-square error (RMSE) and mean-absolute error (MAE) are used to evaluate the model fit.

A.7 in Appendix B.[9] A more detailed analysis of these data, which also includes an implementation of the Schwartz three-factor model, featuring a stochastic interest rate, is presented in Chapter 2.

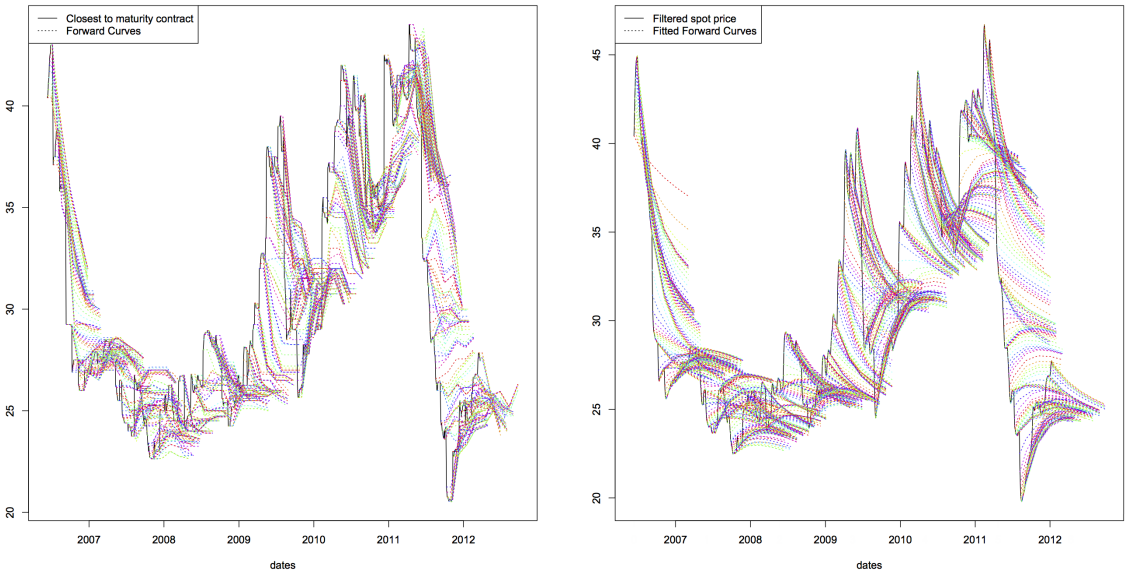

Figure 4.1. Term structures for Panel A: actual forward curves on the left; model generated forward curves on the right

Note: Each colored curve is a static picture of futures prices (y-axis) against contract maturities (x-axis), which is analogous to a plot of the term structure of interest rates. On the left side of the figure, the solid line represents the price of the closest-to-maturity futures contract, i.e., $F1$ in this case; while the dashed line consists of the actual prices of other futures contracts with different maturities in this panel. On the right side of the figure, the solid line is the filtered spot price obtained through the estimation procedure; while the dashed line consists of the estimated futures prices given by the pricing formula.

[9]The slightly odd looking actual term structure for longer dated salmon futures contracts is likely to be caused by the rather low trading volume of these contracts.

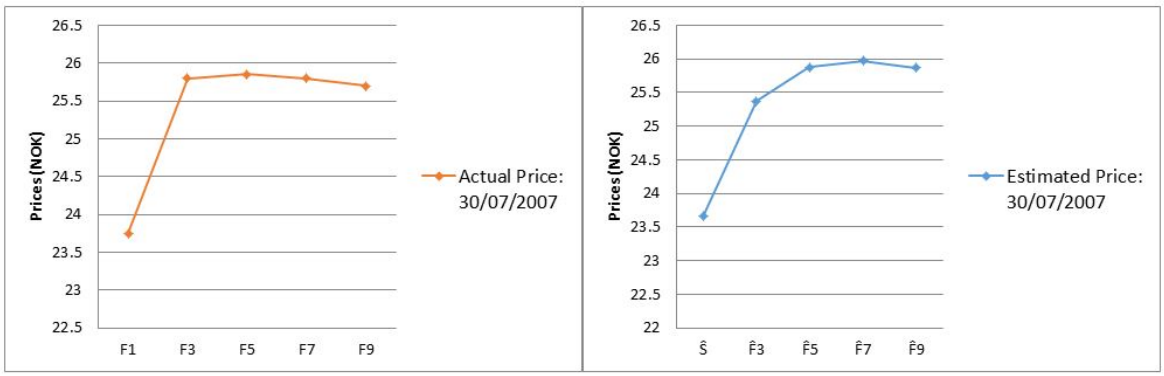

Figure 4.2. Term structure on 30/07/2007: actual forward curve on the left; model generated forward curve on the right

Note: This figure shows the term structure on a specific day. Each line corresponds to one colored line in Figure 4.1 on the same side. The observed term structure of salmon prices is on the left; while the estimated term structure is on the right. F1 - F9 denote the actual futures prices with different maturities on 30/07/2007. $\hat{S}$ is the filtered spot price on that day and $\hat{F}3$ - $\hat{F}9$ represent the estimated futures prices.

4.4 Optimal Harvesting Decision for an individual Fish Farmer and Valuation of the Fish Farm

In this section we discuss the problem of optimal fish farming in the context of the previous sections. We consider a model fish farm, whose manager can decide when to harvest the fish. In this context and in the following we use the word Manager and Fish Farmer synonymously. Both, the case of a single rotation as well as the case of sequential harvesting (infinite number of rotations), will be investigated. We assume that the manager of the fish farm acts rationally and chooses the harvesting time(s) in order to maximize benefits. The so determined value corresponds to the value of a lease (single rotation) respectively ownership (infinite number of rotations) of the fish farm. The methodology applied in this section is usually referred to as the real option approach and shares similarities with the valuation of financial option type derivatives, specifically those of American type, see Dixit and Pindyck (1994) for an overview.

Generally speaking, the fish farmer faces two major uncertainties, i.e., biological and economic uncertainties, which are generated from the stochastic growth and the highly volatile price of fish. Essentially the fish farmer's problem at each point in time is to decide whether it is better to postpone harvest, let the biomass in the pond grow and hope for beneficial movements in the salmon spot price while paying the costs for feeding and maintenance, or harvest the fish and cash in the revenue from selling on the spot market while paying a one time cost for harvesting. In the case of an infinite number of rotations, the salmon farmer will after harvest be able to start a new harvesting cycle.

In his decision whether to harvest now or postpone harvest, the fish farmer weighs up current benefits against expected future benefits. In the absence of the futures market discussed in the earlier sections, this expectation about future benefits would be based on the fish farmer's subjective beliefs, under which the price dynamics and convenience yield follow the dynamics (4.1) and (4.2). This is the standard approach taken in the aquaculture literature. However, the presence of the salmon futures allow

the fish farmer to efficiently hegde the idiosyncratic risk in the salmon spot price.[10] This has the effect, that the rational decision making process of the salmon farmer has to be based on the beliefs expressed by the measure $\mathbb{Q}$ which is used for pricing the salmon future contracts and which has been introduced previously. In fact, only by following this approach, risk premia are correctly accounted for. The fish farmer follows a harvesting strategy which maximizes the financial value of the fish farm, which is an appropriate objective in the corporate setting that fish farms operate nowadays in the real world. This is in line with Schwartz (1997) for crude oil exploration, Chen et al. (2011) for lumber and many other studies.

The model discussed in this article is more complex than most of the models considered in the existing fish farming and aquaculture literature. Next to the two stochastic state variables, spot price and convenience yield, which we introduced in the previous sections, we now include a third state variable into our model which represents the biomass. For simplicity we assume that the average weight $w(t)$ of one individual fish during the harvesting cycle follows a deterministic dynamics represented by a von Bertalanffy's growth function, i.e.

$$w(t) = w_\infty \left(a - be^{-ct}\right)^3. \tag{4.10}$$

Here w_∞ is the asymptotic weight. This growth function has been widely applied in the aquaculture literature. We assume that the total number of fish $n(t)$ at the fish farm unit during the harvesting cycle follows the dynamics

$$dn(t) = -m(t) \cdot n(t)dt, \tag{4.11}$$

where $m(t)$ denotes the mortality rate.[11] Note that salmon does not reproduce in the

[10] Note that the fish farmer can use an appropriate number of futures contracts to eliminate entirely the risk attached to selling a fixed quantity at a pre-determined time in the future. However in the optimal stopping context discussed here, the fish farmer does not know in advance the time when he will harvest nor the quantity. The assumption here is that the fish farmer could run a dynamic portfolio of futures contract to hedge the idiosyncratic risk.

[11] At this point we may well assume that the mortlity rate $m(t)$ is stochastic. In fact this is assumed in Ewald, Nawar, Ouyang, and Siu (2016) and it is shown there how a stochastic mortality rate feeds into the stochastic convenience yield, as it adds to the the cost of storage. In the examples discussed later we assume for simplicity that the mortality rate is constant deterministic.

pens, and therefore the number of salmon in each pen has to decrease over time. The total biomass at the fish farm unit is then given as

$$X(t) = n(t)w(t). \tag{4.12}$$

4.4.1 Single-Rotation Fish Farming

Let us first consider the case of a single rotation. In this case the manager earns revenue from operating the fish farm but returns the fish farm to its owner when one harvesting cycle has been completed. The value determined in that way will correspond to the lease over the period of one harvesting cycle. We assume that to begin with, the fish farm is equipped with a fixed population of smolt[12] and hence initial release costs will not be explicitly accounted for in the single rotation problem. At the time of harvest, the fish farmer will make a profit of $P(t)X(t) - CH(t)$, where $P(t)X(t)$ constitutes the revenue and $CH(t)$ the harvesting costs. This potential profit needs to be evaluated against the option to defer harvest to a later time, and in the mean time pay for certain costs, e.g. feeding the fish. These costs are denoted as $CF(t)$. The optimal harvesting time is the stopping time τ, which is the solution of

$$\max_{\tau} \mathbb{E}_{\mathbb{Q}} \left(e^{-r\tau} \left(P(\tau)X(\tau) - CH(\tau) \right) - \int_0^{\tau} e^{-rt} CF(t) dt \right). \tag{4.13}$$

It is not possible to obtain analytic solutions for an optimal stopping problem of such complexity. For this reason we revert to a numerical approach pioneered by Longstaff and Schwartz (2001) as well as Cortazar, Gravet, and Urzua (2008). This approach is widely known as Longstaff-Schwartz or Least Square Monte Carlo approach.

Longstaff-Schwartz Approach

Following the Longstaff-Schwartz approach we proceed in steps as follows:

Step 1. Path Simulation

A number M of simulated paths over the time horizon T with time-discretization

[12] Infant salmon is commonly referred to as smolt.

$\Delta t = \frac{T}{N-1}$ for the two-factor model presented in the second section are obtained by discretization of (4.6) and (4.7):

$$P_m(t_{n+1}) = P_m(t_n) + (r - \delta_m(t_n))P_m(t_n)\Delta t + \sigma_1 P_m(t_n)\Delta\tilde{Z}_1(t_n) \quad (4.14)$$

$$\delta_m(t_{n+1}) = \delta_m(t_n) + (\kappa(\alpha - \delta_m(t_n)) - \lambda)\Delta t + \sigma_2\Delta\tilde{Z}_2(t_n) \quad (4.15)$$

with

$$\begin{aligned} P_m(t_0) &= P_0, \\ \delta_m(t_0) &= \delta_0, \\ \Delta\tilde{Z}_1(t_n) &= \sqrt{\Delta t}\epsilon_1(t_n), \\ \Delta\tilde{Z}_2(t_n) &= \rho\Delta\tilde{Z}_1(t_n) + \sqrt{1-\rho^2}\sqrt{\Delta t}\epsilon_2(t_n), \end{aligned}$$

where P_0 and δ_0 denote the initial values, $\epsilon_1(t_n) \sim \mathcal{N}(0,1)$, $\epsilon_2(t_n) \sim \mathcal{N}(0,1)$, $m = 1, 2, \ldots, M$ indicates the number of the path that is being generated and $n = 0, 1, \ldots,$ *(N-1)*.

Step 2. Valuation Procedure

Similar as in the valuation and exercising of an American option, the fish farmer makes a decision by comparing the immediate harvesting value (VH) with the expected continuation value (VC) at each point in time. The harvesting value VH originates from sale revenue minus the harvesting cost (CH) while VC accounts for all possible discounted expected future rewards attached to waiting as well as costs for feeding (CF). Suppose the fish farmer makes decisions at K discrete points in time $0 < t_1 \leq t_2 \leq t_3 \cdots \leq t_K = T$. Let $x_{t_n} = [P_{t_n}, \delta_{t_n}]'$ denote the two combined stochastic state variables and as before X_{t_n} the biomass of fish based at the farm, while the σ-algebra $\mathcal{F}_{t_n}$ represents the information available at time t_n.[13] Then the optimal stopping time can be obtained from solving the following Bellman equation:

$$\begin{aligned} V(t_n, x_{t_n}) = \max\{&P_{t_n}X_{t_n} - CH_{t_n}, \\ &-CF_{t_n}\Delta t + e^{-r\Delta t}\mathbb{E}_{\mathbb{Q}}[V(t_{n+1}, x_{t_n+1})|\mathcal{F}_{t_n}]\} \end{aligned} \quad (4.16)$$

[13] In the time discretized setup, we indicate time dependence via sub-indices, i.e. $P_{t_n} = P(t_n)$, which is common in the literature.

where $V(t,x)$ denotes the value function of the problem at time t and state $x = [P, \delta]'$.[14] Expressing the harvesting value VH and the continuation value VC as

$$VH(t_n, x_{t_n}) = P_{t_n} X_{t_n} - CH_{t_n} \tag{4.17}$$

$$VC(t_n, x_{t_n}) = -CF_{t_n}\Delta t + e^{-r\Delta t}\mathbb{E}_{\mathbb{Q}}[V(t_{n+1}, x_{t_n+1})|\mathcal{F}_{t_n}] \tag{4.18}$$

the procedure of determining the optimal harvesting time τ proceeds backwards from time T and harvesting occurs when

$$VC(\tau, x_\tau) < VH(\tau, x_\tau); \tag{4.19}$$

i.e. when the harvesting value is greater than the continuation value.

Step 3. Estimation of the Continuation Value

At each point in time, the harvesting value VH can be readily obtained as a function of the state variables. However the expected continuation value VC is unknown, except at the terminal time T when $VC_T = 0$ as the real option has then expired and fish must be harvested.

However, no-arbitrage pricing dictates that the value of the un-exercised option at time t_n is equal to the sum of the expected remaining future cash flows until expiration, where the expectation is computed under the pricing measure $\mathbb{Q}$. Let C_{t_k} denote the cash-flow generated at time t_k, then the continuation value at time t_n is given as

$$VC(t_n, x_{t_n}) = \mathbb{E}_{\mathbb{Q}}\left[\sum_{k=n+1}^{\tau} e^{-r(t_k - t_n)} C_{t_k} \middle| \mathcal{F}_{t_n}\right], \tag{4.20}$$

with

$$C_{t_k} = \begin{cases} -CF_{t_k}\Delta t + VH_{t_k} & \text{if } \tau = t_k \\ -CF_{t_k}\Delta t & \text{otherwise.} \end{cases}$$

The Longstaff-Schwartz approach provides an easy and efficient way to estimate the

[14] Note that since the biomass $X(t)$ is deterministic, it does not need to be accounted for explicitly as a state variable, but will instead be reflected by the time dependency of the value function.

expected continuation value. The unknown functional form of $VC(t_n, x_{t_n})$ in (4.20) can be expressed as a linear combination of a countable set of measurable basis functions L_j. Assuming the first $J < \infty$ basis functions are used, the continuation value can be approximated as

$$VC_J(t_n, x_{t_n}) = \sum_{j=0}^{J} a_j L_j(t_n, x_{t_n}). \tag{4.21}$$

In this article, we choose a class of quadratic functions for this purpose. As mentioned earlier, state $x = [P, \delta]'$. Let x_1 and x_2 denote the spot price (P) and the convenience yield (δ) respectively. The estimated continuation value at t_n for M simulated paths can then be calculated as,

$$\widehat{VC}_{t_n} = \hat{a_1}{x_1}^2 + \hat{a_2}{x_2}^2 + \hat{a_3}x_1 + \hat{a_4}x_2 + \hat{a_5}x_1x_2 + \hat{a_6}, \tag{4.22}$$

where the estimated coefficients $\hat{a}_j$ are obtained from regressing the discounted values of future cash flows introduced in (4.20), i.e., $\sum_{k=n+1}^{\tau} e^{-r(t_k - t_n)} C_{t_k}$, onto the basis functions for all simulated paths. Moreover Longstaff and Schwartz (2001) suggest that it is more efficient to only use in-the-money paths in the estimation, as the exercise decision is only relevant when the option is in the money. We follow this advice and use only paths with positive harvesting value to run the regression.

Step 4. The Lease Value of the Fish Farm and Harvesting Policy

In the Longstaff-Schwartz approach, harvesting decisions along each path are decoded in matrix form, where rows correspond to different simulated paths, and a 0 resp. 1 matrix entry corresponds to continuation resp. harvesting. Once $\widehat{VC}_{t_n}$ has been obtained, it is compared to the immediate harvesting value VH_{t_n} for each in-the-money path. If the immediate harvesting value is greater than the estimated continuation value, then it is optimal to harvest at t_n and all entries after t_n along that path would be zero, for the fish can only be harvested once. If the continuation value is greater than the immediate harvesting value at t_n, then it is better to wait and the corresponding entry will be set to 0. The procedure starts at $T - \Delta t$ and will be repeated backwards until harvesting decisions at each time point along each path have been determined. More

specifically, let $Flag_m(t_n)$ denote the element in this decision matrix at time t_n for the m-th path, then

a) if $VH_m(t_n) > \widehat{VC}_m(t_n)$,

$$\begin{cases} Flag_m(t_n) = 1 \\ Flag_m(t_i) = 0 \quad \text{for } t_n < t_i \leq T \end{cases}$$

b) if $VH_m(t_n) \leq \widehat{VC}_m(t_n)$, $Flag_m(t_n) = 0$.

The so obtained matrix is then complemented by adding the cost of feeding in each row from left to right, i.e. for each path, up to the "1" entry and replacing the "1" entry with the harvesting value. In this way, each row of the matrix represents the cash flows according to the optimal harvesting decision and the corresponding simulated path. We can then compute the real option value by discounting the realized cash-flows along each path to t_0, and taking the average over all paths. Furthermore, the average harvesting time can be computed by averaging the harvesting times across all simulated paths.

Results

We apply the Longstaff-Schwartz approach presented as above to the fish farming problem, using our estimated parameters for the two-factor model in Table 4.2 reflecting the values of futures contracts traded at the fish pool market during the sample period. A number of other parameters which are relevant to the fish farming process but can (and should) not be inferred explicitly from the salmon futures contracts are listed in Table 4.4. These parameters include elements relevant to feeding costs, mortality and weight function[15] and have been obtained from Asche and Bjorndal (2011), pages 182 and 183. Plots of growth and biomass functions can be found in Appendix B. To calculate the feeding cost, a conversion ratio is used to measure the relationship between feeding quantity and growth/weight of the fish. We use the method of antithetic variates in

[15]The von Bertalanffy's growth function is derived from the polynomial function provided in the book via $w(t) = w_\infty \left(a - be^{-ct}\right)^3$, where w_∞=6, a=1.113, b=1.097, c=1.43.

order to improve the performance of the Longstaff-Schwartz method. In this article, 25,000 paths and corresponding 25,000 antithetic paths are simulated for 72 exercise points over 3 years. In other words, we assume that the fish farmer can make a decision about harvesting twice a month.

Table 4.4. Relevant Parameters for Fish Farming

Parameters	Value
Mortality Rate	10%
Conversion Rate	1.1
Number of Recruits	10000
Time Horizon (*years*)	3
Asymptotic Weight (*kg*)	6
Variable Harvesting Cost per kg (*NOK*)	3
Variable Feeding Cost per kg per year (*NOK*)	7

Note: Parameters which are relevant to the fish farming process but can not be inferred explicitly from the salmon futures contracts are obtained from Asche and Bjorndal (2011).

When should the fish farmer harvest? In the corresponding continuous time model where harvesting can occur at every instantaneous point in time, the optimal harvesting time can be characterized as the first time when $VC(t, x_t) = VH(t, x_t)$ with $x_t = [P_t, \delta_t]'$. This condition describes a two dimensional surface in the (t, P, δ) space, or equivalently for each time t a one-dimensional boundary which splits the (P, δ) space into two regions. In the first region it is optimal to postpone harvesting, while in the second region it is optimal to harvest. This boundary changes over time. In the partial differential equation formulation of the Bellman equation, the so called Hamilton-Jacobi-Bellman equation, this corresponds to the so called free boundary. The original work by Longstaff and Schwartz (2001) as well subsequent work is less conclusive as to how to obtain such a boundary. While under sufficient regularity assumption, in theory the free boundary is a smooth curve in the (P, δ) space which changes shape over time, the time discretization as well as the Monte Carlo/regression element in the Longstaff-Schwartz approach lead to a discrete set of combinations of $(P_m(t_n), \delta_m(t_n))$ where harvesting occurs. These combinations are affected by various estimation and

discretization errors. In this article the free boundary/exercise threshold is obtained by non-linear least squares curve fitting for a class of functions, which we chose to be of the form $f(x) = ax^b + c$. This has been carried out for all scenarios introduced previously. Figure 4.3 shows the result for Panel A while figures for Panel B, Panel C and Panel D are included in Appendix B. Blue spots in the figure represent combinations of P and δ where harvesting occurred. In consequence of the random nature of the problem as well as discretization error, these points do not all lie on the single fitted (thick red) line in the middle. For this reason we also present the boundaries of the 80% confidence intervals above and below the fitted line. These boundaries can also be interpreted as more or less conservative exercise thresholds.[16] The upward sloping concave shape of the curves is characteristic and has been observed in Schwartz (1997) (Table XX and page 970) as well as Chen et al. (2011) Figure 15. For smaller δ the threshold price which triggers harvesting is lower than for larger δ. As Schwartz (1997) page 970 explains, the intuition behind this is that when δ is low at current, because of the mean reversion feature it is likely to be higher in the next period. This will decrease the expected option value (which is decreasing in the convenience yield), and a lower P at current will suffice to make the harvesting payoff larger than the expected option value in the next period, which triggers harvesting. Further, from the dynamics of P, if delta is expected to go up, the growth rate of P is expected to decrease, and as the expected option value is also tied to the expected growth rate, this additionally contributes to decreasing the expected option value and hence lowering the threshold.

Table 4.5 shows for each panel, the lease value of the fish farm over one harvesting cycle and the average harvesting time, that is the average length of the harvesting cycle under the optimal harvesting rule along the different trajectories in the simulation. It can be observed that with the parameter settings obtained from the Fish Pool data as well as Asche and Bjorndal (2011), the average harvesting times are around 2 years, which is a realistic value. The lease values vary between 1.1142 million NOK (0.1186 million EUR) and 1.6467 million NOK (0.1752 million EUR).[17]

[16] Alternative simple harvesting rules are discussed in a later section of this article.

[17] These are realistic values. A comparison with actual prices paid for the acquisition of fish farms is however difficult for the reason that some of the data are confidential. In December 2014, Marine Harvest acquired the assets of Acuinova, a former Chilean salmon farming company, for a total of 125

(a)

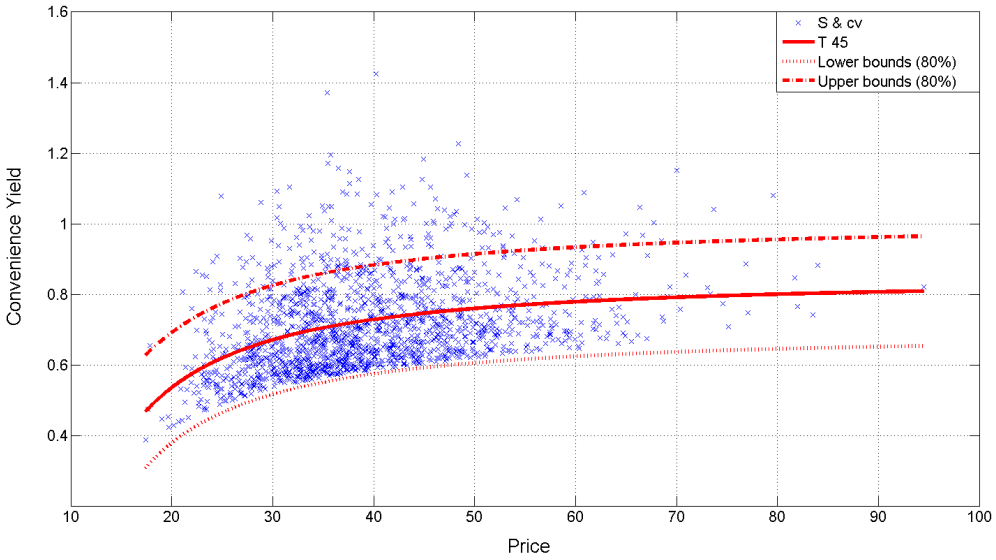

(b)

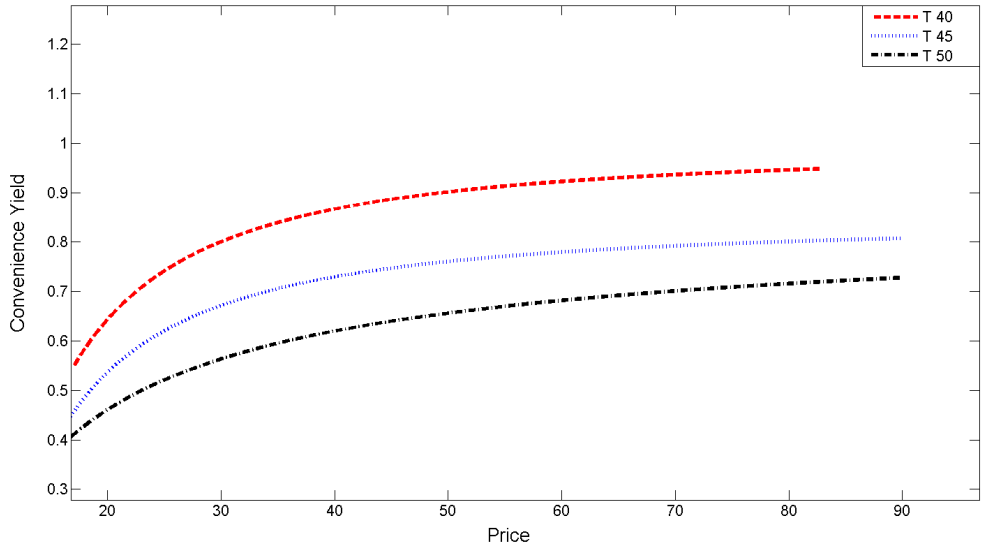

Figure 4.3. Threshold for Panel A: (a) threshold at one time; (b) threshold at different times

Note: S and cv denote spot price and convenience yield respectively. Blue spots in (a) represent combinations of S and cv where harvesting occurred at time point 45. The boundaries of 80% confidence intervals above and below the fitted (thick red) line are also presented and can be interpreted as more or less conservative exercise thresholds. Thresholds at time point 40, 45 and 50 are shown as red, blue and black line accordingly in (b).

Table 4.5. Lease Value of Fish Farm and Harvesting Time

Contracts	Avg. Harvesting Time ($year$)	Pond Value (NOK)	Pond Value (EUR)
$Panel_A$	2.0715	1.5124e+06	1.6092e+5
$Panel_B$	2.4043	1.2220e+06	1.3002e+5
$Panel_C$	2.3550	1.1142e+06	1.1855e+5
$Panel_D$	2.2347	1.6467e+06	1.7521e+5

Note: The table shows for each panel, the lease value of the fish farm over one harvesting cycle and the average harvesting time, that is the average length of the harvesting cycle under the optimal harvesting rule along the different trajectories in the simulation. Exchange rate used here is 1 $NOK = 0.1064$ EUR, http://www.xe.com/ [last access: 02/10/2015].

The impact of the level of mean reversion in the price process on the harvesting decision in the forestry management context has been discussed in Insley (2002) and Insley and Rollins (2003). Specifically, Insley (2002) demonstrates that in the context of their one factor model, a lower level of mean reversion leads to later harvests. The situation in our two factor model is slightly more complex, as the mean reversion is only generated implicitly through the correlation between spot price and convenience yield, as explained previously. An analogue case can be made on the following basis though. By increasing the mean reversion speed κ in the convenience yield, the mean reversion feature in the spot price will be diminished as the convenience yield will become more and more like a constant convenience yield. In the extreme case, $\kappa = \infty$, the spot price will be a geometric Brownian motion which in average grows at the rate of $\mu - \alpha$, which is negative for Panels A, B and C, but positive for Panel D. Panels A and D show a significant larger estimate for κ than Panels B and C, hence the level of mean reversion in prices is less for Panels A and D, than it is for Panels B and D. The corresponding exercise boundaries in Figure 4.3 and Figure A.8 - Figure A.10 indicate that for the same level of convenience yield harvesting occurs at lower prices in Panels A and D than in Panels B and C. We may conclude from this that lower mean reversion in prices leads to earlier harvesting at lower prices. This finding is also supported by Table 4.5, which shows average harvesting times for the four different panels. The result appears to be inverse to the result obtained in Insley (2002) however, this may be explained

million USD. Included in this deal are a hatchery, smolt facility, 36 seawater licenses and primary and secondary processing facilities. The expected harvest volume of this unit lies above 15,000 metric tons in 2015, according to Seafoodsource (2014). The relationship between Fish Pool salmon futures and the share prices of Marine Harvest and The Scottish Salmon Company has been investigated in Ewald and Salehi (2015).

by the different sign in the asymptotic drift term, where in our case $\mu - \alpha$ tends to be negative, while in Insley (2002) and Insley and Rollins (2003) the drift term, at least in the geometric Brownian motion case, is positive. Overall, an exact comparison between the two models is very difficult as the mean reversion feature in our model is far more complex and depending on the combination of a number of parameters.

4.4.2 Infinite-Rotation Fish Farming

We now consider the situation, when the fish farmer/manager initiates a new harvesting cycle, each time the previous harvesting cycle has been completed. This means, that at the time of harvest, the fish farmer not only receives revenue from selling the fish, but in addition obtains the value of the fish farm in its initial state, i.e. harvestable biomass zero, but with smolt released and current values for state variables P_t and δ_t. In addition to the harvesting costs, costs for releasing new smolts into the empty pen accrue at the end of the harvesting cycle. This enables the fish farmer to start a new harvesting cycle, and this procedure continues ad infinitum. As such this problem reflects ownership of the fish farm and its value will hence correspond to the value of ownership. Intuitively, the prospect of starting a new harvesting cycle after completing a previous harvesting cycle provides an incentive for the fish farmer to harvest earlier. It also presents an additional value, i.e. ownership costs more than a lease. For this reason we expect the average harvesting time to decrease and the value to increase. This is confirmed by our technical analysis. Methodologically, this problem is more difficult to solve than the single rotation problem as the value function will now also appear in the harvesting value VH on the right hand side of the Bellman equation.[18] To solve this problem we use a combination of the Longstaff-Schwartz approach with value function iteration.

Analysis

All assumptions and methods adopted in the analysis of single rotation farming are valid for the infinite rotation farming as well. Additionally, since harvesting allows the farmer to start a new cycle, the harvesting value (VH) consists of two parts: the

[18] It always appears in the continuation value VC.

first part is attached to the harvesting itself, namely the sales revenue of fish minus the harvesting cost; the second part is attached to releasing new salmon smolts, where releasing costs (CR), feeding costs and all possible future rewards need to be considered. The latter are implicitly known as the value of the fish farm, in its original state, but under present state variables i.e. $V_0 = V(t_0, P_t, \delta_t)$.[19] We continue to use the notation $x_{t_n} = [P_{t_n}, \delta_{t_n}]'$. To take account of this, the Bellman equation (4.16) needs to be adjusted in the following way:

$$\begin{aligned} V(t_n, x_{t_n}) &= \max\{P_{t_n}X_{t_n} - CH_{t_n} - CR_{t_0} + V_0, \\ &\quad -CF_{t_n}\Delta t + e^{-r\Delta t}\mathbb{E}_{\mathbb{Q}}[V(t_{n+1}, x_{t_n+1})|\mathcal{F}_{t_n}]\}\,. \end{aligned} \tag{4.23}$$

This equation takes into account that the smolt has to be fed in the periods after release.

As indicated before, the algorithm used to solve equation (4.23) is an extension of the algorithm used for the single rotation problem, which now however also entails value function iteration. We proceed in steps as follows:

Step 1. Obtain the farm value ${V_0}^1$ as an initial approximation with harvesting value function $VH(t_n, x_{t_n}) = P_{t_n}X_{t_n} - CH_{t_n} - CR_{t_0}$.

Step 2. Decode the value function in matrix form, set domain and choose grid points for price and convenience yield. If n prices and m convenience yield values are selected, we obtain the $n \times m$ values for the matrix by running the Longstaff-Schwartz algorithm as in the previous section with all combinations for price and convenience yield.

Step 3. Obtain the updated farm value (as a matrix) ${V_0}^2$ with $VH(t_n, x_{t_n}) = P_{t_n}X_{t_n} - CH_{t_n} - CR_{t_0} + {V_0}^1$.[20]

[19] The time t_0 is just a reference time at which the biomass is in its initial state. It can be assumed as $t_0 = 0$ if convenient.

[20] In order to efficiently evaluate the value function on non-grid points, which arise in the Monte Carlo part of the Longstaff-Schwartz approach, an interpolant for the data set that supports interpolation within the grid is created in each iteration. In this article, the method of linear interpolation is selected.

Step 4. If the termination condition is satisfied, ${V_0}^2$ would be chosen as the value matrix. If not, we update the value matrix ${V_0}^3$ with $VH(t_n, x_{t_n}) = P_{t_n} X_{t_n} - CH_{t_n} - CR_{t_0} + {V_0}^2$ and check whether the termination condition is met. We operate iteratively until the termination condition is reached. The termination condition itself measures the relative distance (in matrix norm) between two consecutive value matrices, i.e. $\frac{\|V_0^{k+1} - V_0^k\|}{\|V_0^k\|}$. The algorithm terminates if this value falls below a certain threshold.

Results

Once the value function V_0 has been obtained, we can obtain other relevant results, such as the average harvesting time and thresholds for the infinite rotation fish farming problem. In this part of the article, we consider Panel B over the whole sample period 12/06/2006-22/03/2012 as an example to illustrate the results for the infinite rotation case.[21] We adopt the average 10-year Norwegian bond rate as the proxy of infinite interest rate, i.e., 3.93%, during the sample period and estimates are shown in Table 4.6. This rate suites the time-frame of the problem best. Nevertheless, to get a sense about the robustness of our results, we have considered the other panels as well as three appropriate sub-periods corresponding to three different regimes in the Norwegian base rate. These results are summarized in Chapter 2.

For technical reasons (we rely on a finite set of grid points) we have to disqualify paths in the Monte-Carlo part of the Longstaff-Schwartz method, which leave the grid space. In our particular application we chose these limits to be $P_t \in [10, 100]$ and $\delta_t \in [-1.5, 1.5]$. In theory, this presents an alteration of the Schwartz (1997) two-factor model, however in reality, prices outside the grid space have not been observed since the fish pool market has been created in 2006 and would in fact be highly questionable. The same holds for the convenience yields. As such, we expect that this feature of our analysis actually leads to better and more realistic results. Taking both accuracy and

[21] Panel B represents the medium-term contracts and covers an appropriate mix of maturities, suited to the nature and time frame of the problem. Contracts in panel B are also among the most liquid contracts and hence the price information obtained from these contracts is likely to be the most reliable. Contracts with longer maturities than those present in panel B are far less liquid and hence less reliable for our purpose.

Table 4.6. Estimation Results for Panel B, Avg. Rate 3.93%, 12/06/2006-22/03/2012

Parameter	Medium-term Contract (F12, F14, F16, F18, F20)
μ	$0.654\ (0.103)^{***}$
κ	$1.012\ (0.096)^{***}$
α	$1.135\ (0.193)^{***}$
σ_1	$0.153\ (0.002)^{***}$
σ_2	$0.206\ (0.014)^{***}$
ρ	$0.736\ (0.037)^{***}$
λ	$1.142\ (0.293)^{***}$
Log-Likelihood	-22101.70

Note: Standard errors in parentheses. [***] significant at 1% level; [**] significant at 5% level; [*] significant at 10% level. μ is the expected return on the spot commodity; κ is the speed of mean-reversion of the convenience yield; α is the mean level of the convenience yield; σ_1 is the volatility of the spot price; σ_2 is the volatility of the convenience yield; ρ is the correlation coefficient of spot price and convenience yield; λ is the market price of the convenience yield risk.

efficiency into consideration, 7×7 grid points are chosen, equidistant in each state variable. The termination criterion reflects the average matrix norm (L^1-norm) and termination occurs when this norm falls below 1%. Overall, we observe good convergence of our scheme.

Figure 4.4 below shows the plot of the value function V_0 as a function of the two-state variables P and δ. This function represents the value for ownership of the fish-farm. It can be clearly observed that the convenience yield has a negative impact on the value of the fish farm, while the salmon spot price obviously has a positive impact. The former can be explained as follows: As discussed previously, ownership of the fish-farm has similar characteristics as holding an option contract on the commodity, but not the commodity itself. As the convenience yield benefits the commodity holder but not the option holder, an increase in the convenience yield will decrease the value of the fish-farm.[22]

[22]This can also be observed for options on dividend paying equity in the classical Black-Scholes framework, where the continuously paid dividend replaces the convenience yield.

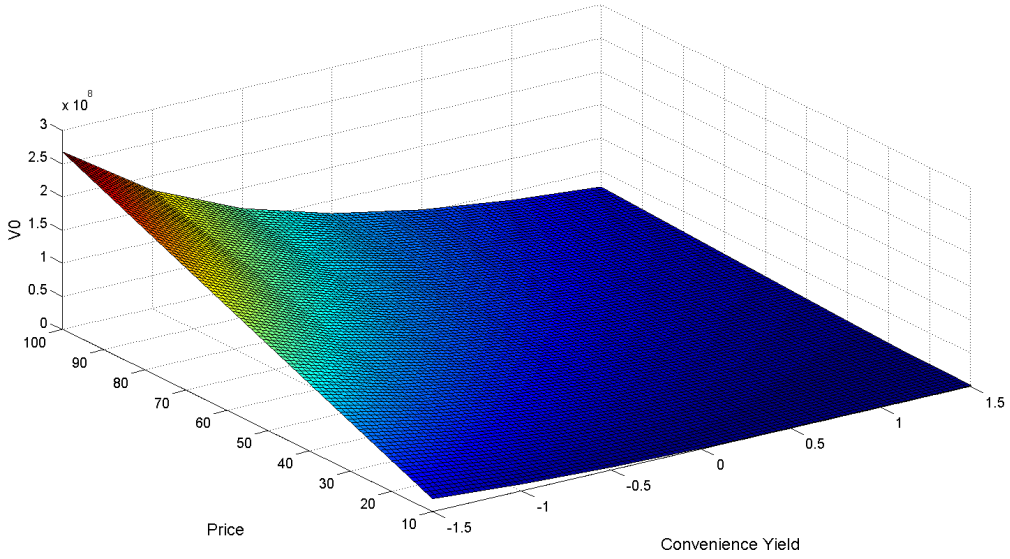

Figure 4.4. Value of ownership of the fish farm for parameters obtained from Panel B, 12/06/2006-22/03/2012

Note: The ownership value of the fish-farm V_0 is expressed as a function of the two-state variables, i.e., price and convenience yield. It can be clearly observed that the convenience yield has a negative impact on the value of the fish farm, while the salmon spot price has a positive impact.

Figure 4.5 shows the thresholds (free boundary for harvesting) for the infinite rotation problem. These have been obtained by appropriately adjusting the methods from the previous section. Compared to single-rotation fish farming, the average harvesting time in the infinite rotation fish farming problem reduces significantly from 2.4251 years to 2.1396 years. As indicated earlier, this is expected, as the prospect of starting a new harvesting cycle provides an incentive for earlier harvesting. The value for ownership of the fish-farm based on the estimates obtained from panel B has been computed as 20.6410 million NOK (2.1962 million EUR) while the lease value is 1.2324 million NOK (0.1311 million EUR). This value is about 17 times larger than the lease value, which is realistic as well.[23]

[23]Note that with the computed average harvesting time of 2.1396 years in the infinite rotation case, ownership entitles to roughly 23 harvesting cycles in 50 years, which considering discounting makes this value seem realistic as well.

(a)

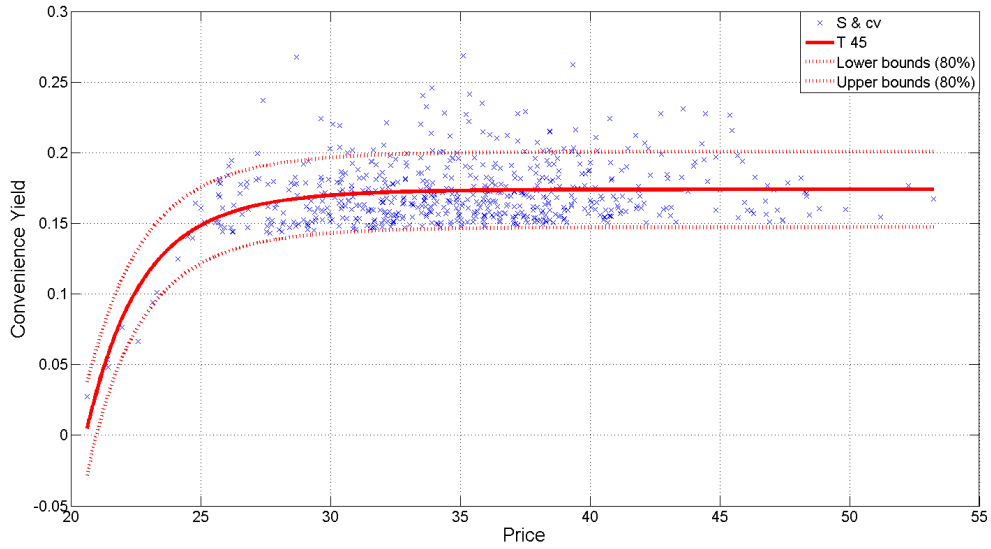

(b)

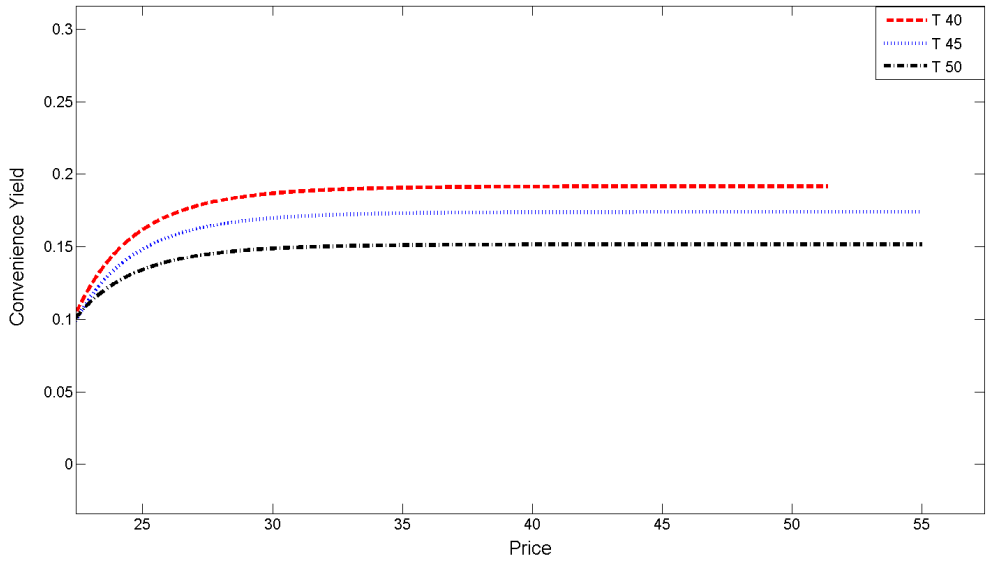

Figure 4.5. Infinite rotation fish farming, threshold for Panel B: (a) threshold at one time; (b) threshold at different times

Note: S and cv denote spot price and convenience yield respectively. Blue spots in (a) represent combinations of S and cv where harvesting occurred at time point 45. The boundaries of 80% confidence intervals above and below the fitted (thick red) line are also presented and can be interpreted as more or less conservative exercise thresholds. Thresholds at time point 40, 45 and 50 are shown as red, blue and black line accordingly in (b).

4.4.3 Is it worth it ? The value of managerial flexibility.

Mcdonald (2000) assessed in a general context optimal exercise rules obtained from a real option approach against simple rules of thumbs, including exercise at an optimal predetermined time. In this way he captured the value of managerial flexibility as well as the usefulness of the real option approach. In this section, we do a similar comparison within the context of the model presented here, which is of higher complexity than the one considered in Mcdonald (2000). As such we assess the real option approach discussed in the previous sections against a scenario where the manager sets a fixed harvesting date at the beginning of the harvesting cycle, disregarding any information updates over the harvesting cycle. The manager aims at setting this harvesting date optimally. The valuation problem corresponding to this setup is similar to the valuation of a a European option. Taking Panel A as an illustration, with $P_0 = 40.4$ and $\delta_0 = 0$, adopting the real option policy, the true lease value is computed as 1.5124 million NOK (*approx.* 0.1609 million EUR). Table 4.7 shows the values, fractions of optimal value covered and absolute difference between real option policy and fixed date strategies for various harvesting dates. We apply the calculation to each panel, including the case of infinite rotation, and find that these suboptimal policies can cover up to 90% of the optimal value on average if the fixed harvesting date is set at about 2 years. While this is substantial, it also means that following any of the suboptimal strategies, the fish farm would voluntarily give up 10% of its value, when additional computational costs attached to the real option approach are only marginally higher than those attached to the fixed date strategies. As such we think, yes, the real option approach for the valuation of fish farms is worth it.[24]

[24]Using different combination of initial values for price and convenience yield, i.e., $P_0 \in (35, 40.4, 45)$ and $\delta_0 \in (-0.5, 0, 0.5)$, in addition to Table 4.7, eight additional cases have been considered and the results are presented in Appendix C. While absolute values such as the optimal value and suboptimal value do vary with different initial values, the fractions of value captured by the corresponding suboptimal policies are relatively stable, with the highest values all occurring at the 2nd year.

Table 4.7. Optimal Policy vs. Suboptimal Policy: Panel A with $(P_0 = 40.4, \delta_0 = 0)$

Fixed Harvesting Date	Suboptimal Value NOK (EUR)	Suboptimal Value/Optimal Value	Optimal Value - Suboptimal Value NOK(EUR)
1.0 year	0.8931e+6 (0.9503e+5)	59.05%	6.1935e+5 (0.6590e+5)
1.5 years	1.2291e+6 (1.3078e+5)	81.27%	2.8333e+5 (0.3015e+5)
2.0 years	1.3172e+6 (1.4015e+5)	87.09%	1.9522e+5 (0.2077e+5)
2.5 years	1.2647e+6 (1.3456e+5)	83.62%	2.4773e+5 (0.2636e+5)
3.0 years	1.1511e+6 (1.2248e+5)	76.11%	3.6133e+5 (0.3845e+5)

Note: The suboptimal value is produced under the scenario where the manager sets a fixed harvesting date at the beginning of the harvesting cycle, disregarding any information updates over the harvesting cycle; while the optimal value is obtained via the real option policy, which is computed as 1.5124 million NOK (*approx.* 0.1609 million EUR) in this case. Exchange rate used here is 1 NOK = 0.1064 EUR, http://www.xe.com/ [last access: 02/10/2015].

4.5 Risk Aversion: What is the Impact of Having a Salmon Futures Market ?

As we indicated earlier, in the presence of a complete salmon futures market, the fish farmer is able to efficiently hedge idiosyncratic risk in the salmon spot price. Individual risk preferences are aggregated in the market measure and its pricing kernel is in fact determined by marginal utilities. The specific level of risk aversion of one particular fish farmer who uses salmon futures appropriately hence has no effect on this fish farmer's harvesting decision, the optimal harvesting time is independent of the level of risk aversion. But what if the fish farmer does not use the futures market, or what if there were no salmon futures market ? In this section, we assume that the fish farmer does not have access to the salmon futures market and hence is unable to hedge price risk. We further assume that the fish farmer is risk averse and that preferences are characterized by a CRRA utility function $U(x) = \frac{x^{1-\gamma}}{1-\gamma}$, where γ represents the level of risk aversion.

Real options have been studied in the context of risk aversion with no or partial spanning in Hugonnier and Morellec (2007), Henderson (2007) and Ewald and Yang (2008). Hugonnier and Morellec (2007) assume that the project generates an instantaneous cash flow given by a geometric Brownian motion. They show that under the assumption of CRRA, the investment threshold is increasing with the level of risk aversion and the level of volatility. Investment is henceforth delayed and the difference in project value between firm- and utility maximizing policies can reach up to 20% for reasonable parameter values. A disadvantage of the the modelling framework in Hugonnier and Morellec (2007) is that it cannot cope with negative cash flows, at least for the CRRA case. Additionally, the assumption that instantaneous cash flows follow a geometric Brownian motion is limiting, given that the presence of mean reversion can significantly alter investment behavior. Henderson (2007) uses a different setup, where the payoff of the investment project is given by a geometric Brownian motion (which is similar to Hugonnier and Morellec (2007)), but utility is of exponential type. In addition it is assumed that a partial spanning asset exist. However, the case of

no spanning asset is included by setting the relevant correlation $\rho = 0$. In this setup Henderson (2007) observes that increased volatility can in fact speed up investment behavior. Extending the setup in Henderson (2007) and including a mean reversion feature in the project's payoff, Ewald and Yang (2008) in fact demonstrate that the investment threshold can be decreasing with the level of risk aversion (with and without mean reversion). There is hence no clear indication as to how the level of risk aversion would in general affect investment behavior.

Let us now assume that in the context of the single-rotation fish farming model discussed earlier, the fish farmer's preferences are given by a CRRA utility function and that the fish farmer does not have access to the salmon futures market. To account for negative cash flows prior to harvest, e.g. feeding costs, we assume that these are made from bank loans which are redeemed at the time of harvest, when profits are made. This is a necessary assumption as CRRA utility $U(x) = \frac{x^{1-\gamma}}{1-\gamma}$ is not defined for negative values of x, but it is also a very realistic assumption. We only consider the single rotation case. The previous analysis to obtain the optimal harvesting time is then repeated, but under the real world measure (which reflects the fish farmer's subjective believes) and computing utilities for both harvesting and continuation value. We perform this analysis for varying levels of risk aversion γ and observe that for all panels the averaging harvesting time is decreasing with the level of risk aversion. Table 4.8 shows this for Panel D as an example. In this particular case the average harvesting time ranges from 2.5232 years with $\gamma = 0$ to 1.1979 years with $\gamma = 50$. The average harvesting time for the same panel with salmon futures is 2.2347 years (compare Table 4.5). Perhaps more important than the average harvesting time is the relative loss in value, defined as in Hugonnier and Morellec (2007) as the relative difference in project value between firm- and utility maximizing policies. Table 4.8 shows that the relative loss in value can be significant, but crucially depends on the level of risk aversion. For very low risk aversion $\gamma \in [0, 1]$, the losses are only around 1.5%, but start to become more noticeable at $\gamma = 2.6$ where losses exceed 5% and become very large for high level of risk aversion at $\gamma = 8$, where they exceed 20% and reach a similar level as those reported in Hugonnier and Morellec (2007). The corresponding results for Panels A,

B and C are similar and contained in Appendix D. In consequence, the salmon futures market provides a valuable service, in particular to those fish farmers which exhibit a high degree of risk aversion.

Table 4.8. Lease Value of Fish Farm and Harvesting Time Under CRRA: Panel D

γ	Harvesting Time (years)	Pond Value (million)		Percentage Loss
0	2.5232	1.6199 *NOK*	0.1724 *EUR*	1.63%
0.1	2.5198	1.6207	0.1724	1.58%
0.3	2.5090	1.6220	0.1726	1.50%
0.5	2.4969	1.6224	0.1726	1.48%
0.9	2.4635	1.6208	0.1725	1.57%
1.1	2.4424	1.6179	0.1721	1.75%
2	2.3252	1.5885	0.1690	3.53%
5	2.0057	1.4510	0.1544	11.88%
8	1.7075	1.2558	0.1336	23.74%
18	1.5840	1.1675	0.1242	29.10%
33	1.4131	1.0538	0.1121	36.01%
50	1.1979	0.9559	0.1017	41.95%

Note: γ measures the level of risk aversion. Percentage Loss = relative difference in project value between firm- and utility maximising policies, which reflects the percentage loss due to not having access to the futures market at different levels of risk aversion. Exchange rate used here is 1 $NOK = 0.1064$ EUR, http://www.xe.com/ [last access: 02/10/2015].

4.6 Conclusions

In this article we presented a methodological approach, which can be used to determine the values of lease or ownership of a fish farm in a way which is consistent with market data obtained from the fish pool market, a recently established exchange in Bergen (Norway), where futures on fresh farmed salmon are traded. Our approach correctly accounts for risk premia due to stochastically fluctuating prices. Specifically, we considered the optimal harvesting problem for a fish farmer in a model where the price dynamics is determined by a Schwartz (1997) two-factor model. We looked at both cases of single and infinite rotations. The arbitrage-free value of lease and ownership of the fish farm have then been obtained from the value function of the harvesting problem with single and infinite rotation respectively. The data set used for this analysis contains a large set of futures contracts with different maturities traded at the Fish Pool market between 12/06/2006 and 22/03/2012. In the calibration of our model we adopted the Kalman filter approach, while our numerical approach to solve the optimal stopping problem embedded in the harvesting decision of the fish farmer made use of the Least Square Monte Carlo and function iteration methods. We found this approach to be numerically stable and obtained very realistic results for a model fish farm.

We assessed the optimal strategy, harvesting time and value against the alternatives where the fish farmer has either no managerial flexibility or no access to the salmon futures market but exhibits risk aversion as modeled by a CRRA utility function. We observed that in both cases, the loss in project value can be very significant, and in the second case is only negligible for extremely low levels of risk aversion. As such we have established that the presence of a salmon future market as well as managerial flexibility are of high importance to risk-averse fish farmers.

Our approach is of practical interest to companies in the fish farming business and can guide their decision process in the context of the acquisition of fish farm units. There are a number of ways how this study can be extended. One way is the inclusion of a stochastic mortality rate, possibly in a regime switching framework, where a high

mortality regime corresponds to periods with disease outbreak such as fish lice or salmon anemia. It would be very interesting to understand how markets price the risk of disease outbreak and how this effects the valuation of fish farms. Stochastic growth as well as stochastic feed costs would be other interesting lines of research to pursue.

Bibliography

Arnason, R. (1992). Optimal feeding schedules and harvesting time in aquaculture. *Marine Resource Economics*, 15–35.

Asche, F., & Bjorndal, T. (2011). *The economics of salmon aquaculture* (Vol. 10). John Wiley & Sons.

Asche, F., Bjørndal, T., & Young, J. A. (2001). Market interactions for aquaculture products. *Aquaculture Economics & Management*, *5*(5-6), 303–318.

Asche, F., Bremnes, H., & Wessells, C. R. (1999). Product aggregation, market integration, and relationships between prices: an application to world salmon markets. *American Journal of Agricultural Economics*, *81*(3), 568–581.

Baxter, J., Conine, T. E., & Tamarkin, M. (1985). On commodity market risk premiums: Additional evidence. *Journal of Futures Markets*, *5*(1), 121–125.

Bessembinder, H. (1992). Systematic risk, hedging pressure, and risk premiums in futures markets. *Review of Financial Studies*, *5*(4), 637–667.

Bjerksund, P. (1991). *Contingent claims evaluation when the convenience yield is stochastic: analytical results*. Institutt for foretaksøkonomi, Institute of Finance and Management Science.

Bjørndal, T. (1988). Optimal harvesting of farmed fish. *Marine Resource Economics*, 139–159.

Black, F. (1976). The pricing of commodity contracts. *Journal of financial economics*, *3*(1), 167–179.

Cacho, O. J. (1997). Systems modelling and bioeconomic modelling in aquaculture. *Aquaculture Economics & Management*, *1*(1-2), 45–64.

Carter, C. A., Rausser, G. C., & Schmitz, A. (1983). Efficient asset portfolios and the theory of normal backwardation. *Journal of Political Economy*, *91*(2), 319–331.

Chen, S., Insley, M., & Wirjanto, T. (2011). The impact of stochastic convenience yield on long-term forestry investment decisions.

Cortazar, G., Gravet, M., & Urzua, J. (2008). The valuation of multidimensional american real options using the lsm simulation method. *Computers & Operations Research*, *35*(1), 113–129.

Dixit, A. K., & Pindyck, R. S. (1994). *Investment under uncertainty*. Princeton university press.

Dusak, K. (1973). Futures trading and investor returns: An investigation of commodity market risk premiums. *The Journal of Political Economy*, 1387–1406.

Ewald, C.-O., Nawar, R., Ouyang, R., & Siu, T. K. (2016). The market for salmon futures: an empirical analysis of fish pool using the schwartz multifactor model. *Quantitative Finance*.

Ewald, C.-O., & Salehi, P. (2015). Salmon futures and the fish pool market in the context of the capm and the fama & french three-factor model. *Available at SSRN 2567737*.

Ewald, C.-O., & Yang, Z. (2008). Utility based pricing and exercising of real options under geometric mean reversion and risk aversion toward idiosyncratic risk. *Mathematical Methods of Operations Research*, *68*(1), 97–123.

Forsberg, O. I., & Guttormsen, A. G. (2006). The value of information in salmon farming. harvesting the right fish at the right time. *Aquaculture Economics & Management*, *10*(3), 183–200.

Guttormsen, A. G. (2008). Faustmann in the sea: optimal rotation in aquaculture. *Marine Resource Economics*, 401–410.

Heaps, T. (1995). Density dependent growth and the culling of farmed fish. *Marine Resource Economics*, 285–298.

Henderson, V. (2007). Valuing the option to invest in an incomplete market. *Mathematics and Financial Economics*, *1*(2), 103–128.

Hugonnier, J., & Morellec, E. (2007). Real options and risk aversion. *Swiss Finance Institute Research Paper*.

Insley, M. (2002). A real options approach to the valuation of a forestry investment. *Journal of environmental economics and management*, *44*(3), 471–492.

Insley, M., & Rollins, K. (2003). *Real options in harvesting decisions on publicly owned forest lands (revised).*

Jamshidian, F., & Fein, M. (1990). Closed-form solutions for oil futures and european options in the gibson-schwartz model: A note. *Merril Lynch Capital Markets*.

Longstaff, F. A., & Schwartz, E. S. (2001). Valuing american options by simulation: a simple least-squares approach. *Review of Financial studies*, *14*(1), 113–147.

Mcdonald, R. L. (2000). Real options and rules of thumb in capital budgeting. In *Oxford university.*

Schwartz, E. S. (1997). The stochastic behavior of commodity prices: Implications for valuation and hedging. *The Journal of Finance*, *52*(3), 923–973.

Solibakke, P. B. (2012). Scientific stochastic volatility models for the salmon forward market: forecasting (un-) conditional moments. *Aquaculture Economics & Management*, *16*(3), 222–249.

Xu, Y., & Malkiel, B. G. (2004). Idiosyncratic risk and security returns. In *Afa 2001 new orleans meetings.*

Yu, R., & Leung, P. (2006). Optimal partial harvesting schedule for aquaculture operations. *Marine Resource Economics*, 301–315.

Appendix A:

Seasonality Model Estimation

Considering $N = 2$ as an example, i.e., γ_1, γ_1^*, γ_2 and γ_2^* are included in the model, by using the sample data ranging from 12/06/2006 to 22/03/2012, we obtain the following estimates as shown in Table A.1. Compared to Table 4.2 in the main article, estimates obtained from Panel A, B and D are slightly modified but the figures produced, such as term structures, are quite similar. The results obtained from the longer maturities contracts, Panel C, are rather poor. The reason for this is likely that on top of lower liquidity of these contracts, over the long time that it takes until these contracts mature, seasonal effects average out and become blurred in a way, that it negatively effects the filter process. Therefore, we won't include Panel C in the following analysis.

Table A.1. Estimation Results of Whole Sample with Seasonality Model, Avg. Rate 3.03%, 12/06/2006-22/03/2012

Parameter	Panel A F1, F3, F5, F7, F9 (Short Term)	Panel B F12, F14, F16, F18, F20 (Medium Term)	Panel C F24, F25, F26, F28, F29 (Long Term)	Panel D F1, F7, F14, F20, F25 (Mixed Term)
μ	0.327 (0.076)***	0.524 (0.068)***	6.643 (0.847)***	0.291 (0.087)***
κ	3.044 (0.129)***	1.274 (0.077)***	1.123 (0.095)***	1.220 (0.036)***
α	1.438 (0.181)***	0.563 (0.079)***	-0.065 (1.949)	0.634 (0.137)***
σ_1	0.163 (0.005)***	0.121 (0.002)***	0.850 (0.246)***	0.168 (0.005)***
σ_2	0.662 (0.031)***	0.202 (0.009)***	0.941 (0.274)***	0.271 (0.013)***
ρ	0.671 (0.032)***	0.690 (0.045)***	0.840 (0.086)***	0.889 (0.012)***
λ	0.908 (0.342)***	0.670 (0.127)***	0.272 (1.927)	0.746 (0.162)***
γ_1	1.000 (0.140)***	-0.231 (0.032)***	-0.072 (0.205)	-0.310 (0.063)***
γ_2	-0.861 (0.124)***	-0.143 (0.023)***	1.018 (0.100)***	-1.005 (0.103)***
γ_1^*	-1.764 (0.250)***	-0.116 (0.022)***	0.738 (0.108)***	0.116 (0.034)***
γ_2^*	-1.437 (0.204)***	0.685 (0.083)***	-0.400 (0.180)**	1.986 (0.213)***
Log-Likelihood	-17065.9	-21934	-21883.8	-16120.2

Note: Standard errors in parentheses. [***] Significant at 1% level; [**] Significant at 5% level; [*] Significant at 10% level. μ is the expected return on the spot commodity; κ is the speed of mean-reversion of the convenience yield; α_0 is the constant term in the mean level of the convenience yield; σ_1 is the volatility of the spot price; σ_2 is the volatility of the convenience yield; ρ is the correlation coefficient of spot price and convenience yield; λ is the market price of the convenience yield risk; γ_1, γ_2, γ_1^* and γ_2^* are the coefficients of trigonometric terms in the mean level of the convenience yield.

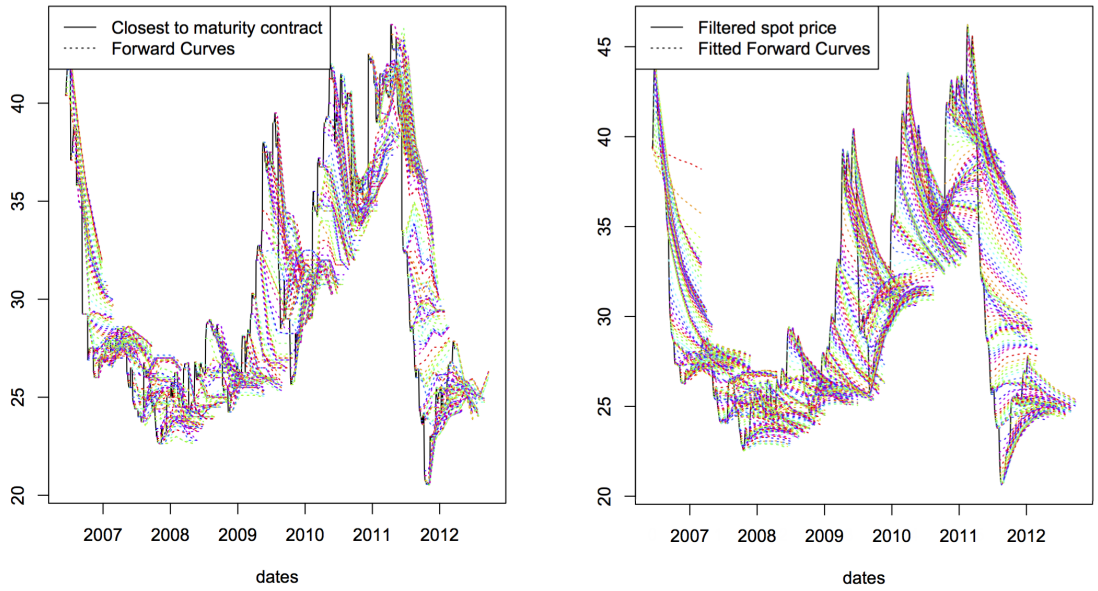

Figure A.1. Term structures for Panel A (seasonality model): actual forward curves on the left; model generated forward curves on the right

Note: Each colored curve is a static picture of futures prices (y-axis) against contract maturities (x-axis), which is analogous to a plot of the term structure of interest rates. On the left side of the figure, the solid line represents the price of the closest-to-maturity futures contract, i.e., $F1$ in this case; while the dashed line consists of the actual prices of other futures contracts with different maturities in this panel. On the right side of the figure, the solid line is the filtered spot price obtained through the estimation procedure; while the dashed line consists of the estimated futures prices given by the pricing formula.

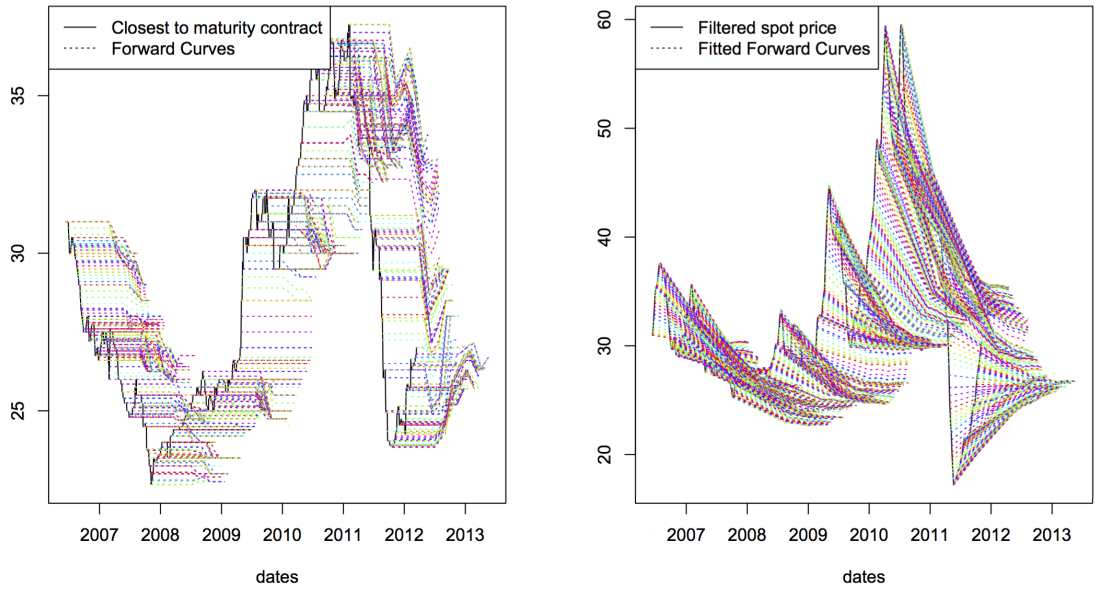

Figure A.2. Term structures for Panel B (seasonality model): actual forward curves on the left; model generated forward curves on the right

Note: Each colored curve is a static picture of futures prices (y-axis) against contract maturities (x-axis), which is analogous to a plot of the term structure of interest rates. On the left side of the figure, the solid line represents the price of the closest-to-maturity futures contract, i.e., $F12$ in this case; while the dashed line consists of the actual prices of other futures contracts with different maturities in this panel. On the right side of the figure, the solid line is the filtered spot price obtained through the estimation procedure; while the dashed line consists of the estimated futures prices given by the pricing formula.

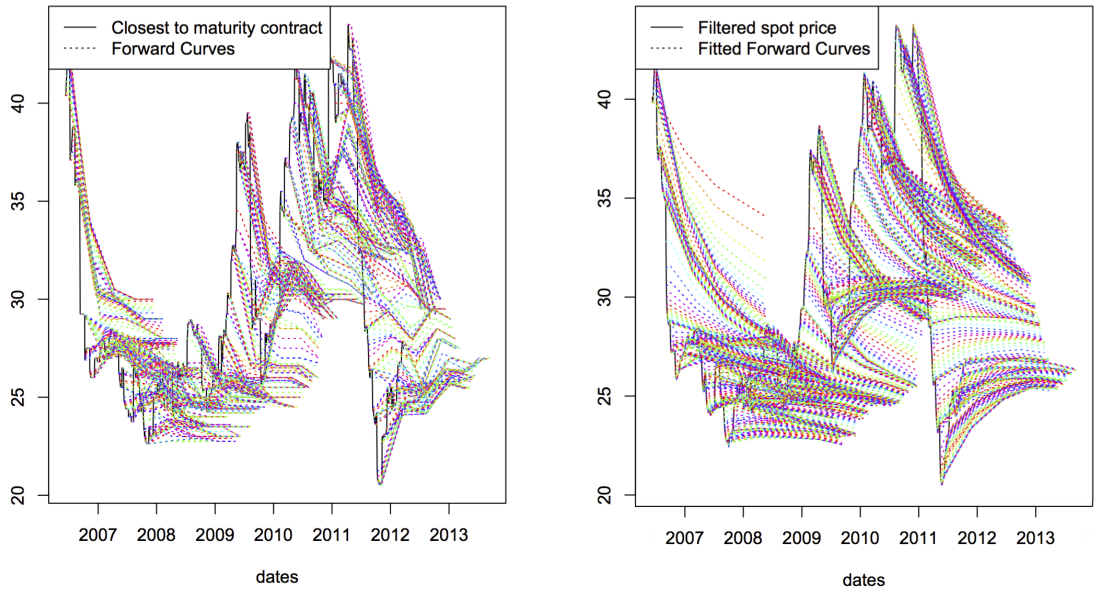

Figure A.3. Term structures for Panel D (seasonality model): actual forward curves on the left; model generated forward curves on the right

Note: Each colored curve is a static picture of futures prices (y-axis) against contract maturities (x-axis), which is analogous to a plot of the term structure of interest rates. On the left side of the figure, the solid line represents the price of the closest-to-maturity futures contract, i.e., $F1$ in this case; while the dashed line consists of the actual prices of other futures contracts with different maturities in this panel. On the right side of the figure, the solid line is the filtered spot price obtained through the estimation procedure; while the dashed line consists of the estimated futures prices given by the pricing formula.

Table A.2. RMSE and MAE of Log Price with Seasonality Model

Panel A						
	F1	F3	F5	F7	F9	ALL
RMSE	0.0221	0.0270	0.0180	0.0140	0.0224	0.0212
MAE	0.0166	0.0209	0.0131	0.0096	0.0167	0.0154
Panel B						
	F12	F14	F16	F18	F20	ALL
RMSE	0.0102	0.0136	0.0118	0.0093	0.0102	0.0111
MAE	0.0075	0.0096	0.0088	0.0062	0.0068	0.0078
Panel D						
	F1	F7	F14	F20	F25	ALL
RMSE	0.0240	0.0365	0.0212	0.0155	0.0240	0.0252
MAE	0.0187	0.0293	0.0147	0.0109	0.0163	0.0180

Note: The root-mean-square error (RMSE) and mean-absolute error (MAE) are used to evaluate the model fit.

Appendix B: Additional Figures

Figure A.4 depicts the growth/weight and biomass of fish.

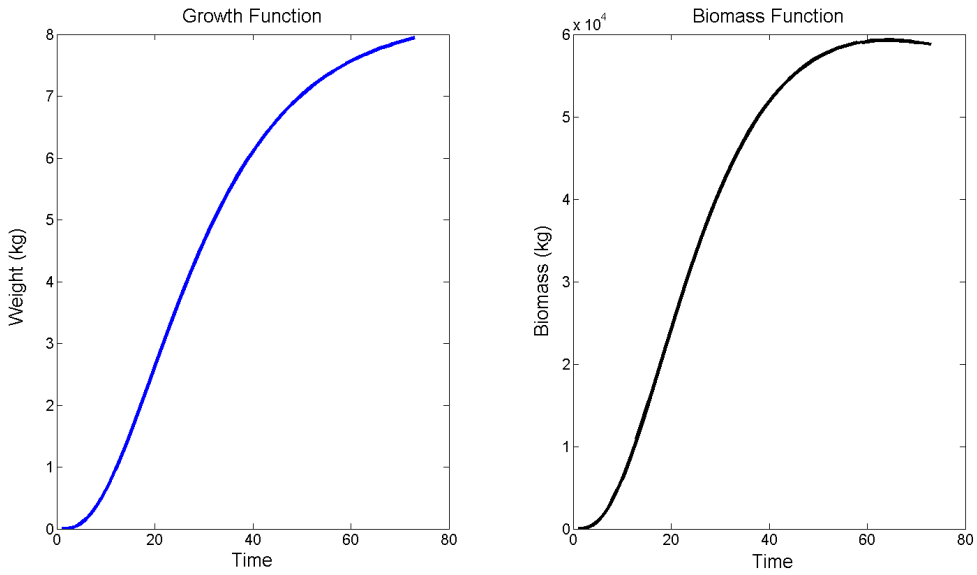

Figure A.4. Growth and biomass functions plotted by using relevant parameters in Asche and Bjorndal (2011)

Figure A.5 - Figure A.7 show the term structures for Panel B, Panel C, Panel D respectively. The graphs show the proxies for the spot (closest future on the left and filtered spot on the right) as the solid continuing line from 2006 until 2012, and attached at each date the forward curve originating from that date (actual forward curve on the left and model generated forward curve on the right). It can be observed that both contango and backwardation are present in the market at different times.

Figure A.8 - Figure A.10 show the thresholds for each panel accordingly.

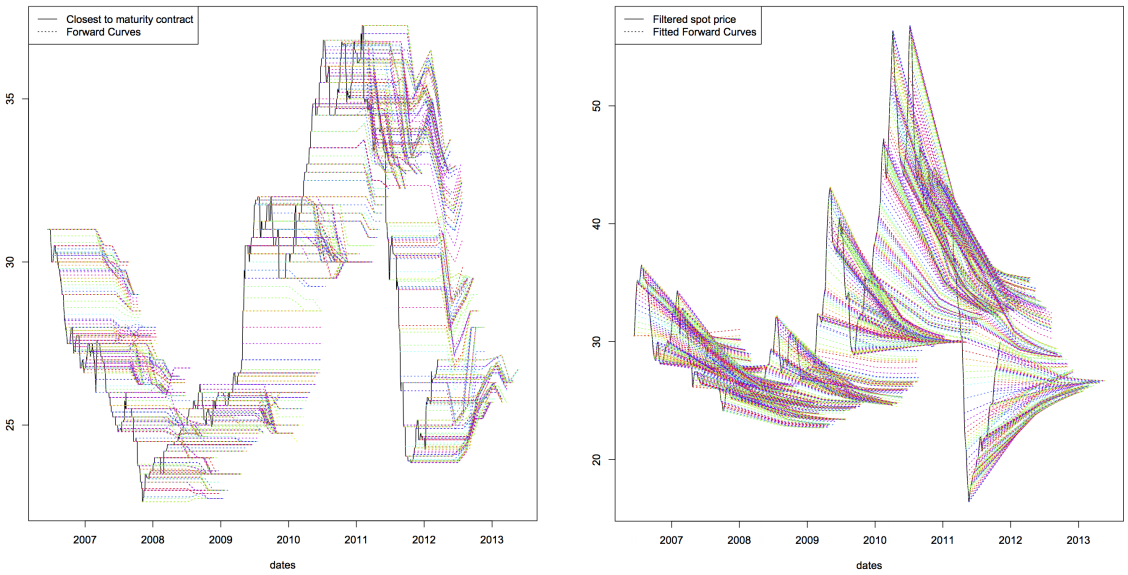

Figure A.5. Term structures for Panel B: actual forward curves on the left; model generated forward curves on the right

Note: Each colored curve is a static picture of futures prices (y-axis) against contract maturities (x-axis), which is analogous to a plot of the term structure of interest rates. On the left side of the figure, the solid line represents the price of the closest-to-maturity futures contract, i.e., $F12$ in this case; while the dashed line consists of the actual prices of other futures contracts with different maturities in this panel. On the right side of the figure, the solid line is the filtered spot price obtained through the estimation procedure; while the dashed line consists of the estimated futures prices given by the pricing formula.

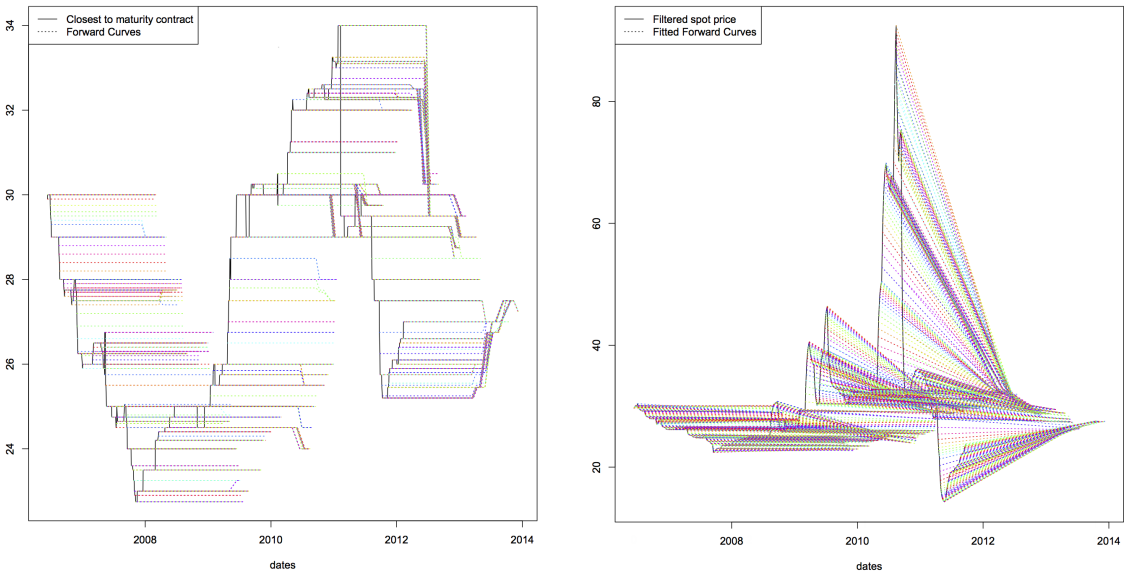

Figure A.6. Term structures for Panel C: actual forward curves on the left; model generated forward curves on the right

Note: Each colored curve is a static picture of futures prices (y-axis) against contract maturities (x-axis), which is analogous to a plot of the term structure of interest rates. On the left side of the figure, the solid line represents the price of the closest-to-maturity futures contract, i.e., $F24$ in this case; while the dashed line consists of the actual prices of other futures contracts with different maturities in this panel. On the right side of the figure, the solid line is the filtered spot price obtained through the estimation procedure; while the dashed line consists of the estimated futures prices given by the pricing formula.

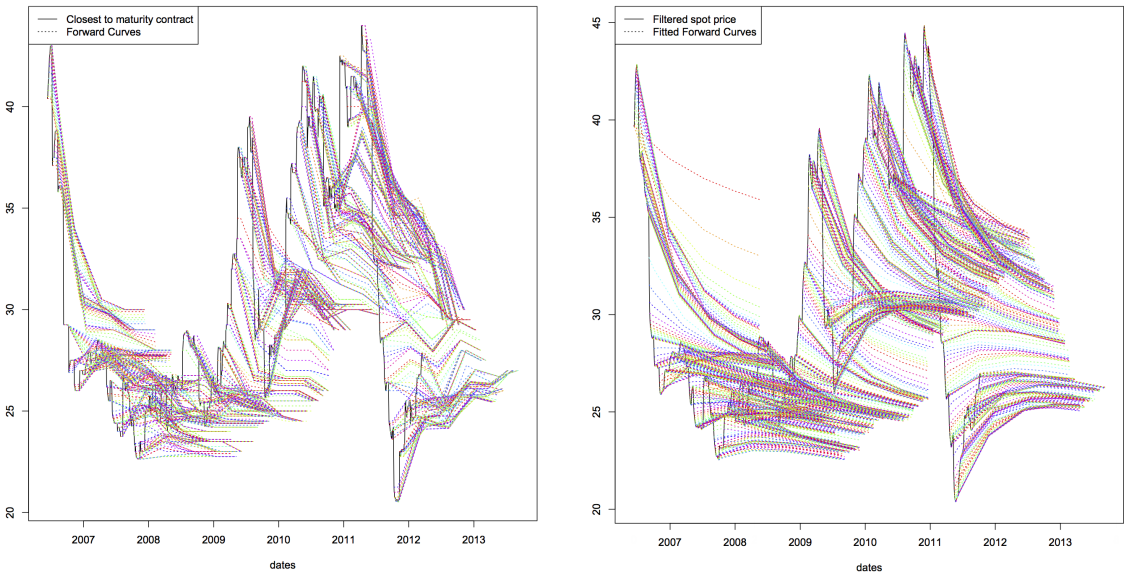

Figure A.7. Term structures for Panel D: actual forward curves on the left, model generated forward curves on the right

Note: Each colored curve is a static picture of futures prices (y-axis) against contract maturities (x-axis), which is analogous to a plot of the term structure of interest rates. On the left side of the figure, the solid line represents the price of the closest-to-maturity futures contract, i.e., $F1$ in this case; while the dashed line consists of the actual prices of other futures contracts with different maturities in this panel. On the right side of the figure, the solid line is the filtered spot price obtained through the estimation procedure; while the dashed line consists of the estimated futures prices given by the pricing formula.

(a)

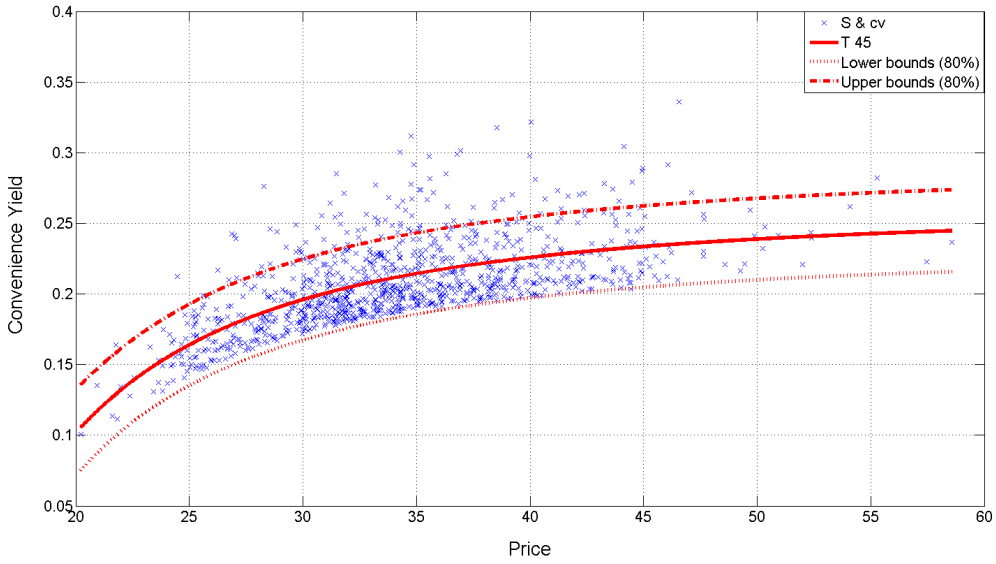

(b)

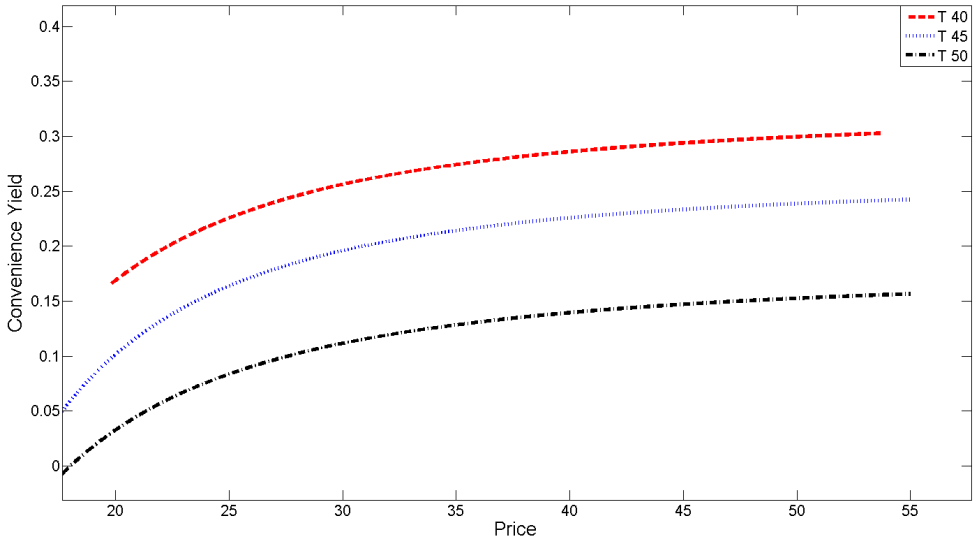

Figure A.8. Threshold for Panel B: (a) threshold at one time; (b) threshold at different times

Note: S and cv denote spot price and convenience yield respectively. Blue spots in (a) represent combinations of S and cv where harvesting occurred at time point 45. The boundaries of 80% confidence intervals above and below the fitted (thick red) line are also presented and can be interpreted as more or less conservative exercise thresholds. Thresholds at time point 40, 45 and 50 are shown as red, blue and black line accordingly in (b).

(a)

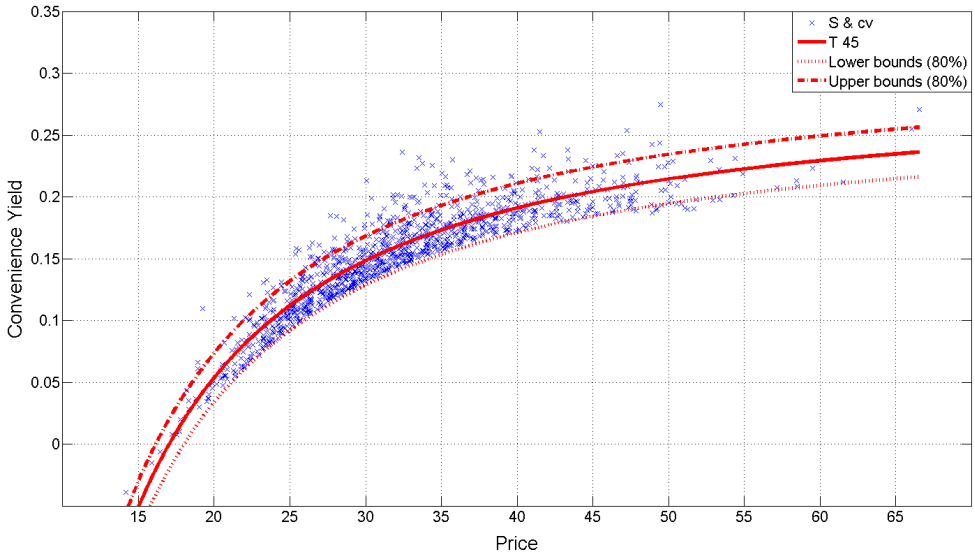

(b)

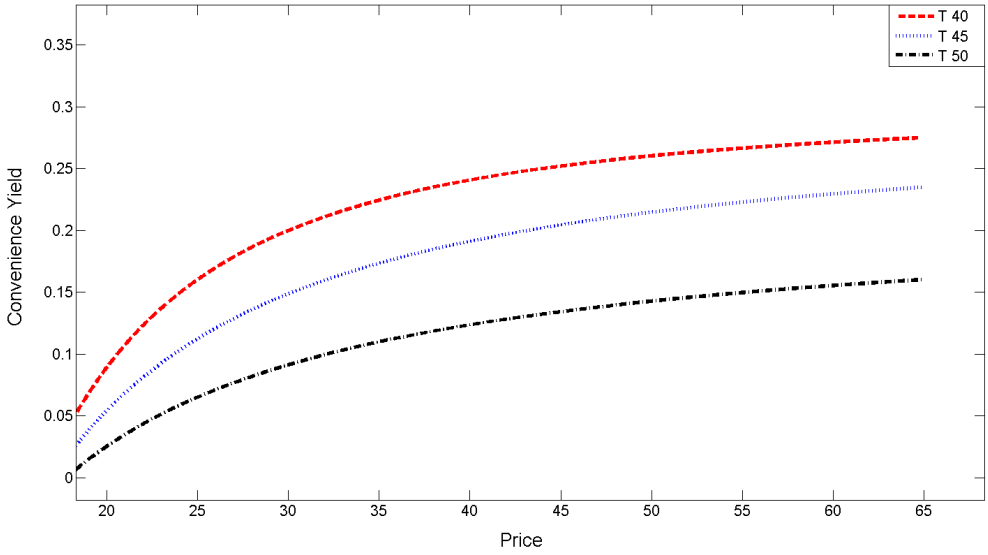

Figure A.9. Threshold for Panel C: (a) threshold at one time; (b) threshold at different times

Note: S and cv denote spot price and convenience yield respectively. Blue spots in (a) represent combinations of S and cv where harvesting occurred at time point 45. The boundaries of 80% confidence intervals above and below the fitted (thick red) line are also presented and can be interpreted as more or less conservative exercise thresholds. Thresholds at time point 40, 45 and 50 are shown as red, blue and black line accordingly in (b).

(a)

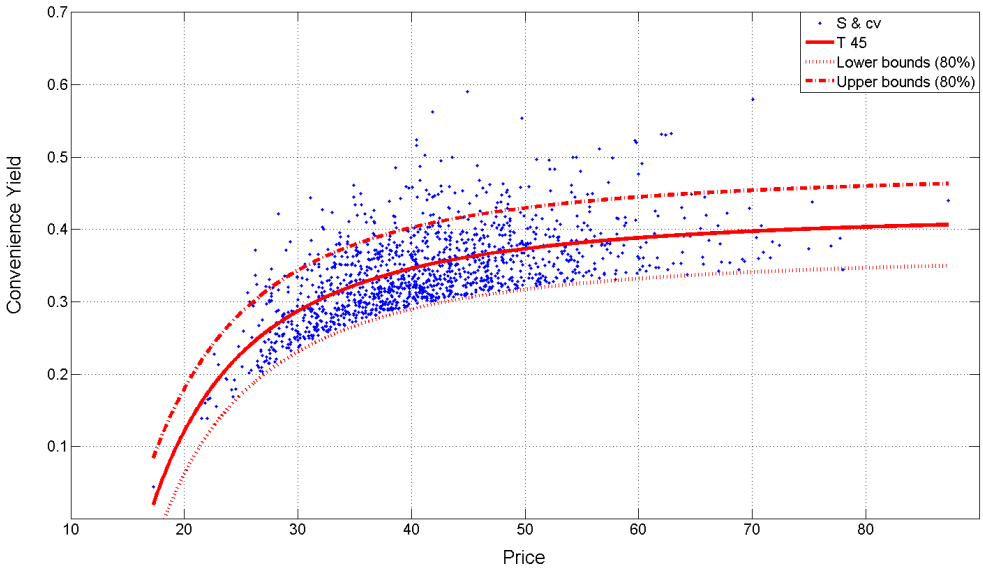

(b)

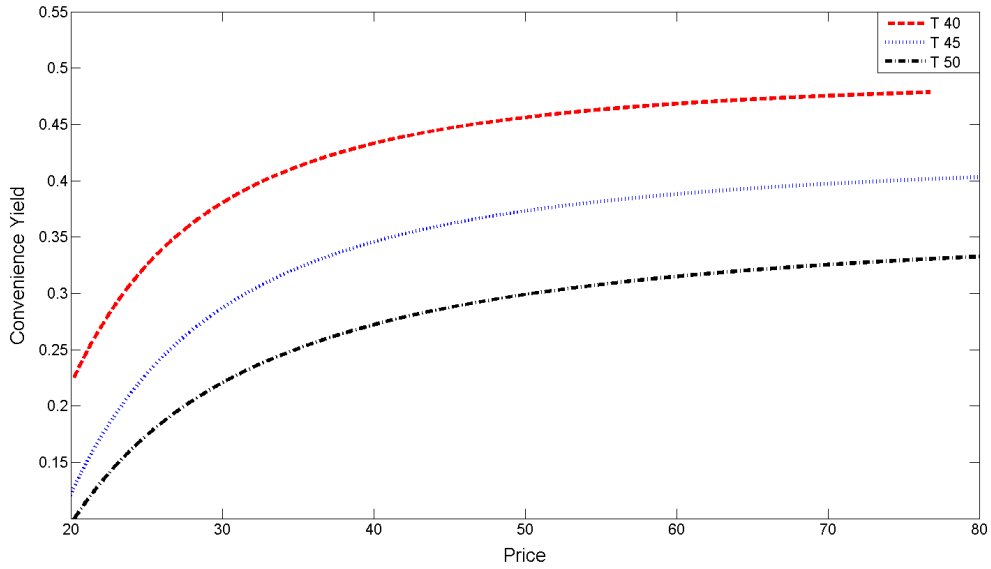

Figure A.10. Threshold for Panel D: (a) threshold at one time; (b) threshold at different times

Note: S and cv denote spot price and convenience yield respectively. Blue spots in (a) represent combinations of S and cv where harvesting occurred at time point 45. The boundaries of 80% confidence intervals above and below the fitted (thick red) line are also presented and can be interpreted as more or less conservative exercise thresholds. Thresholds at time point 40, 45 and 50 are shown as red, blue and black line accordingly in (b).

Appendix C:

Optimal Policy vs. Suboptimal Policy

Using different combination of initial values for price and convenience yield, i.e., $P_0 \in (35, 40.4, 45)$ and $\delta_0 \in (-0.5, 0, 0.5)$, in addition to Table 4.7 in the main article, eight additional cases have been considered.

Table A.3. Optimal Policy vs. Suboptimal Policy: Panel A

Case 1: ($P_0 = 40.4$, $\delta_0 = 0$), $V^1_{optimal}$=1.5124e+6 NOK (1.6092e+5 EUR)			
Fixed Harvesting Date	Suboptimal Value NOK (EUR)	Suboptimal Value/Optimal Value	Optimal Value - Suboptimal Value $NOK(EUR)$
1.0 year	0.8931e+6 (0.9503e+5)	59.05%	6.1935e+5 (0.6590e+5)
1.5 years	1.2291e+6 (1.3078e+5)	81.27%	2.8333e+5 (0.3015e+5)
2.0 years	1.3172e+6 (1.4015e+5)	87.09%	1.9522e+5 (0.2077e+5)
2.5 years	1.2647e+6 (1.3456e+5)	83.62%	2.4773e+5 (0.2636e+5)
3.0 years	1.1511e+6 (1.2248e+5)	76.11%	3.6133e+5 (0.3845e+5)
Case 2: ($P_0 = 40.4$, $\delta_0 = 0.5$), $V^2_{optimal}$=1.2787e+6 NOK (1.3605e+5 EUR)			
Fixed Harvesting Date	Suboptimal Value NOK (EUR)	Suboptimal Value/Optimal Value	Optimal Value - Suboptimal Value $NOK(EUR)$
1.0 year	0.7570e+6 (0.8504e+5)	59.20%	5.2164e+5 (0.5550e+5)
1.5 years	1.0359e+6 (1.1022e+5)	81.01%	2.4279e+5 (0.2583e+5)
2.0 years	1.1039e+6 (1.1745e+5)	86.33%	1.7479e+5 (0.1860e+5)
2.5 years	1.0525e+6 (1.1199e+5)	82.31%	2.2613e+5 (0.2406e+5)
3.0 years	0.9498e+6 (1.0106e+5)	74.28%	3.2888e+5 (0.3499e+5)
Case 3: ($P_0 = 40.4$, $\delta_0 = -0.5$), $V^3_{optimal}$=1.7723e+6 NOK (1.8857e+5 EUR)			
Fixed Harvesting Date	Suboptimal Value NOK (EUR)	Suboptimal Value/Optimal Value	Optimal Value - Suboptimal Value $NOK(EUR)$
1.0 year	1.0438e+6 (1.1106e+5)	58.90%	7.2841e+5 (0.7750e+5)
1.5 years	1.4434e+6 (1.5358e+5)	81.45%	3.2883e+5 (0.3499e+5)
2.0 years	1.5539e+6 (1.6533e+5)	87.68%	2.1840e+5 (0.2324e+5)
2.5 years	1.5001e+6 (1.5961e+5)	84.64%	2.7219e+5 (0.2896e+5)
3.0 years	1.3744e+6 (1.4624e+5)	77.55%	3.9784e+5 (0.4233e+5)
Case 4: ($P_0 = 35$, $\delta_0 = 0$), $V^4_{optimal}$=1.2273e+6 NOK (1.3058e+5 EUR)			
Fixed Harvesting Date	Suboptimal Value NOK (EUR)	Suboptimal Value/Optimal Value	Optimal Value - Suboptimal Value $NOK(EUR)$
1.0 year	0.7258e+6 (0.7723e+5)	59.14%	5.0153e+5 (0.5336e+5)
1.5 years	0.9932e+6 (1.0568e+5)	80.93%	2.3410e+5 (0.2491e+5)
2.0 years	1.0569e+6 (1.1245e+5)	86.12%	1.7038e+5 (0.1813e+5)
2.5 years	1.0058e+6 (1.0702e+5)	81.96%	2.2145e+5 (0.2356e+5)
3.0 years	0.9055e+6 (0.9635e+5)	73.78%	3.2181e+5 (0.3424e+5)
Case 5: ($P_0 = 35$, $\delta_0 = 0.5$), $V^5_{optimal}$=1.0254e+6 NOK (1.0910e+5 EUR)			
Fixed Harvesting Date	Suboptimal Value NOK (EUR)	Suboptimal Value/Optimal Value	Optimal Value - Suboptimal Value $NOK(EUR)$
1.0 year	0.6079e+6 (0.6468e+5)	59.28%	4.1748e+5 (0.4442e+5)
1.5 years	0.8258e+6 (0.8787e+5)	80.54%	1.9958e+5 (0.2124e+5)
2.0 years	0.8721e+6 (0.9279e+5)	85.05%	1.5328e+5 (0.1631e+5)
2.5 years	0.8220e+6 (0.8746e+5)	80.17%	2.0335e+5 (0.2164e+5)
3.0 years	0.7311e+6 (0.7779e+5)	71.30%	2.9430e+5 (0.3131e+5)
Case 6: ($P_0 = 35$, $\delta_0 = -0.5$), $V^6_{optimal}$=1.4519e+6 NOK (1.5448e+5 EUR)			
Fixed Harvesting Date	Suboptimal Value NOK (EUR)	Suboptimal Value/Optimal Value	Optimal Value - Suboptimal Value $NOK(EUR)$
1.0 year	0.8564e+6 (0.9112e+5)	58.99%	5.9547e+5 (0.6336e+5)
1.5 years	1.1789e+6 (1.2543e+5)	81.20%	2.7298e+5 (0.2905e+5)
2.0 years	1.2620e+6 (1.3428e+5)	86.92%	1.8991e+5 (0.2021e+5)
2.5 years	1.2098e+6 (1.2872e+5)	83.32%	2.4210e+5 (0.2576e+5)
3.0 years	1.0990e+6 (1.1693e+5)	75.69%	3.5289e+5 (0.3755e+5)

Table A.3. continued

Case 7: ($P_0 = 45$, $\delta_0 = 0$), $V^7_{optimal}$=1.7560e+6 NOK (1.8684e+5 EUR)			
Fixed Harvesting Date	Suboptimal Value NOK (EUR)	Suboptimal Value/Optimal Value	Optimal Value - Suboptimal Value $NOK(EUR)$
1.0 year	1.0356e+6 (1.1019e+5)	58.97%	7.2041e+5 (0.7665e+5)
1.5 years	1.4300e+6 (1.5215e+5)	81.44%	3.2595e+5 (0.3468e+5)
2.0 years	1.5389e+6 (1.6374e+5)	87.64%	2.1707e+5 (0.2310e+5)
2.5 years	1.4852e+6 (1.5803e+5)	84.58%	2.7079e+5 (0.2881e+5)
3.0 years	1.3603e+6 (1.4474e+5)	77.47%	3.9568e+5 (0.4210e+5)
Case 8: ($P_0 = 45$, $\delta_0 = 0.5$), $V^8_{optimal}$=1.4951e+6 NOK (1.5908e+5 EUR)			
Fixed Harvesting Date	Suboptimal Value NOK (EUR)	Suboptimal Value/Optimal Value	Optimal Value - Suboptimal Value $NOK(EUR)$
1.0 year	0.8840e+6 (0.9406e+5)	59.13%	6.1107e+5 (0.6502e+5)
1.5 years	1.2148e+6 (1.2925e+5)	81.25%	2.8028e+5 (0.2982e+5)
2.0 years	1.3013e+6 (1.3846e+5)	87.04%	1.9380e+5 (0.2062e+5)
2.5 years	1.2489e+6 (1.3288e+5)	83.53%	2.4623e+5 (0.2620e+5)
3.0 years	1.1361e+6 (1.2088e+5)	75.99%	3.5903e+5 (0.3820e+5)
Case 9: ($P_0 = 45$, $\delta_0 = -0.5$), $V^9_{optimal}$=2.0450e+6 NOK (2.1759e+5 EUR)			
Fixed Harvesting Date	Suboptimal Value NOK (EUR)	Suboptimal Value/Optimal Value	Optimal Value - Suboptimal Value $NOK(EUR)$
1.0 year	1.2035e+6 (1.2805e+5)	58.85%	8.4148e+5 (0.8953e+5)
1.5 years	1.6688e+6 (1.7756e+5)	81.60%	3.7623e+5 (0.4003e+5)
2.0 years	1.8025e+6 (1.9179e+5)	88.14%	2.4248e+5 (0.2580e+5)
2.5 years	1.7474e+6 (1.8592e+5)	85.45%	2.9763e+5 (0.3167e+5)
3.0 years	1.6091e+6 (1.7121e+5)	78.68%	4.3594e+5 (0.4638e+5)

Note: The suboptimal value is produced under the scenario where the manager sets a fixed harvesting date at the beginning of the harvesting cycle, disregarding any information updates over the harvesting cycle; while the optimal value is obtained via the real option policy. Exchange rate used here is 1 $NOK = 0.1064$ EUR, http://www.xe.com/ [last access: 02/10/2015].

Appendix D:

Additional Tables for Risk Aversion and No Access to Salmon Futures Market

Table A.4. Lease Value of Fish Farm and Harvesting Time Under CRRA: Panel A

γ	Harvesting Time (years)	Pond Value (millon)	
0	1.8351	1.4895 *NOK*	0.1585 *EUR*
0.1	1.8313	1.4885	0.1584
0.3	1.8224	1.4863	0.1581
0.5	1.8113	1.4821	0.1577
0.9	1.7869	1.4683	0.1562
1.1	1.7666	1.4542	0.1547
2	1.6109	1.3251	0.1410
5	1.4503	1.0663	0.1135
8	1.3435	0.9325	0.0992
18	1.1383	0.7737	0.0823
33	1.0501	0.7315	0.0778
50	0.9956	0.7046	0.0750

Note: γ measures the level of risk aversion. Exchange rate used here is 1 $NOK = 0.1064$ EUR, http://www.xe.com/ [last access: 02/10/2015].

Table A.5. Lease Value of Fish Farm and Harvesting Time Under CRRA: Panel B

γ	Harvesting Time (years)	Pond Value (million)	
0	1.6701	1.0819 *NOK*	0.1151 *EUR*
0.1	1.6686	1.0812	0.1150
0.3	1.6642	1.0797	0.1149
0.5	1.6583	1.0771	0.1146
0.9	1.6468	1.0721	0.1141
1.1	1.6407	1.0693	0.1138
2	1.6018	1.0479	0.1115
5	1.3975	0.9334	0.0993
8	1.4398	0.9339	0.0994
18	1.2194	0.8101	0.0862
33	1.0857	0.7189	0.0765
50	0.9900	0.6415	0.0683

Note: γ measures the level of risk aversion. Exchange rate used here is 1 $NOK = 0.1064$ EUR, http://www.xe.com/ [last access: 02/10/2015].

Table A.6. Lease Value of Fish Farm and Harvesting Time Under CRRA: Panel C

γ	Harvesting Time (years)	Pond Value (million)	
0	2.2301	1.1041 *NOK*	0.1175 *EUR*
0.1	2.2252	1.1039	0.1175
0.3	2.2110	1.1021	0.1173
0.5	2.1955	1.1001	0.1171
0.9	2.1442	1.0905	0.1160
1.1	2.1199	1.0858	0.1155
2	2.0011	1.0518	0.1119
5	1.7770	0.9462	0.1007
8	1.6375	0.8778	0.0934
18	1.4362	0.7666	0.0816
33	1.3860	0.7494	0.0797
50	1.3195	0.7210	0.0767

Note: γ measures the level of risk aversion. Exchange rate used here is 1 $NOK = 0.1064$ EUR, http://www.xe.com/ [last access: 02/10/2015].

Chapter 5

Conclusion

In this PhD thesis, we first discuss the valuation of futures on fresh farmed salmon as traded on the Fish Pool exchange and then explore how information reflected in the prices of futures contracts can be used to compute arbitrage free prices for lease and ownership of fish farms.

We established a link between the popular Schwartz (1997) multifactor model used for the pricing of commodity derivatives and classical models originating in the aquaculture/fish farming literature. Specifically we looked at future contracts written on fresh farmed salmon, which have been actively traded at the Fish Pool Market in Norway since 2006. The link with the fish farming literature, has been established following first principles, starting by modeling the aggregate salmon farming production as well as modeling salmon demand using a Cobb-Douglas utility function for a representative consumer. We further extended the Schwartz (1997) two-factor model by adding a seasonality feature to the mean-level of convenience yield. We estimated all models using a rich data set of futures contracts with different maturities traded at Fish Pool by means of Kalman filter. Our results show that the framework presented is able to produce an excellent fit to the actual term structure of salmon futures. The results are then discussed in the context of other commodity markets, specifically live cattle which acts as a substitute. The comparison with live cattle futures traded within the same period reveals subtle difference, for example within the level of the convenience yield, the speed of mean reversion of the convenience yield and the convenience yield

risk premium.

Thereafter, the implications in the decision process of an individual fish-farmer have been investigated in the associated and accordingly calibrated model using a real option approach adopting the Longstaff-Schwartz-Method in the context of multiple state variables. Monetary values for lease and ownership of a model fish farm as well as the expected duration of harvesting cycles in the infinite and single rotation cases are determined. The values so determined take correctly account of the fish farmer's ability to efficiently diversify idiosyncratic risk contained in the salmon spot price by trading in the Fish Pool market. We assess the optimal strategy, harvesting time and value against two alternative setups. The first alternative involves simple strategies which lack managerial flexibility, the second alternative allows for managerial flexibility and risk aversion as modeled by a constant relative risk aversion utility function, but without access to the salmon futures market. In both cases, the loss in project value can be very significant, and in the second case is only negligible for extremely low levels of risk aversion. In consequence, for a risk averse fish farmer, the presence of a salmon futures market as well as managerial flexibility are highly important. Our approach is of practical interest to companies in the fish farming business and can guide their decision process in the context of the acquisition of fish farm units.

This study can be extended in several ways. One way is to investigate how markets price the risk of disease outbreak, such as fish lice or salmon anemia, and how this effects the valuation of fish farms. Moreover, stochastic factors like stochastic growth as well as stochastic feeding costs could be considered in the model. One can also examine the hedging effects of salmon futures. Other interesting research topics could be the possibility of creating financial markets for similar products, and introducing financial derivatives other than futures, e.g., swaps and options, to such markets.